Solution isomerization of commercial C_2-symmetric metallocene catalysts

By

Omar Soltan

Thesis presented for the degree of

Master of Science (Polymer Science)

at the

University of Stellenbosch

Promoter:
Dr. A.J. van Reenen

Stellenbosch
February 2006

Declaration

I, the undersigned hereby declare that the work contained in this thesis is my own original work and that I have not previously in its entirety or in part submitted it at any university for a degree.

Signature: …….. Date ……..

Acknowledgement

I would first like to thank Allah (God) who gave me the strength, health and opportunity to carry out this study in a proper way.

My appreciation and gratitude go to my parents, for providing me with all the opportunities and guidance throughout my life. My mother is especially thanked for her love, worrying, patience and praying to make this success possible. My father is gratefully thanked for his continuous encouragement and support. I would also like to extend my sincere thanks to all my brothers and sisters for their love.

I would also like to express my thanks to my promoter Dr. AJ van Reenen, for his advice and guidance throughout this study, and for opportunity to carry out this project in his group.

I would also like to thank the following people for their contributing to this study: All the staff and students at Polymer Science department, for their assistance and encouragement (Special thanks to the members of polyolefins group); Jean and Elsa, for all the NMR analyses done during this study; Derek and Nyambeni, for their assistance in CRYSTAF analyses; Valerie, for her assistance in HTGPC analyses; Dr. M. Hurndall for her assistance and advice in the proofreading of this thesis.

Centre of Macromolecules and Materials science (Libya) is gratefully acknowledged for the financial support of this research.

ABSTRACT

This study concerns the investigation of the isomerization of different metallocene catalysts in solution, and the effects thereof on the microstructure of polypropylenes prepared with these catalysts.

Two C_2 symmetric *ansa* metallocenes, ethylene-bis(indenyl) zirconium dichloride (EI) and dimethylsilyl-bis(2-methyl benzoindenyl) zirconium dichloride (MBI) were exposed, in solution, to both sunlight and UV radiation. The *rac-meso* isomerization of these catalysts were followed by ^{1}H NMR spectroscopy. The reaching of a photostationary state is described, as well as the effect of isomerization of these catalysts in solution on the polymerization of propylene.

Results show that metallocene structure has an effect on the isomerization rate and photostationary state. Results also show that the wavelength of light plays a role in the isomerization process.

Effects on stereochemistry and molecular weight of the formed polymer as well as the catalyst activity is described and discussed. In addition the effect of activating the catalysts with MAO before exposure to light is discussed.

OPSOMMING

Hierdie studie behels die ondersoek na die isomerisasie van verskillende metalloseen kataliste in oplossing, en die uitwerking daarvan op die mikrostruktuur van polipropileen wat deur hierdie kataliste berei word.

Twee C_2 simmetriese *ansa* metallosene, etileen-bis(indeniel) sirkonium dichloried (EI) en dimetielsiliel-bis(2-metiel bensoindeniel) sirkonium dichloried (MBI) in oplossing is blootgestel aan beide sonlig en UV bestraling. Die *rac-meso* isomerisasie van die kataliste is met behulp van ^{1}H KMR spektroskopie bestudeer. Die bereiking van ‘n foto-stasionêre toestand word beskryf, asook die effek van die isomerisasie van die kataliste in oplossing op die polimerisasie van propileen..

Resultate wys dat die metalloseen struktuur ‘n uitwerking het op die tempo van isomerisasie en die foto-stasionêre toestand. Resultate dui ook aan dat die golflengte van die lig ‘n rol speel tydens die isomerisasie-proses.

Die uitwerking vand die isomerisasie op die stereochemie en die molekulêre gewig van die gevormde polimeer, sowel as die katalis-aktiwiteit word beskryf en bespreek. Voorts word die uitwerking van aktivering van die katalis met MAO voor blootstelling aan lig ook bespreek.

Contents

List of Contents

CHAPTER 5: CONCLUSIONS AND RECOMMENDATIONS

List of Figures

List of Tables

List of Charts and Schemes

List of abbreviations

Cp	Cyclopentadienyl
Cp_2ZrCl_2	Bis(cyclopentadienyl)zirconium dichloride
CRYSTAF	Crystallization analysis fractionation
d	Metal-Cp distance
DSC	Differential scanning calorimetry
$\Delta\Delta E^{\ddagger}$	Difference in activation energy
ΔT	Temperature range
EI	Ethylene bis(1-indeyl)zirconium dichloride (rac-Et(Ind)2ZrCl2)
Flu	Flourenyl
GPC	Gel permeation chromatography
HT-GPC	High temperature gel permeation chromatography
Ind	Indenyl
i-PP	Isotactic polypropylene
MAO	Methylaluminoxane
MBI	Dimethylsilyl bis(2-methyl-4,5-benzo-indenyl)zirconium dichloride (*rac*-Me_2Si(2-Me-4,5-benzoind)$_2$]$ZrCl_2$)
Mn	Number average molecular wieght
Mw	Weight average molecular weight
MWD	Molecular weight distribution
NMR	Nuclear magnetic resonance spectroscopy
PP	Polypropylene
Tc	Crystallization temperature
Tm	Melting temperature
TMA	Trimethyl aluminium
TREF	Temperature rising elution fractionation
UV	Ultraviolet
Wi	Weight fraction
Wi%	Weight fraction percentage
ΣWi%	Wum of weight fraction percentage
α	Cp-Mt-Cp angle

δ	Chemical shift (ppm)

Chapter 1

Introduction and objectives

1.1 Introduction

Ansa C_2-symmetric metallocene catalysts is one of the research topics that has received a great deal of attention in the last two decades. These catalysts are highly iso-selective in propylene polymerization and have high activity. This allows for their use in most industrial applications for the production of PP homopolymer and PP copolymers.

The structure of the formed polymer is strongly related to the structure of the C_2-symmetric metallocene used for the polymerization. Any change to the C_2-symmetry during the preparation of the catalyst solution will affect the activity and the stereoselectivity of the catalyst.

The same catalyst can exist in 2 isomeric forms, resulting in a chiral C_2 symmetric compound or an achiral C_s symmetric compound. Inter-conversion between the two isomers, caused by UV radiation, has been observed and used [1-3] for promoting formation of the *racemic* (C_2) isomer over the *meso* (C_s) isomer during the synthesis of the catalyst.

It is common practice to prepare a catalyst solution in advance and to use this solution when required. Catalyst solutions could be kept for long periods of time before being used. During this period, the catalyst solution could be exposed to UV light from different sources. This process could result in a change in the polymer structure, and hence the inherent physical, thermal, and mechanical properties of the polymers prepared.

1.2 Objectives

The first objective of this study was to examine the isomerization of different *ansa* C_2-symmetric metallocene catalysts solutions using different types of UV sources. The isomerization process could be followed using ^{1}H NMR.

To this end, two C_2 symmetric *ansa* metallocenes that have a wide use, ethylene-

bis(indenyl) zirconium dichloride (EI) and dimethylsilyl-bis(2-methyl benzoindenyl) zirconium dichloride (MBI), were studied.

The second objective of this thesis was to synthesize and characterize polypropylene using solutions of C_2 symmetric *ansa* metallocenes which have been exposed to UV radiation, and study the effect of the isomerization process on stereochemistry of the formed polymer as well as the catalyst activity.

1.3 Thesis Outline

Chapter 1 presents a short introduction on the study as well as the main objectives of the study. Chapter 2 provides a brief historical overview of the development of metallocene catalyst. The structure-property relationship between polymer microstructure, crystallization behaviour and morphology is discussed. The mechanism of stereo-selectivity is presented, as well as the brief background on the photochemistry of metallocene catalysts.

Chapter 3 describes the investigation of the structure of the two isomers of different C_2-symmetric metallocene catalysts by ^{1}H NMR. The rate of the isomerization of these catalysts is discussed, using both sunlight and a UV lamp as a source of UV radiation.

Chapter 4 discusses the effect of the isomerization process on polypropylene microstructure and relates it to the change in the catalyst structure as studied by ^{1}H NMR. In addition the effect of activating the catalysts with MAO before exposure to light is also discussed.

Chapter 5 summarizes the main conclusions on all the previous chapters and provides some recommendations for future studies.

1.4 References

1. Wild, F. Zsolnai, L. Huttner, G. Brintzinger, H. J. Organomet. Chem, 1982. 232: p. 233.

2. Wild, F. Wasiucionek, M. Huttner, G. Brintzinger, H. J. Organomet. Chem., 1985. 288: p. 63.

3. Kaminsky, W. Chauwienold, A. Freidanck, F. J. Mol. Catal. A: Chem., 1996. 112: p. 37.

Chapter 2

Metallocene catalysts: Historical background and theory

2.1 Introduction

Since the discovery of stereoselective olefin polymerization in 1954, [1] and development of PP by Natta [2] using Ziegler type catalysts, PP has become an important commercial thermoplastic. PP consumption is still increasing more rapidly than any other polymer and will continue to do so in the future.

This growth in production is due to relatively low polymer cost that, in turn, can be attributed to low monomer cost and efficient polymerization technology. Also, PP has the ability to be processed at low cost, which in turn allows for economic use in most commercial fabrication techniques. PP can also be modified for a variety of applications.

With the development of metallocene catalytic systems for the isospecific polymerization of olefins, new isotactic polypropylenes (iPP) showing a wide variety of microstructures have become available. [3-7] Depending on the specific metallocene complex used as catalyst, [8] as well as on the polymerization conditions (i.e., monomer concentration, temperature, nature of cocatalyst, etc.), iPP samples containing different amounts and combinations of stereoregularity (primary insertions with the wrong enantioface, or stereodefects) and regioregularity (*meso* and *racemic* secondary insertions, or regiodefects) can be obtained. [9]

The tacticity distribution of PP is a reflection of the homogeneity of active sites in a catalyst. In the conventional Ziegler-Natta catalyst there are many active sites and the PP obtained has a broad tacticity distribution. Homogeneous metallocene catalysts are believed to have a `single active site', and the tacticity distribution of the prepared PP is very narrow by comparison.

This chapter discusses development of metallocene catalysts and gives some background to the structure property relationships for PP. The development of olefin polymerization in terms of the proposed mechanisms will also be

discussed. Some background on the photoisomerization of metallocene catalyst is also discussed.

2.2 Historical background of metallocene catalysts

Metallocenes are relatively well-known organometallic complexes that were discovered as early as 1951. The first compound discovered was ferrocene, [10] a simple complex consisting of an iron center and two cyclopentadienyl (Cp) rings surrounding the metal.

The term metallocene was used to describe any complex with a metal centre and Cp ligands surrounding it. Presently, the term is used to describe a wide variety of organometallic complexes including those with altered structures such as substituted Cp rings and bridging atoms.

In 1953 Karl Ziegler and his co-workers [1] discovered catalyst systems based on transition metal compounds (zirconium and titanium halides), which were used to study the polymerization of α-olefins. [11] In the presence of aluminum alkyl activators these catalyst systems were able to polymerize ethylene to yield HDPE at low pressure, but could not polymerize propylene.

In 1954 Natta reported the successful polymerization of propylene using the same catalyst system. [2] After characterization the resulting polymer, he was able to define the three stereoconformations of polypropylene: isotactic, syndiotactic, and atactic. [12, 13]

In 1957, Breslow and Newburg reported the polymerization of ethylene with the titanocene catalyst, CP_2TiCl_2 (Figure 2.1). [11, 14] This was accomplished with the cocatalyst trimethyl aluminium, although the activity of the metallocene was found to very low and there was little promise for commercial use.

In the mid 1970's, during experiments involving a metallocene catalyst of the form Cp_2ZrCl_2 and the cocatalyst Al $(CH_3)_3$, water was accidentally introduced

into the system. [15] It was noted that the activity of the metallocene/alkylaluminum catalysts could be significantly increased by the controlled addition of water to the polymerization reactor. High activity between the catalyst and ethylene monomers to form polymer was achieved. After further research, it was postulated that the high activity was a result of the hydrolysis of the co-catalyst trimethyl aluminum to form methylaluminoxane or MAO. [15, 16]

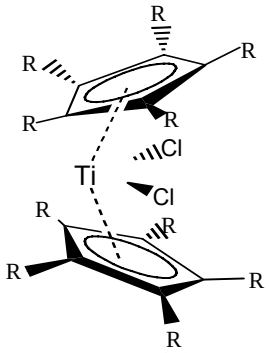

Figure 2.1 Titanocene catalyst

In 1982 Brintzinger *et al.,* [17] reported the synthesis of the *ansa* C_2 –symmetric metallocene catalyst *rac*-Et(Ind)$_2$MtCl$_2$, which allowed for the stereospecific polymerization of propylene. In 1988 Ewen [18] reported a C_s-symmetric zirconocene ([Me$_2$C(Flu)(Cp)]ZrCl$_2$) which allowed for the production of syndiotactic polypropylene in high quantities.

Since then much research has been conducted in the area of metallocenes. The structure of metallocenes has also received a lot of attention in order to optimize it for the polymerization of α-olefins. Metallocenes can be substituted, bridged, unbridged, or of the half sandwich type. Ligands such as indenyl (Ind) and flourenyl (Flu) have been used instead of cyclopentadienyl (Cp). (Figure 2.2)

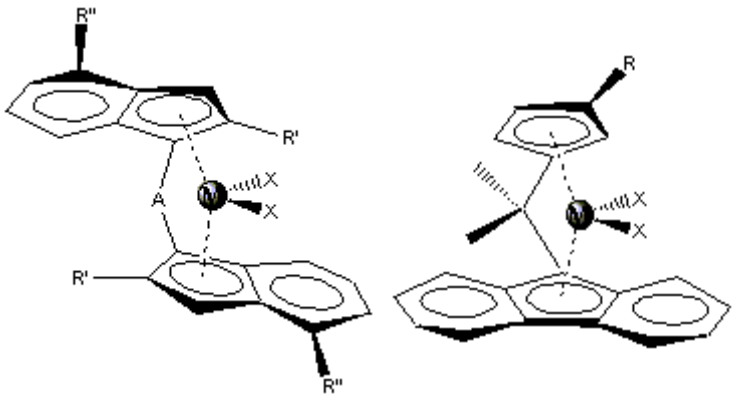

Figure 2.2 Examples of different structures of metallocene catalysts

2.3 Theoretical background

2.3.1 Relationship of structure to morphology and properties

The properties of PP are related to both fabrication history of the material and its molecular structure. The polymer structure is related to the catalyst, polymerization, and compounding technologies. The wide range of PP applications comes from the variation of its properties that can be achieved.

Figure 2.3 is a representation of the relationship between structure, morphology, and end-use properties. The microstructure and the molecular weight of PP strongly determine the crystallization behaviour and its physical properties. [19-25] The physical properties and the crystallization behaviour in turn determine thermal and mechanical properties of the final products. [26-28]

From the figure it can be concluded that polymer morphology provides a bridge between polymer structure, processing, fabrication history, and end-use properties. Understating the effect of these structure variables on PP morphology is essential, because it is the morphology which provides the most direct link with polymer properties.

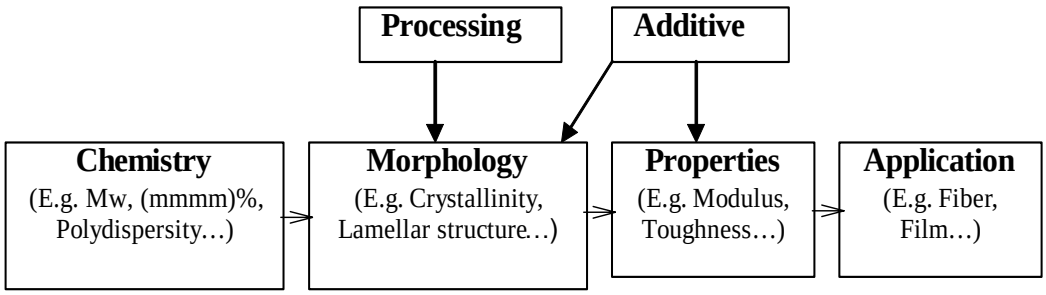

Figure 2.3 Polymer structure, morphology, properties, and end-use relationship

Depending on the tacticity, PP polymers with different percentages of crystallinity can be obtained. The level of tacticity can be varied considerably in PP. As will be discussed in the following section, PP has three different types of stereochemical configurations termed isotactic, syndiotactic, atactic polypropylene.

Isotactic and syndiotactic chains crystallize to a high degree while atactic chains do not. The regioregularity of PP also has a significant impact on the level of crystallinity of the polymer and the crystallization kinetics. Molecular weight also has a significant impact in determining the morphology and consequently on the thermal and mechanical properties.

Polydispersity and details on the intra-chain architecture, which include co-monomer distribution in random copolymers, also play a significant role in determining the end-use of the polymer. Different processing parameters and different types of additives can be used to manipulate the morphology and the final properties of the polymer.

Polymer microstructure can be influenced by catalyst structure, polymerization conditions, the technology used for polymerization, and the types and percentage of the co-monomer that used (Figure 2.4).

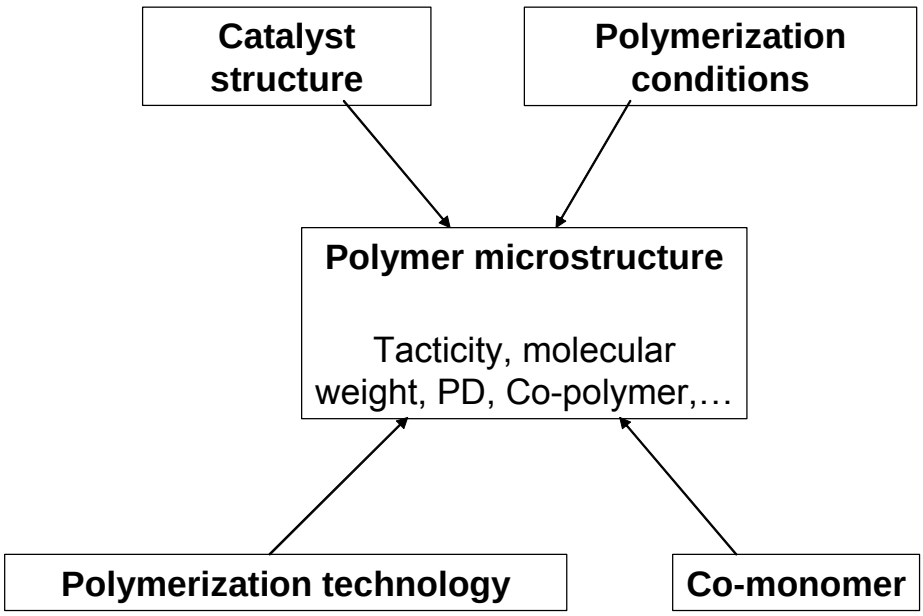

Figure 2.4 Factors that influence the polypropylene microstructure

During the polymerization of propylene monomer any change in the catalyst structure or reduction in catalyst concentration will lead to changes in the structure of the formed polymer.

2.3.2 Polypropylene microstructure

The general chemical structure of propylene chain is shown in Figure 2.5.

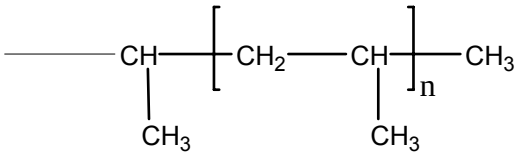

Figure 2.5 General structure of PP

The way in which the monomer inserts into the polymer backbone (head-to-tail or head-to-head or tail-to-tail or right or left hand) determines the polymer's regioregularity and stereoregularity, respectively. From the right hand and the left hand insertions three different PP structures are produced:

Isotactic polypropylene results from the head-to-tail addition of propylene monomer units, where the methyl groups always have the same configuration with respect to the polymer backbone (Figure 2.6 (A)).

Atactic polypropylene results from head-to-tail addition of monomer units, where the methyl groups have a random configuration with respect to the polymer backbone (Figure 2.6 (B)).

Syndiotactic polypropylene results from the same head-to-tail addition of monomer units, where the methyl groups have an alternative configuration with respect to the polymer backbone (Figure 2.6 (C)).

The first isotactic polypropylene with high stereoregularity was produced in 1955 and IR spectroscopy was the only technique used to evaluate the degree of isotacticity. [29] In 1960 ^{13}C NMR became the most powerful tool for the determination of the microstructure of polyolefins and the polymerization mechanism in solution.

Olefin insertion into metallocene Mt-C bonds is predominantly primary (head-to-tail). However, one of the features of most isospecific metallocene catalysts is their generally lower regioselectivity compared to heterogeneous Ziegler-Natta catalysts.

Despite the fact that primary propylene insertion is clearly favoured by electronic factors, isolated secondary propylene units are often detectable in i-PP samples and their presence is the signature of a metallocene catalyst. Tail-to-tail propylene insertions, normally referred to as secondary or 2,1 insertions, occur in i-PP made by isospecific metallocene catalysts with high but opposite (with respect to primary insertions) enantioface selectivity (Figure 2.7).

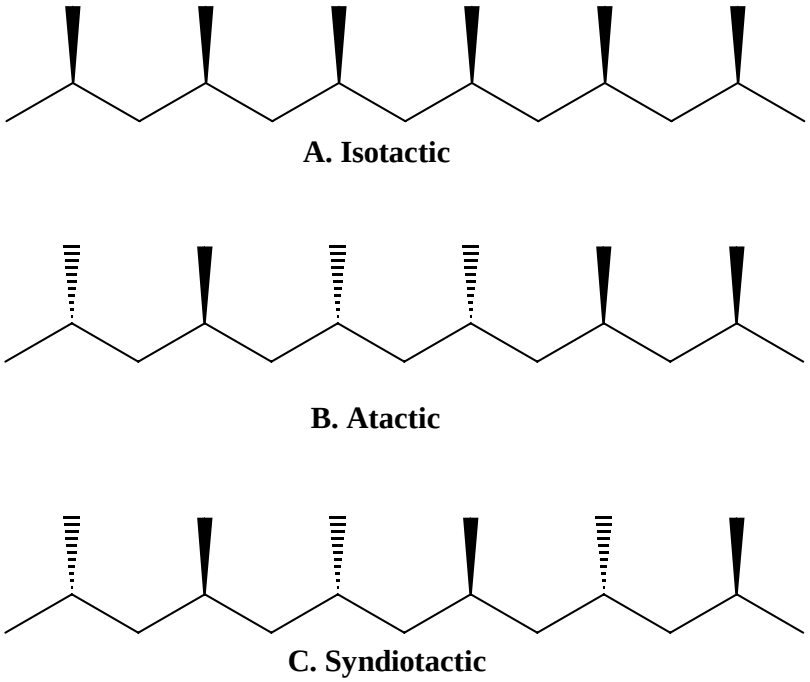

Figure 2.6 The three different types of stereoregularity of PP

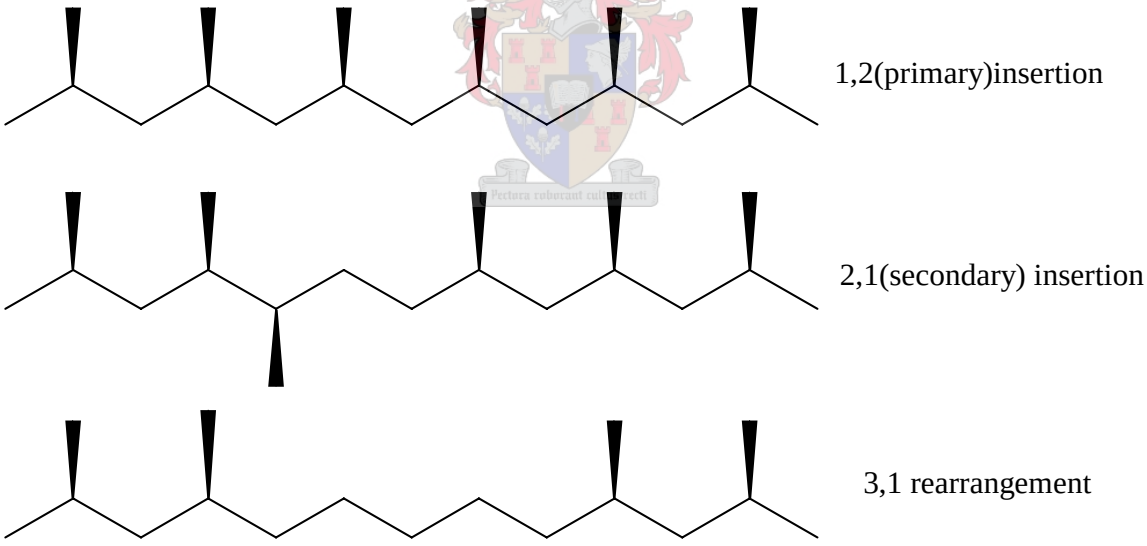

Figure 2.7 Regiochemistry of PP: primary and secondary insertions

Regiodefects have a strong effect in lowering the crystallinity and melting point of i-PP. At the same time, there is also a close correlation between catalyst regioselectivity on one side and catalyst activity and polymer molecular weight on the other, due to the lower monomer insertion rate at a secondary growing

chain end, and the competing H-transfer to the monomer after a secondary insertion.

Two types of regioirregular units are formed in PP chains when a metallocene catalysts are used: 2,1 insertions and 3,1 insertions. Chien, [30] Kaminsky [31] and Brintzinger *et al*. [32] suggest that 1,3 units are formed via isomerization of secondary Zr-alkyl units, resulting from 2,1 monomer insertion, to primary Zr-alkyl units before the next monomer insertion.

2.3.3 ^{13}C NMR Analysis

^{13}C NMR spectroscopy is the main source of information on the stereochemistry and regiochemistry of metallocene, and related transition metal, catalyzed α-olefin polymerizations.

A polymer chain is a permanent record of the statistical chain of events which makes up the polymerization process. From the microstructure, it is possible to identify the reaction modes and to measure their relative rates. It is even possible, at least in principle, to infer the interdependence of these reactions. In this respect, ^{13}C NMR has proved to be a most valuable fundamental technique, particularly in the field of Ziegler-Natta and related transition metal catalyzed α-olefin polymerization reactions. [33-38]

The chemical shift of the methyl groups in polypropylene is highly sensitive to the relative stereochemistry of neighboring monomer units, that is, each methyl carbon has a different chemical shift depending on the configuration of the adjacent methynes, up to five on each side (a sequence length of 11 consecutive monomer units). The degree of isotacticity can be given as the pentad, triad, or diad content (% mmmm, % mm, % m, respectively). The most commonly quoted stereo-sequence is at the pentad level, where the methyl resonance is split in nine or ten major peaks assigned as *mmmm, mmrr, rrrr, mmmr, mmrm, mrrr, rmmr, rmrr, mrrm, rmrm* (Chart 2.1).

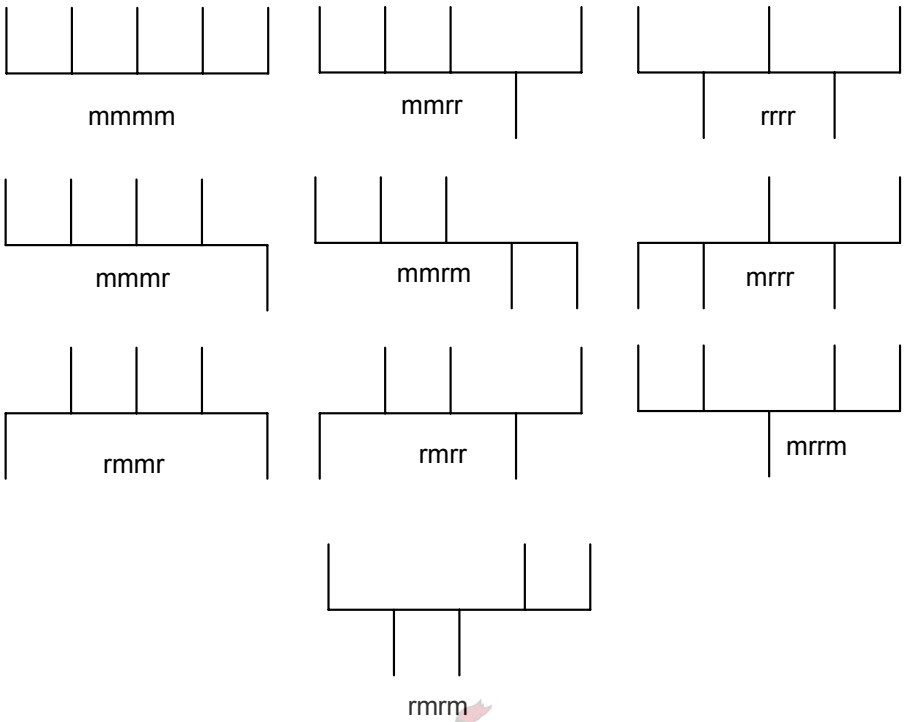

Chart 2.1 Pentad stereosequences in polypropylene

^{13}C NMR analysis has also shown that 2,1 units are always isolated between two isotactic blocks. These 2,1 sequences can give rise to the formation of tetramethylene sequences (3,1 units), if unimolecular isomerization of the secondary unit occurs.

End groups of the polymer chains provide information about the mechanism of termination, chain transfer and polymerization can also be detected using ^{1}H and ^{13}C NMR spectroscopy.

2.3.4 Metallocene catalysts

2.3.4.1 Catalyst structure

Active metallocene catalysts are formed by the reaction of metallocenes and a cocatalyst, which is generally an organoaluminium compound. The exact definition of the catalyst is that group 4 metallocenes (titanium, zirconium or hafnium) are d^{o} pseudotetrahedral organometallic compounds in which the

transition metal bears two η^5 ligands and two σ ligands.

Figure 2.8 shows a general structure of metallocene catalyst. It consists of two cyclopentadienyl (η^5) ligands and a group 4 metal atom (titanium, zirconium or hafnium) with two halogen atoms (σ ligands) attached to the metal.

The carbon atoms of the Cp ligands can bear hydrogen or other groups such as alkyl. Up to ten different substituents are possible on the metallocene. The different substituents change not only the shape and the size of the Cp ligands but also the metal-Cp distance (d) and the Cp-Mt-Cp angle (α).

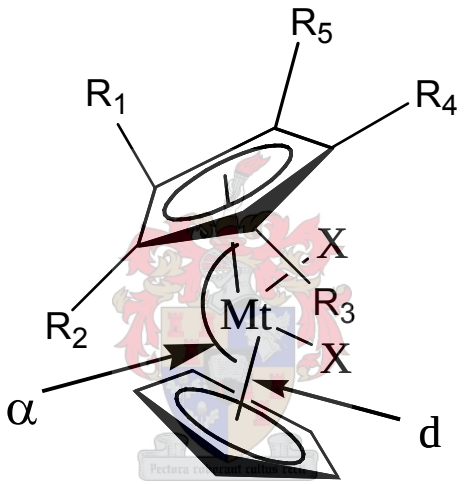

Figure 2.8 General structure of a metallocene catalyst: R_1, R_2, R_3, R_4, and R_5 can be hydrogen or an alkyl group

The most commonly found Cp-type ligands are cyclopentadienyl, alkylated cyclopentadienyl, indenyl, and flourenyl. Figure 2.9 shows the general structures of the different types of ligands used in metallocene catalysts.

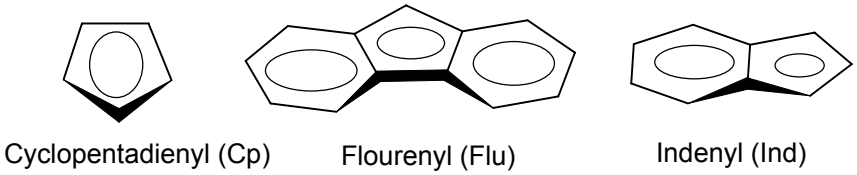

Figure 2.9 The different types of ligands that used in metallocene catalysts

2.3.4.2 Classification of metallocenes

Metallocene catalysts have been classified on the basis of their symmetry. [39] Figure 2.10 is a schematic representation of the different classes of metallocene catalysts. In class I, the two η^5 - cyclopentadienyl ligands can be bridged or not; in the other classes they are bridged. In classes I and II, the two sites occupied by the η^5-ligands are bisected by a horizontal mirror plane and consequently are achirotopic and identical in class I and different in class II. In the other classes, the two above sites are chirotopic; they are related by a two-fold rotation axis in class III and are homotopic (equal). In class IV, the two sites are related by a vertical mirror plane and are enantiotopic (mirror image to each other). No symmetry elements are present in class V, and the two sites are different.

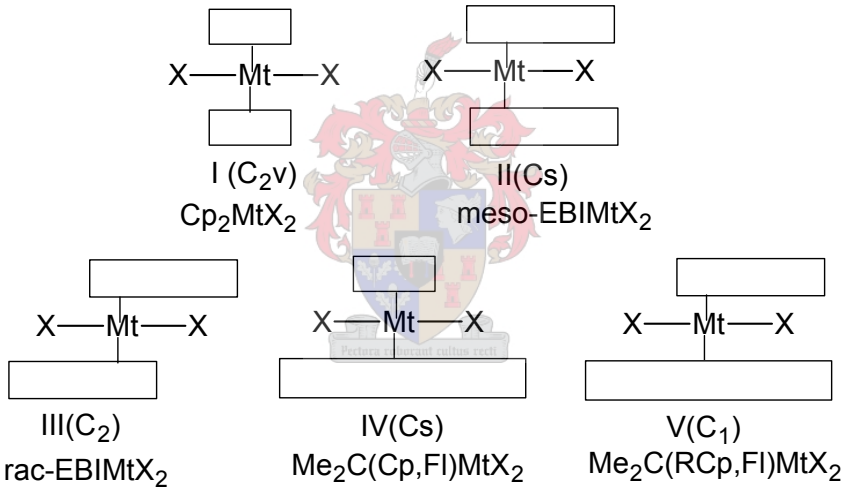

Figure 2.10 Classification of metallocene catalysts according to their symmetry

2.3.4.3 Elements of chirality

The use of cyclopentadienyl, indenyl or fluorenyl ligands can lead to achiral or variety of stereoisomeric metallocenes, depending on the symmetry of the ligands being used. In general, chiral group 4 metallocene catalyst can have “chirality” assoociated with it in three ways: i) the chirality may be based on a stereogenic metal atom with four different ligands; ii) the chirality may be introduced by the coordination of the metal to chiral or prochiral ligands; iii) it

may be due both of these elements. [5, 40]

Stereocontrol is ultimately due to the chiral arrangement of the ligands of the transition metal of the catalyst complex. The stereocontrol as a function of metallocene symmetry is shown in Figure 2.11. It is important to remember that the two η^5 ligands are constant, the two σ ligands are replaced by an alkyl group (or a growing polymer chain during polymerization) and a coordinated monomer. Due to the mechanism of polymerization, the latter two ligands can change their relative position after every monomer insertion.

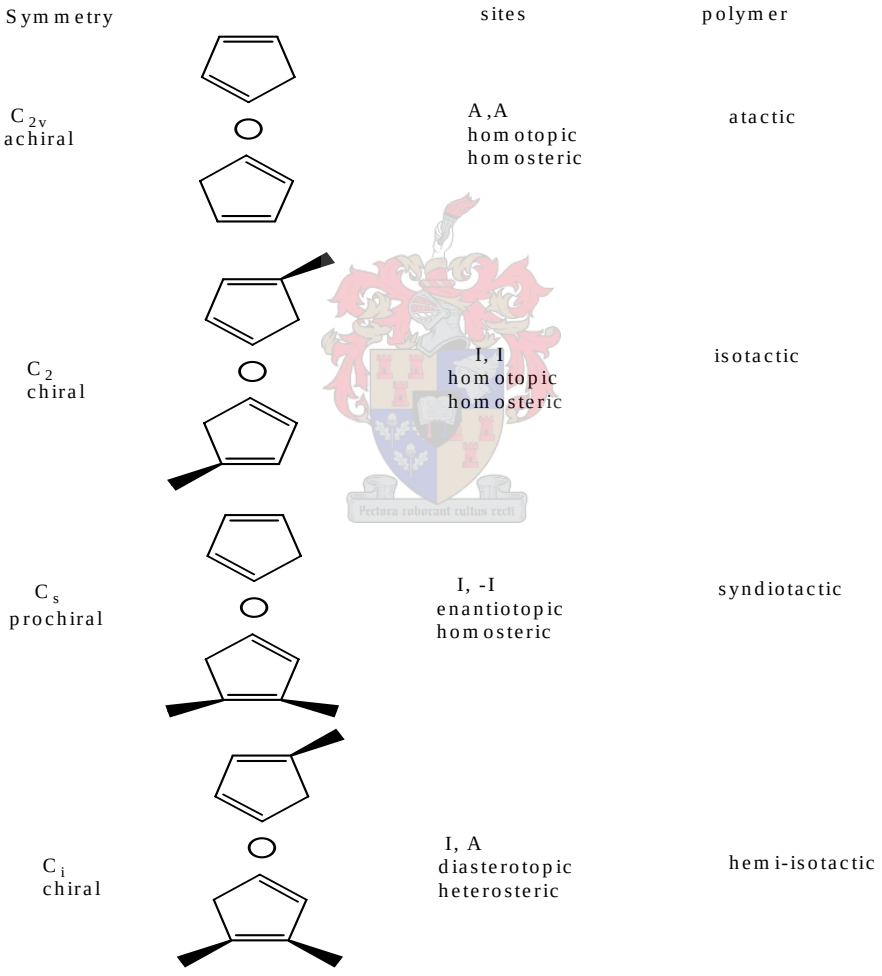

Figure 2.11 Steric control as a function of metallocene symmetry

2.3.4.4 The role of the co-catalyst

The co-catalysts are the key to the activity of the metallocenes. Methylaluminoxane (MAO) is mostly used and is synthesised by the controlled hydrolysis of trimethyl aluminium (TMA). [41, 42] Other bulky anionic complexes which show weak co-ordination, such as borates, [43-46] play an increasing role too.

MAO is an oligomeric compound with a molecular weight of 1 000 – 1 500 g/mol, obtained by the controlled hydrolysis of trimethylaluminum ($AlMe_3$). Studies have shown that MAO is a mixture of several different compounds, including residual (coordinated) $AlMe_3$ and possibly AlO_3 units, in dynamic equilibrium. [47]

The exact structure of MAO has not yet been determined. They supposedly exist as a mixture of different cyclic or linear oligomers with degrees of oligomerization commonly varying from 6 to 20. MAO, the most commonly used aluminoxane, may have the structures shown in Figure 2.12. Some recent experimental studies have suggested that MAO can also have a three-dimensional open cage structure. [41]

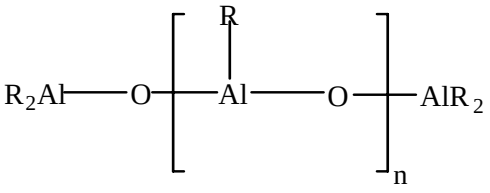

1

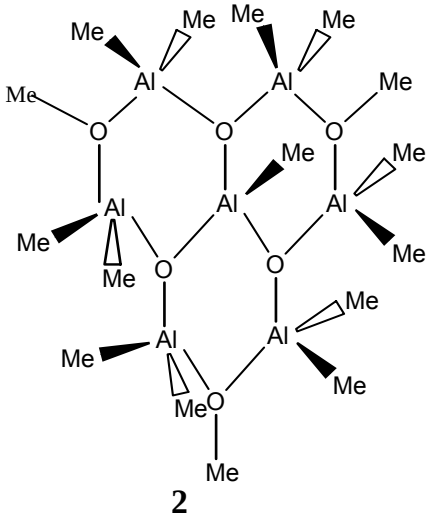

2

Figure 2.12 Proposed structures of MAO

The first function of the MAO is the alkylation of the halogenated metallocene complex. Monomethylation takes place within seconds, and an excess of MAO leads to dialkylated species. [48] The generally accepted mechanism of metallocene activation by MAO is shown schematically in Figure 2.13.

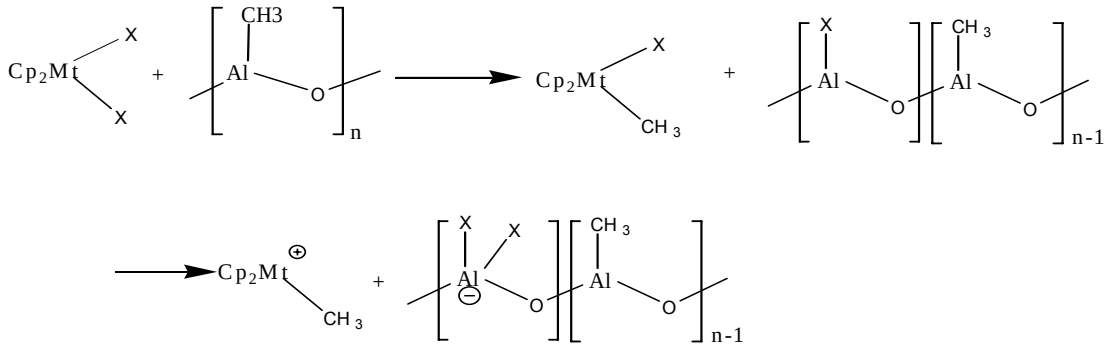

Figure 2.13 The mechanism of metallocene activation by MAO

2.3.4.5 Mechanism of olefin polymerization with metallocenes

In order for the polymerization to take place, the active metal atom centre bearing the growing alkyl chain must have a site for coordination. Insertion occurs via chain migration to the closest carbon of the olefin double bond, which undergoes *cis* opening with formation of the new M-C and C-C bonds.

Four mechanisms for olefin polymerization have been proposed: the first of these mechanisms is the so-called Cossee mechanism [14, 49] and essentially involves two steps, being (i) olefin coordination and (ii) alkyl migration of the σ-coordinated growing chain to the π-coordinated olefin. This results in a net migration of the Mt-chain σ-bond to the coordination position previously occupied by the coordinated olefin. (Scheme 2.1)

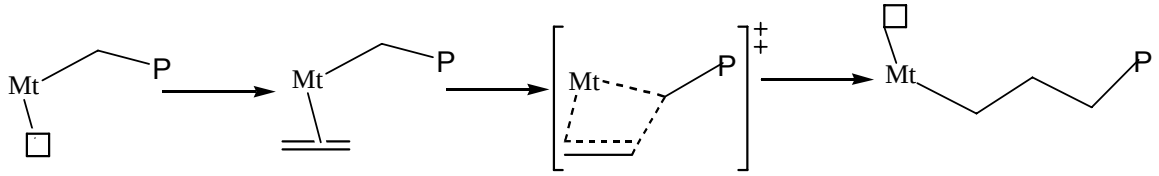

Scheme 2.1 Cossee mechanism

The second mechanism is the so-called Green and Rooney mechanism, [50] but this involves an oxidative 1,2-hydrogen shift from the first C atom of the growing chain to the metal. This is not possible, for the cationic d^o complexes that are effective polymerization catalysts lack the electrons required for this reaction.

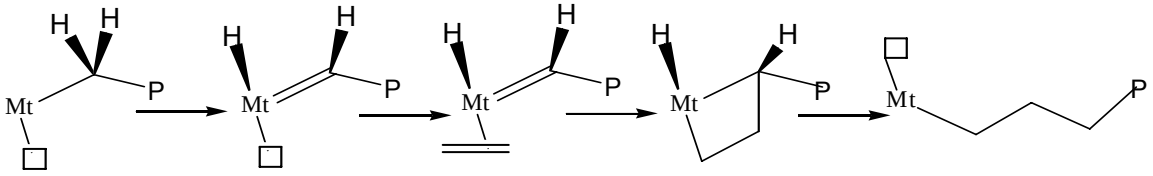

Scheme 2.2 Green and Rooney mechanism

The "Modified Green-Rooney mechanism" was developed by Green, Rooney, and Brookhart [51] and requires a stabilizing α-agostic interaction in various stages of the reaction. The fourth mechanism which is very similar to the modified Cossee mechanism (Scheme 2.4) also requires the presence of an α-agostic interaction.

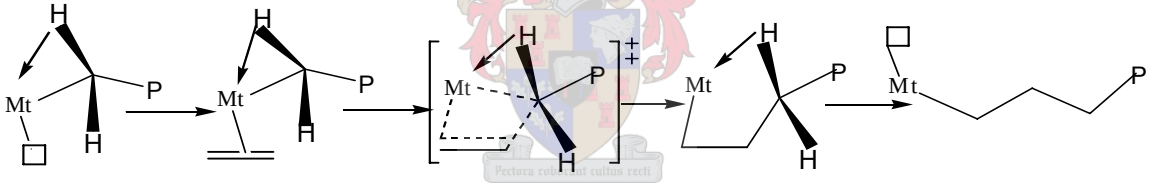

Scheme 2.3 Ground and transition state α-agostic mechanism

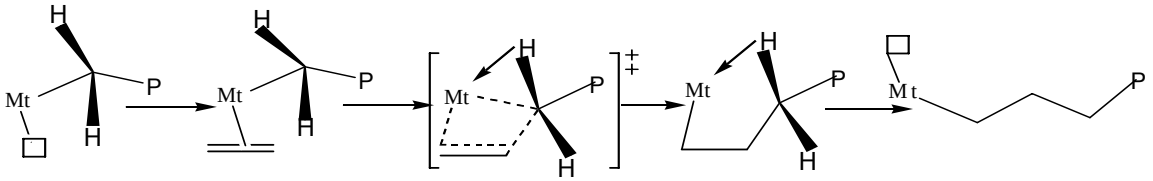

Scheme 2.4 Transition state α-agostic mechanism

All the presented mechanisms show that the olefin insertion occurs by *cis* opening of the double bond and with chain migratory insertion. In metallocene catalysts, every metal atom is regarded as an active centre and every active centre has two active sites in which coordination can take place. Because of the two sites, and the mechanism of chain migratory insertion with site switching,

metallocene catalysts allow for the formation of different olefin structures. This can be predicted by knowing the relationship between metallocene site symmetry and polymer stereochemistry.

2.3.4.6 Mechanisms of stereocontrol in propylene polymerization

Stereoselectivity or enantioface selectivity of olefin insertion can be due to 2 mechanisms. The most effective one is that which is generally called enantiomorphic site control, that is, the chirality arises from the catalytic site. This is due to the spatial arrangement of the 2 η^5 -coordinated Cp ligands, the growing polymer chain and the coordinated monomer itself. The arrangement is largely determined by energy considerations and the lowest energy state will determine the preferred monomer coordination. If the last coordinated monomer is able to influence the coordination of the next monomer, the mechanism is called chain-end control. This is far less common.

The isomerization of a C_2-symmetric compound will result in the production of an achiral C_s-symmetric compound in solution, thus it significant to discuss the mechanisms of stereocontrol in these two types of metallocene catalysts.

a) Mechanism of enantiomorphic site control (isospecific catalysts)

If we assume that 1,2 or primary insertion of the monomer is prevalent, then there are two ways for a prochiral monomer like propylene to coordinate. These two stereospecific processes can have a difference in activation energy [52] ($\Delta\Delta E^{\ddagger}$) of up to 5 kcal/mol, so the possibility for the stereoerror to occur is theoretically very low.

In C_2-symmetric catalysts, such as *rac*-Et(Ind)$MtCl_2$, the two active sites available for the incoming monomer and the growing chain are the same (homotopic) and, therefore, the configuration of the central metal atom does not change after the chain migratory insertion of the coordination monomer (Figure 2.14).

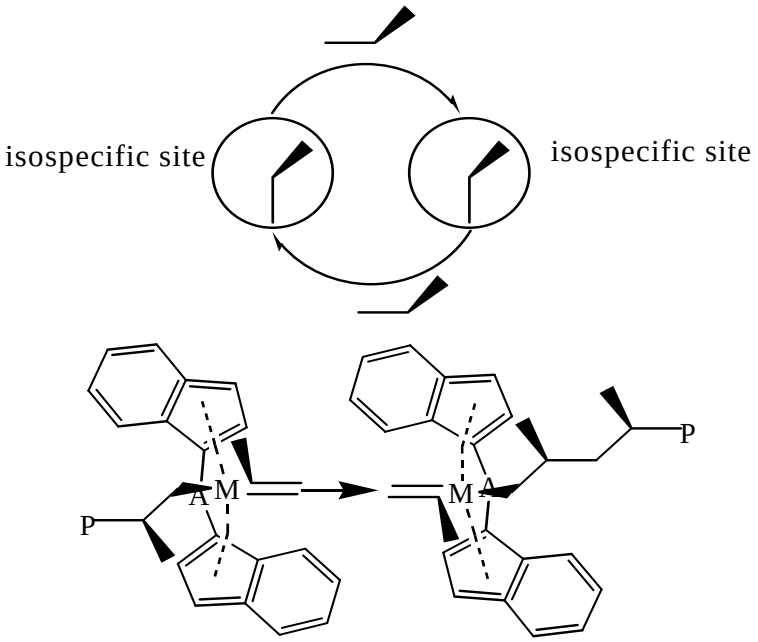

Figure 2.14 Propylene polymerisation mechanism with C_2-symmetric metallocene catalysts

b) Lack of control (aspecific catalyst)

In achiral C_s-symmetric catalysts, such as *meso*-Et(Ind)$MtCl_2$, the positions of the coordinated olefin and of the alkyl ligands are not chirotopic (fixed by energy considerations) and, therefore, the catalyst control is completely lacking (Figure 2.15).

Chain-end control could be functional here, and is less effective than site control, the ($\Delta\Delta E^{\ddagger}$) between the insertion of the two enantiofaces being around 2 kcal/mol, so the stereoerror is more likely than in the case of the enantiomorphic site control. The types of stereoerrors arising from chain end control (or a lack of site control) are diagnostic of this state of affairs and clearly be seen in ^{13}C NMR. [52]

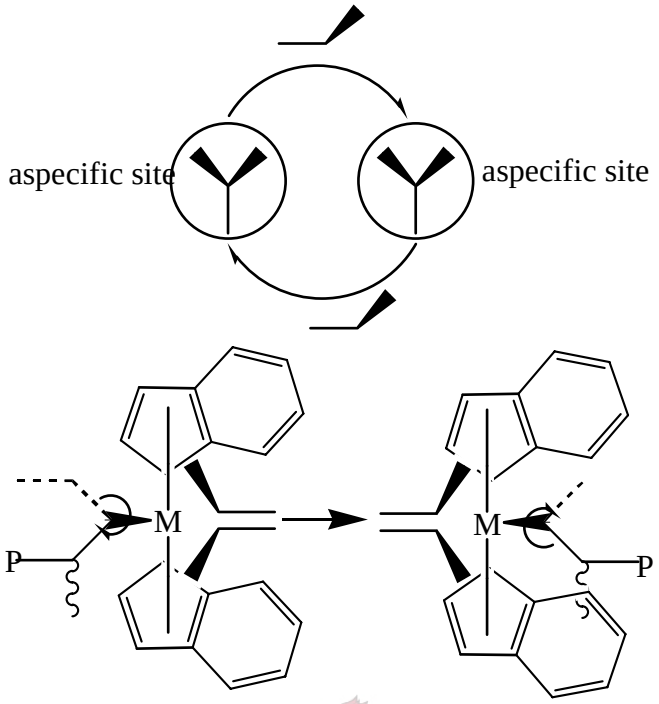

Figure 2.15 Propylene polymerization mechanism with achiral Cs-symmetric metallocenes (meso isomers of C_2 symmetry)

2.3.5 The photochemistry of metallocene catalysts

The first investigation on the effect of the ultravilet radiation on metallocenes was applied on ferrocene with no significant result. [53, 54]

After that, the photochemistry of metallocene was investigated by Harrigan [54] using a Cp_2TiCl_2 catalyst. He found that in the titanocence dihalide photolytic scission occurs to give cyclopentadieny radicals. In the same work Harrigan proposed the mechanism of the photochemistry, which is:

$$Cp_2TiCl_2 \underset{}{\overset{h\nu}{\rightleftharpoons}} CpTiCl_2 \xrightarrow{CHCl_3} CpTiCl_3 + \bullet CHCl_2$$

where reaction takes place via a homolytic cleavage of the η^5-metal cyclopentadienyl ring bond. Harrigan proved this mechanism by performing the irradiation in a halogenated solvent.

Since then many researchers have focused on the isomerization of metallocene catalysts and utilizing this phenomenon during in the synthesis of the catalyst and also to study the effect of light on the catalyst strucuture. [55-59]

Kaminsky [7] investigated the isomerization of *racemic* and *meso* isomers of $SiMe_2(Ind)_2ZrCl_2$ catalyst by ultraviolet radiation. He achieved the same result, which is that the radiation caused a homolytic cleavage of the η^5-metal-cyclopentadienyl ring bond (Figure 2.16).

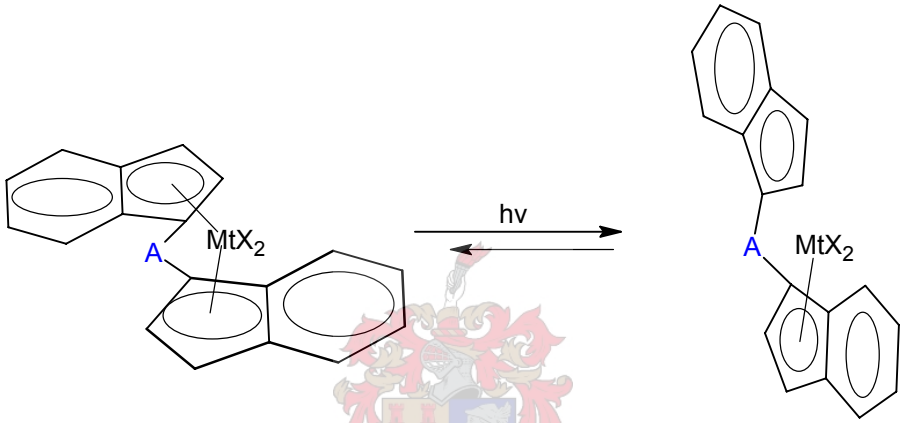

Figure 2.16 The first step in the mechanism of the photoinduced *rac/meso* intercoversion [7]

After the photolytic scission of the η^5-metal-cyclopentadienyl ring bond, light causes the rotation of the ligands followed by the recombination of the η^5-metal-cyclopentadienyl ring bond (Figure 2.17).

It seems that the scission of the η^5 -metal-cyclopentadienyl ring bond is promoted by a wide range of wavelengths. [58] The rotation of the ligands, however, is promoted by more selected, suitable wavelengths, and the recombination of the η^5-metal-cyclopentadienyl ring bond does not need any light source.

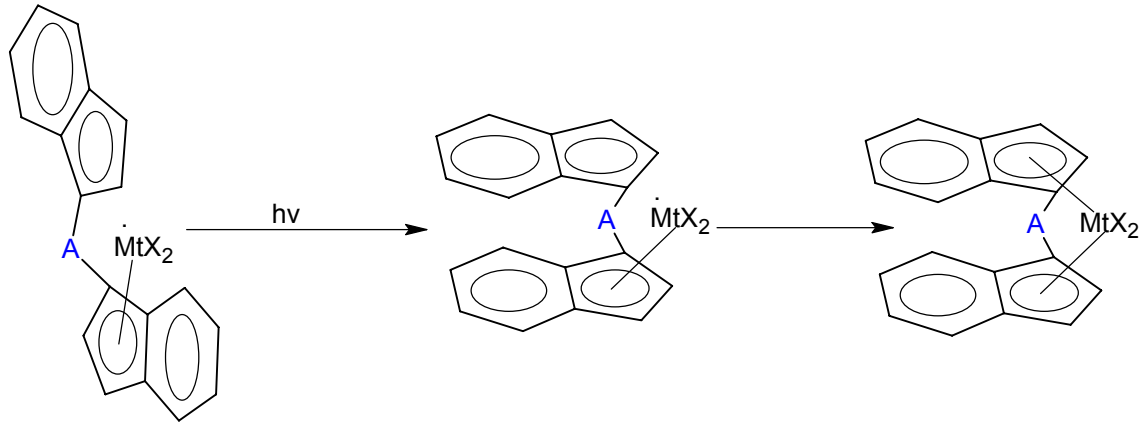

Figure 2.17 The second step in the mechanism of the photoinduced *rac/meso* intercoversion [7]

2.4 References

1. Ziegler, K.; Holzkamp, E.; Breil, H., Angew. Chem., 1955. 67: p. 541.

2. Natta, G., Angew. Chem., 1956. 68: p. 393.

3. Coates, G., Chem. Rev., 2000. 100: p. 1223.

4. Ewen, J.; Elder, M.; Jones, R.; Haspeslagh, L.; Atwood, J.; Bott, S., Macromol Symp., 1991. 49: p. 253.

5. Resconi, L.; Cavallo, L.; Fait, A.; Piemontesi, F., Chem. Rev., 2000. 100: p. 1253.

6. Brintzinger, H.; Fischer, D.; Mulhaupt, R.; Rieger, B.; Waymouth, R., Angew. Chem. Int. Ed. , 1995. 34: p. 1143.

7. Kaminsky, W., Macromol. Chem. Phys., 1996. 197: p. 3907.

8. Roll, W.; Kuber, F.; Winter, A.; Rohrmann, J.; Antberg, M.; Doll, V.; Paulus. E., Organometallics, 1994. 13: p. 954.

9. Busico, V.; Cipullo, R., Prog. Polym. Sci., 2001. 26: p. 443.

10. Wilkinson, G.; Birmingham, M. , J. Am. Chem. Soc., 1954. 76: p. 4281.

11. Breslow, D.; Newburg, N. , J. Am. Chem. Soc., 1957. 79: p. 5072.

12. Edward, P.; Moore, J., Polypropylene Handbook. 1996: Hanser Publishers, Munich Vienna New York.

13. Pavan, A.; Provasoli, A.; Moraglio, G.; Zambelli, A., Makromol. Chem., 1977. 178: p. 1099.

14. Breslow, D.; Newburg, N., J. Am. Chem. Soc., 1959. 81: p. 81.

15. Reichert, K.; Meyer, R., Makromol. Chem., 1973. 169: p. 163.

16. Sinn, H.; Kaminsky, W., Adv. Organomet. Chem., 1980. 18: p. 99.

17. Wild, F.; Zsolnai, L.; Huttner, G.; Brintzinger, H., J. Organomet. Chem., 1982. 232: p. 233.

18. Ewen, J.; Jones, R.; Razavi, A.; Ferrara, J., J. Am. Chem. Soc., 1988. 110: p. 6255.

19. Auriemma, F.; De Rosa, C.; Boscato, T.; Corradini, P. , Macromolecules, 2001. 34: p. 4815.

20. De Rosa, C.; Auriemma, F.; Perretta, C. , Macromolecules, 2004. 37: p. 6843.

21. De Rosa, C.; Auriemma, F.; Circelli, T.; Waymouth, R., Macromolecules, 2002. 35: p. 3622.

22. Auriemma, F.; De Rosa, C., Macromolecules, 2002. 35: p. 9057.

23. De Rosa, C.; Auriemma, F.; Circelli, T.; Longo, P.; Boccia, A., Macromolecules, 2003. 36: p. 3465.

24. De Rosa, C.; Auriemma, F.; Spera, C.; Talarico, G.; Tarallo, O., Macromolecules, 2004. 37: p. 1441.

25. De Rosa, C.; Auriemma, F.; Ruiz de Ballesteros, O.; Resconi, L.; Fait, A.; Ciaccia, E.; Camurati, I., J. Am. Chem. Soc., 2003. 125: p. 10913.

26. Katti, S.; Schultz, J., Polym. Eng. Sci., 1982. 22: p. 1001.

27. Fujiyama, M.; Wakino, T.; Kawasaki, Y., J. Appl. Polym. Sci., 1988. 35: p. 29.

28. Fujiyama, M.; Wakino, T., J. Appl. Polym. Sci., 1991. 43: p. 97.

29. Natta, G.; Pino, P.; Corradini, P.; Danusso, P.; Mantica, E.; Mazzanti, G., J. Am. Chem. Soc., 1955. 77: p. 1708.

30. Rieger, B.; Mu, X.; Mallin, D.; Rausch, M.; Chien, J., Macromolecules, 1990. 23: p. 3559.

31. Schupfner, G.; Kaminsky, W., J. Mol. Catal. A: Chem., 1995. 102: p. 59.

32. Prosenc, M.; Brintzinger, H., Organometallics., 1997. 16: p. 3889.

33. Brintzinger, H.; Fischer, D.; Muelhaupt, R.; Rieger, B.; Waymouth, R., Angew. Chem. Int. Ed. Engl., 1995. 34: p. 1143.

34. Zambelli, A.; Dorman, D.; Brewster, A.; Bovey, F., Macromolecules, 1973. 6: p. 925.

35. Zambelli, A.; Locatelli, P.; Bajo, G.; Bovey, F., macromolecules, 1975. 8: p. 687.

36. Ferro, D.; Zambelli, A.; Provasoli, A.; Locatelli, P.; Rigamonti, E., Macromolecules, 1980. 13: p. 179.

37. Busico, V.; Cipullo, R.; Monaco, G.; Vacatello, M., Macromolecules, 1997. 30: p. 6251.

38. Grassi, A.; Zambelli, A.; Resconi, L.; Albizatti, E.; Mazzochi, R.,

Macromolecules, 1988. 21: p. 617.

39. Farina, M.; Di Silvestro, G.; Terragni, A., Macromol. Chem. Phys., 1995. 196: p. 353.

40. Janiak, C.; Schumann, H., Adv. Organomet. Chem., 1991. 33: p. 291.

41. Mason, M.; Smith, J.; Bott, S.; Barron, A., J. Am. Chem. Soc., 1993. 115: p. 4971.

42. Harlon, c.; Mason, M.; Barron. A., Organometallics, 1994. 13: p. 2957.

43. Yang, X.; Stern, C.; Marks, T., J. Am. Chem. Soc., 1991. 113: p. 3623.

44. Yang, X.; Stern, C.; Marks, T., J. Am. Chem. Soc., 1994. 116: p. 10015.

45. Bochmann, M.; Lancaster, S., Organometallics, 1993. 12: p. 633.

46. Chien, J.; Tsai, W.; Rausch, M., J. Am. Chem. Soc., 1991. 113: p. 8570.

47. Sugano, T.; Matsubara, K.; Fujita, T.; Takahashi, T., J. Mol. Catal., 1993. 82: p. 93.

48. Jordan, R., adv. Organomet. Chem., 1991. 32: p. 325.

49. Arlman, E.; Cossee, P., J. Catal., 1964. 33: p. 99.

50. Green, M., Pure Appl. Chem., 1972. 30: p. 373.

51. Brookhart, M.; Green, M., J. Organomet. Chem., 1983. 250: p. 395.

52. Ewen, J., J. Am. Chem. Soc., 1984. 106: p. 6355.

53. Bozak, R., Adv. Photochem, 1971. 8: p. 227.

54. Harrigan, R. Hammond, G. Gray, H., J. Organomet. Chem, 1974. 81: p. 79.

55. Wiesenfeldt, H.; Barsties, E.; Evertz, Z.; Brintzinger, H., J. Organomet. Chem.,

1989. 369: p. 359.

56. Wild, F.; Huttner, G.; Brintzinger, H., J. Organomet. Chem., 1982. 232: p. 233.

57. Schmidt, K.; Rief, U.; Diebold, J.; Brintzinger. H., Organometallics, 1997. 16: p. 1724.

58. Rheingold, A.; Whelan, J.; Bosnich, B., Organometallics, 1992. 11: p. 1869.

59. Collins, S.; Ramachandran, R.; Taylar, N., Organometallics, 1991. 10: p. 2349.

Chapter 3

Isomerization of the metallocene catalysts (MBI and EI)

Abstract

Solutions of 2 metallocene catalysts, dimethylsilyl bis(2-methyl-4,5-benzo-indenyl)zirconium dichloride (*rac*-Me_2Si(2-Me-4,5-benzoind)$_2$]$ZrCl_2$) (MBI), and ethylene bis(1-indeyl)zirconium dichloride (rac-Et$(Ind)_2ZrCl_2$) (EI) were prepared under nitrogen in NMR tubes using deuterated dichloromethane (CD_2Cl_2) as solvent. These solutions were exposed to UV light (UV lamp and daylight) for different periods of time. Then ^{1}H-NMR spectra of these samples were recorded.

Results showed that, for the MBI catalyst, when using the daylight as a source of UV, conversion of the *rac*-isomer into *meso*-isomer occurred over time. But no conversion occurred when using a UV lamp as light source. The rate of conversion for this catalyst is discussed in this chapter. It was also found that the catalyst decomposed at long exposure times (using either UV lamp or sunlight as light source). The conversion of *rac*-isomer into *meso*-isomer continued until it reached photostationary state, where the two isomers are in equilibrium in the solution mixture. The ratio between the two isomers at the photostationary state was about 1:1.17 (*meso*-isomer:*rac*-isomer), and it took about 300 minutes (exposure time) to reach this ratio.

On the other hand the IE catalyst did not show any conversion from one isomer to the other, upon exposure the catalyst solution to the UV source (either UV lamp or sunlight) even after long period of time. Decomposition of the EI catalyst took place as a result of exposure of the catalyst to UV light.

3.1 Introduction

During the synthesis of homogenous group 4 transition metal catalysts, different forms of the complex are formed in the reaction. The product is normally a mixture of *racemic* and *meso* forms of the metallocene. When these catalysts are used for propylene polymerization, the *racemic* form produces isotactic polymer, usually with high molecular weight, while the *meso* form produces atactic polymer, usually with low molecular weight. [1-3]

It is therefore not surprising that the *racemic* form is the most used as polymerization catalyst when isotactic polypropylene is required. So during the synthesis of the catalyst it is desirable to produce only the *racemic* form in the mixture, which has not been done so far, or to produce a mixture where the *racemic* form is predominant in order to reduce the cost by obviating the physical separation of the two isomers.

Many methods have been developed in order to minimize the formation of unwanted the *meso*-isomer during the synthesis of the complex, [4-8] especially during the reaction of the ligands with the appropriate metal halides.

Other methods have been developed in order to convert the *meso*-isomer to the *rac*-isomer after the synthesis of the catalyst. [9-12] One of the methods that used to promote the interconversion of the two isomers is the use of the photochemistry.

Although there has been a recent surge of interest in the photochemistry of inorganic and organometallic compounds and in metal containing ligands bound to atoms of the transition metals (which are able to polymerize α-olefins), there are several aspects that have received little attention. Harrigan *et al*. [13] studied the photochemistry of titanocene derivatives (Cp_2TiCl_2) and found that this complex dissociates to give cyclopentadienyl radicals. The mechanism of the photochemistry of C_2-symmetric zirconocene was investigated by Kaminsky [10] using the metallocene catalyst dimethylsilyl bis(indenyl)zirconium

dichloride ($SiMe_2(Ind)_2ZrCl_2$) and UV radiation. They concluded that the conversion takes place via a homolytic cleavage of the η^5-metal-cyclopentadienyl ring bond. It was also reported that the conversion of the two diastereomers from one to the other cannot be carried out to 100%, but reaches a photostationary state where upon it stops.

The investigation of the structure of the two isomers of two different C_2-symmetric metallocene catalysts by ^{1}H-NMR is the main aim of this chapter. The rate of the isomerization of these catalysts will be monitored as a function of the exposure time, using both sunlight and UV lamp as a source of UV radiation. The C_2-symmetric metallocene catalysts used are $Me_2Si(2\text{-}Me\text{-}4,5\text{-}benzoind)_2ZrCl_2$ (MBI) (1) and [*rac*-$Et(Ind)_2$]$ZrCl_2$ (EI) (2).

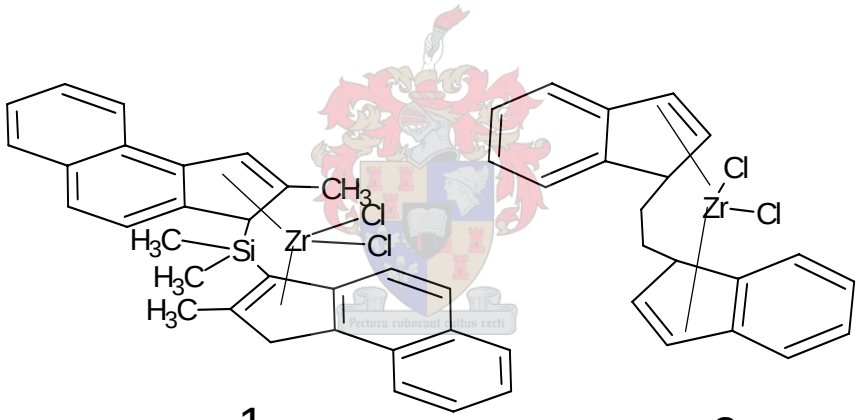

1 2

3.2 Experimental work

3.2.1 Isomerization of $[Me_2Si(2\text{-}Me\text{-}4,5\text{-}benzoind)_2]ZrCl_2$ and $[rac\text{-}Et(Ind)_2]ZrCl_2$ in CD_2Cl_2

The catalysts used were obtained from Boulder Scientific. All procedures were carried out in a nitrogen atmosphere. Typically a solution of the catalyst in CD_2Cl_2 was prepared in an NMR tube (3 mg catalyst was dissolved in 0.5 ml solvent) and the solution exposed to UV light (UV lamp or sunlight) for different times, varying from 0 to 1 500 minutes. The change in the catalyst structure was investigated by ^{1}H-NMR spectroscopy. At every exposure time spectra were recorded on a Varian VXR 600 NMR spectrometer.

Simultaneously, a similar solution of the same catalyst was prepared (for both types of catalysts) and kept in dark (at 4 ^{o}C in a fridge). ^{1}H-NMR spectra of these control solutions were recorded after 24 hours, 12 days, and 35 days. The spectra of the catalyst solution that was kept in the dark were used to investigate the effect of the storage time on the catalysts structure in terms of the symmetry of the catalyst, and the catalyst decomposition. The spectra of the catalyst solutions that were kept in dark were also used to compare the effect of the storage time with the effect of the light, on the catalyst solution, in terms of the catalyst activity.

3.2.2 High resolution ^{1}H NMR

^{1}H NMR spectra were collected using a standard pulse sequence on a 600 Varian ^{Unity}Inova NMR spectrometer equipped with an Oxford magnet (14.09 T) operating at 600 MHz for ^{1}H, using a 5mm inverse detection PFG probe.

3.2.3 Reaction scheme

By exposing the catalyst solution to the UV source (e.g. sunlight), the catalyst will be in high state of energy which in turn will cause in the homolytic cleavage of

the η^5-metal-cyclopentadienyl ring bond (Figure 3.1). The ligands of the catalyst will then start to rotate around its bridge. Later when the catalyst is in the lower energy state the η^5-metal-cyclopentadienyl ring bond will re-combine.

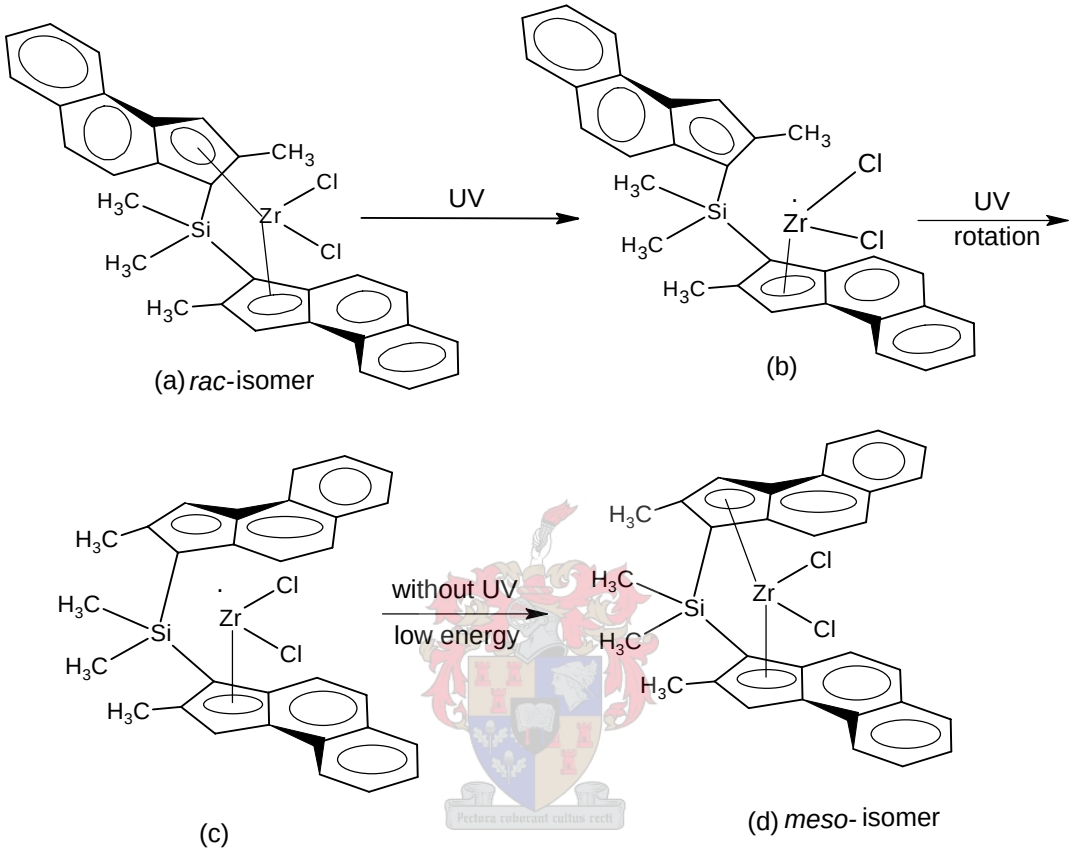

Figure 3.1 Proposed mechanism of the photoinduced *rac/meso* interconversion for C_2-symmetric metallocene catalysts.

3.3 Results and discussion

3.3.1 $Me_2Si(2\text{-}Me\text{-}4,5\text{-}benzoind)_2\ ZrCl_2$

Figure 3.2 shows the structures of the *rac*-isomer and the *meso*-isomer. From those two structures it can be seen that the methyl groups of the silyl bridge are two different environments.

In the *rac*-isomer the methyl groups are pointed away from the aromatic ring (indenyl ligand), so they are surrounded by a lower electron density, thus the protons of these groups will be less shielded. Consequently, in ^{1}H NMR spectra, the signals of these groups will appear down field from those of the *meso*-isomer.

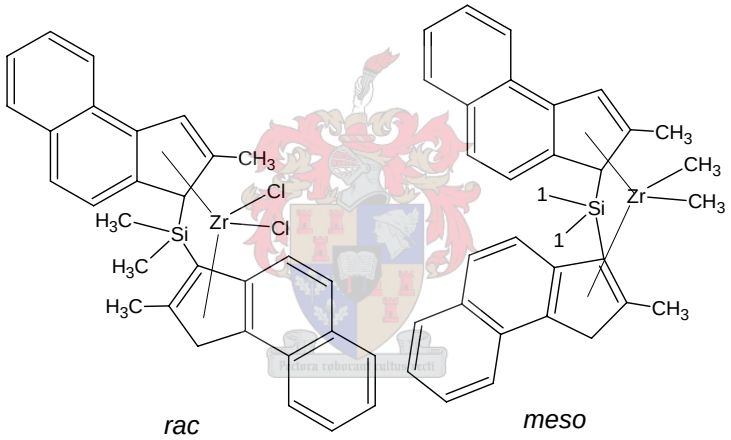

Figure 3.2 Proposed structures of *rac* form and *meso* form of MBI.

The methyl groups of the *meso*-isomer (Figure 3.2) are pointed inward with respect to the indenyl ligands, so they surrounded by a higher electron density. They are more shielded than the methyl groups of the *rac*-isomer, and consequently these groups will appear at higher field.

3.3.1.1 ^{1}H-NMR of the catalyst in CD_2Cl_2

After trying to dissolve the catalyst in different solvents, it was found that the best solubility was achieved by using CD_2Cl_2.

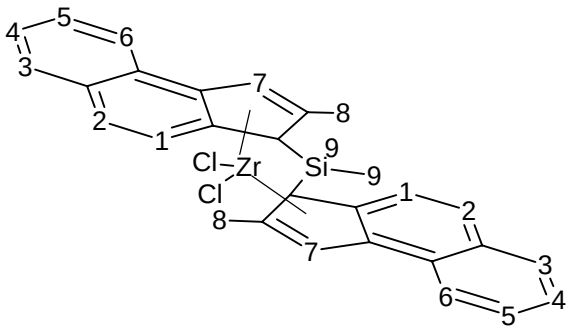

Figure 3.3 General structure of the MBI and numbering of carbons.

The ^{1}H-NMR spectrum a freshly prepared solution of [Me_2Si(2-Me-4,5-benzoind)$_2$]$ZrCl_2$ is shown in Figure 3.3. Table 3.4 summarizes the ^{1}H NMR data of the spectrum.

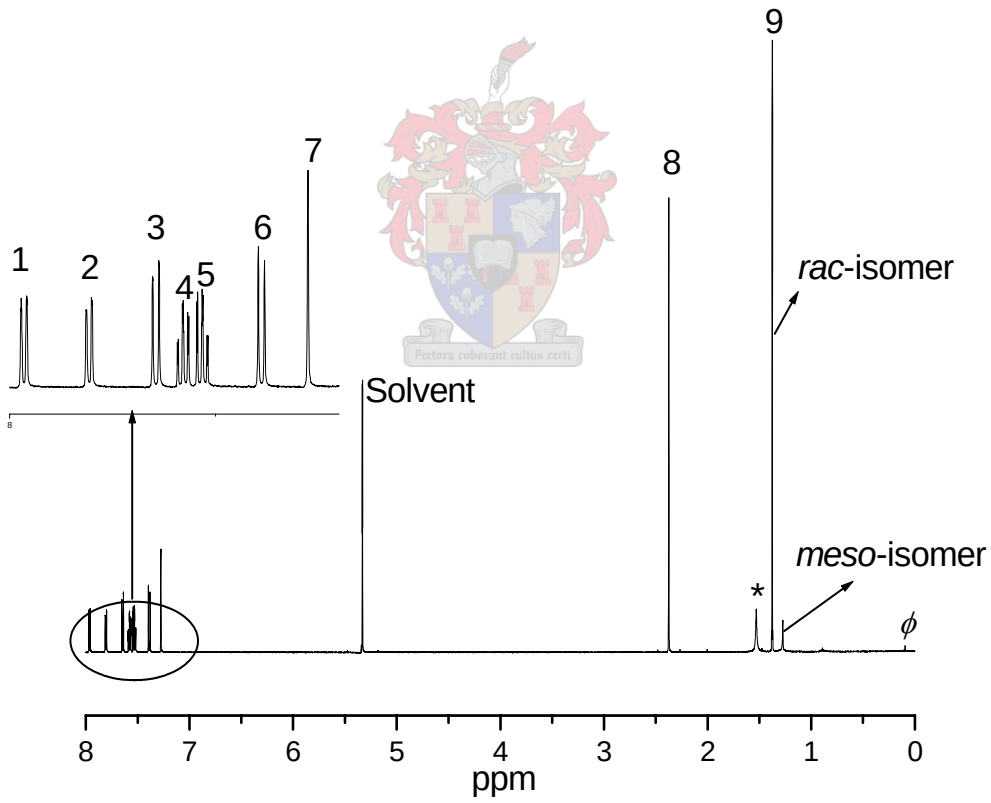

Figure 3.4 ^{1}H-NMR spectrum of the MBI catalyst in CD_2Cl_2, * signal at δ = 0.1 ppm is due to the decomposition of the catalyst, and signal at δ = 1.53 ppm is due to the presence of some moisture.

Table 3.1 ^{1}H NMR data for MBI catalyst

^{1}H NMR in CD_2Cl_2*	NMR shift (ppm)
H(1)	7.958
H(2)	7.801
H(3)	7.636
H(4)	7.567
H(5)	7.53
H(6)	7.38
H(7)	7.052
H(8)	2.301
H(9)	1.303

* see also Figure 3.4

In Figure 3.4, the signal at δ=1.3 ppm is due to the methyl groups attached to the silyl bridge in the *racemic* form of the metallocene catalyst. The signal at δ=1.25 ppm is due to the same groups when the catalyst is in the *meso* form. As expected the *meso* signal appears upfield. These two signals are important for determine the symmetry of the metallocene in solution. These two signals were used to determine the ratio of the two isomers in solution (*meso:rac* ratio).

Table 3.2 summarizes the ^{1}H NMR signals of the methyl groups that are

attached to the indenyl ligands and the methyl groups of the silyl bridge of the catalyst in both the *meso* form and the *rac* form.

For the substituted methyl groups of the indenyl ligand the difference in the signals between the *rac*-isomer and the *meso*-isomer is small, because the difference in the electron density for these methyl groups in the respective isomers is small (see Figure 3.2). As we can see from Table 3.2 and Figure 3.3 the ^{1}H NMR signals of the methyl groups of the ligands appear at 2.30 ppm, and 2.29 ppm for the *rac*-isomer and *meso*-isomer, respectively. But for the methyl groups of the silyl bridge the signals at 1.30 ppm, and 1.20 ppm for the *rac*-isomer and the *meso*-isomer, respectively. [14, 15]

The signal at δ=5.27 ppm, in Figure 3.4, is due to the solvent (dichloromethane) and the signal at 1.53 ppm (designated by * in Figure 3.4) is due to the presence of traces of water in the catalyst.

Table 3.2. Selected NMR data for *rac* and *meso* forms of MBI

^{1}H NMR in CD_2Cl_2	NMR shift (ppm)	
	rac form	*meso* form
H(9)	2.301	2.298
H(8)	1.373	1.251

The signals at δ=0.2 ppm and δ=0.5 ppm (designated by ϕ in Figure 3.4) could be due to the methyl groups of the silyl bridge and the methyl groups attached to the Indenyl ligands respectively, where the catalyst at a state of the homolytic cleavage of the η^5-metal cyclopentadienyl ring bond occurs (Figure 3.1(b)). This homolytic cleavage of the η^5-metal cyclopentadienyl ring bond to give a

Zirconium based radical appears to be obtainable for all wavelengths of the visible and near-UV range. [12, 13]

The reason for assuming that those two peaks (0.2 ppm and 0.5 ppm) could be due to state of the homolytic cleavage of the η^5-metal cyclopentadienyl ring bond, is that the catalyst activity increases if the catalyst placed in the dark before use instead of using it immediately after the exposure to UV.

This result could confirm the mechanism of the isomerization, in that it starts with the cleavage of the η^5 metal-cyclopentadienyl ring bond to give the intermediate component (See Figure 3.1.b, c), and this intermediate component is not active for the α-olefin polymerization. Some time is required for the fragments to re-combine. This occurs by allowing the energy level to drop by removing the light source. The re-combined catalyst species are active for α-olefin polymerization, and might be in the *meso* form or the *rac* form (depending on the UV source)..

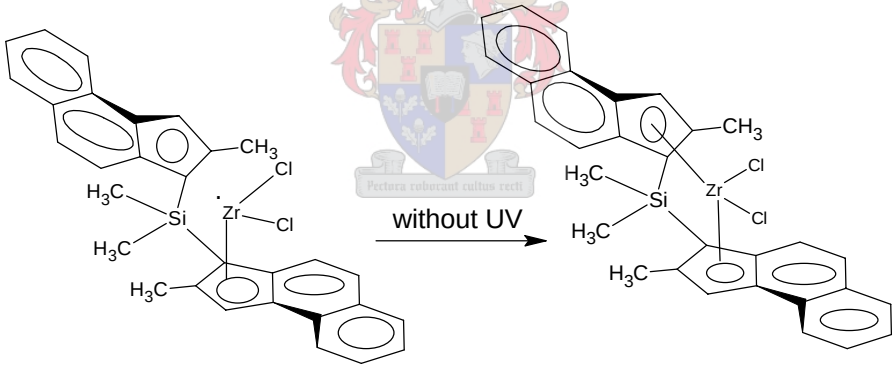

Figure 3.5 The last step of the mechanism of photoisomerization.

It seems that the rotation of the catalyst ligands around its bridge, which the second step of the mechanism of the isomerization, depends on the UV wavelength that used for the isomerization, because when sunlight was used as a source of the UV, interconversion from the *rac*-isomer to the *meso*-isomer was obtained. But when UV lamp was used (discussed later in this chapter) as a source of the UV no interconversion took place. The wide range of wavelengths

that the compounds are exposed to when placed in sunlight enhances the possibility of rotation of the ligands around the bridge, rather than making use of a monochromatic UV source (257 nm).

We found that the catalyst activity increases if the catalyst solution is placed in the dark instead of using it immediately after the UV. Yet, while the catalyst activity increased after allowing the catalyst solution time after removing the light source, the overall activity was still lower than that of the catalyst solution which was not exposed to the UV radiation at all. This indicates that some of the catalyst decomposes irreversibly during exposure to UV light.

It is therefore possible that the appearance of the two peaks (0.2 ppm and 0.5 ppm) might be due to the decomposition of the catalyst.

These results are in agreement with literature. [12] It has been reported that during the photo-isomerization of (*S,S*)-2,3-butylene-1,1'-bis(indenyl) zirconium dichloride in THF to *R,R, R,S*, isomers, that after a few hours of irradiation, extensive decomposition of the complex occurred.

On the other hand, Kaminsky *et al*. [10] investigated the isomerization of *rac*-$[Me_2Si(2\text{-}Me\text{-}4,6\ {}^{i}Pr_2Ind)_2]ZrCl_2$ in benzene-d_6 and toluene-d_8 and no decomposition of the catalyst were observed whether using UV lamp or daylight as a source of UV.

3.3.1.2 Sunlight as UV light source

Figure 3.6 shows the ^{1}H NMR spectra of MBI catalyst after exposure in sunlight for time of 0, 10, 30, and 210 minutes.

Comparing the spectrum in Figure 3.6 (a) with spectra (b), (c), and (d) for the same sample after exposure to daylight for 10, 30, and 210 minutes respectively, it can be seen that a new peak appeared at δ=1.25 ppm, which is due to the *meso*-isomer as shown in Figure 3.3. This peak increases in intensity as the

exposure time increased.

In Figure 3.6 we also observe a decrease in the intensity of the peak at δ=1.37 ppm, which due to the *rac*-isomer. The ratio of *meso*:*rac* in the catalyst solution at 0 minutes exposure time is 1:15.7 (6% *meso*-isomer), and at 10 minutes is 1:5.25 (16% *meso*-isomer). The presence of two peaks for the methyl group in the spectrum of the fresh catalyst Figure 3.6 (a) indicates that the catalyst is not completely in the C_2 symmetric form.

The broadening of the signal at 1.53 ppm, which has been assigned to the presence of a trace of water, with increasing exposure time (Figure 3.6) indicates that there is an ion exchange in the solution caused by the UV. Even though the height of this peak (1.53 ppm) decreases with increasing the time, its integral remained constant.

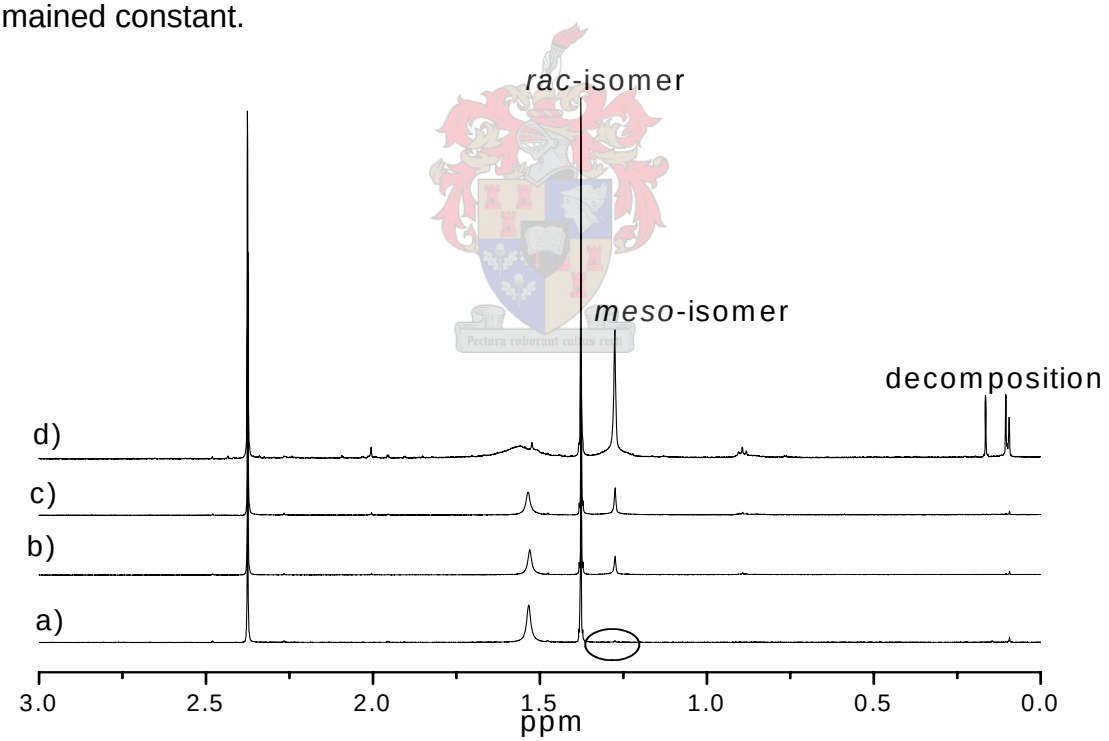

Figure 3.6 ^{1}H-NMR spectra (0 to 3 ppm) of MBI: for 0 min (a), 10 min (b), 30 min (c), 210 min (d) exposure time respectively.

Figure 3.7 shows that there is no further increase in the peaks of the *meso* form of the catalyst with increasing exposure time after 330 minutes. On the other

hand, the peaks which are due to the decomposition of the catalyst continue to increase, which in turns affects the catalytic activity (Chapter 4).

It seems that both isomers decompose at the same rate because the *rac:meso* ratio remain constant after exposure of 330 minutes. It is possible that only one of the isomers has the ability to decompose, which could be followed by the conversion of the other isomer to decomposable isomer in order to keep the relative intensity of the two isomers constant (photostationary state).

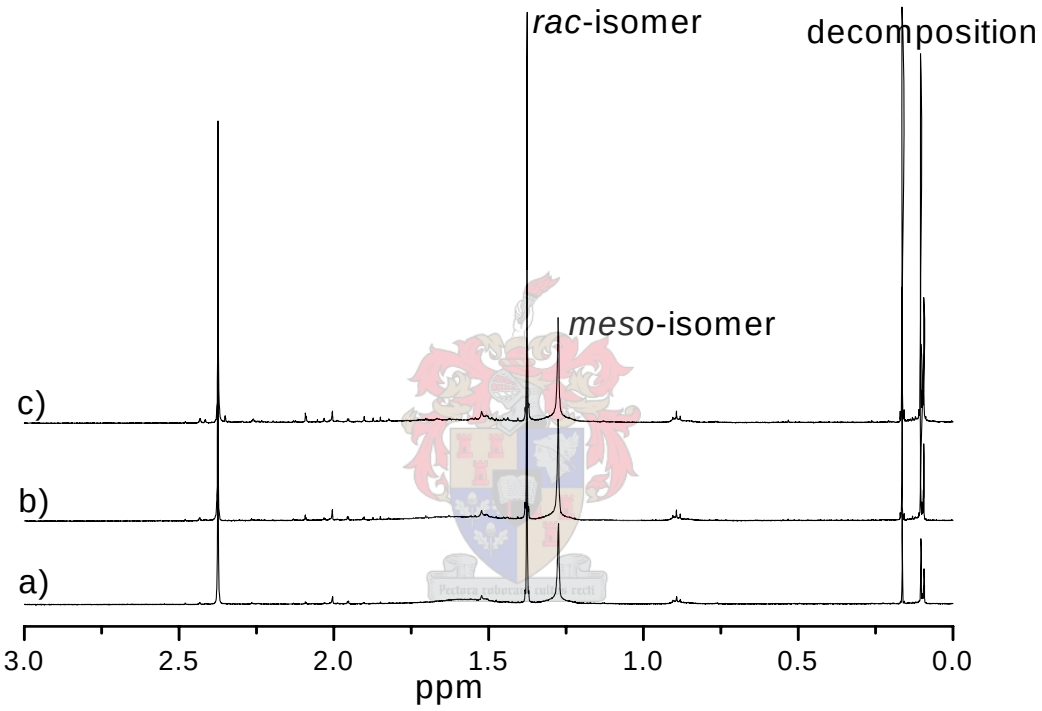

Figure 3.7 ^{1}H-NMR spectra (0 to 3 ppm)of MBI: a, b, c, for 330 min, 600 min, and 1 500 min exposure time respectively.

Table 3.3 shows the integrals of the signals of the *rac* peak and the *meso* peak of the catalyst from the ^{1}H-NMR spectra of the catalyst at different exposure times using sunlight. The table shows that the interconversion rate of the catalyst from the *rac* form to the *meso* form is high for the first 30 minutes of the exposure then the rate decreases (increase in *meso*%).

After 330 minutes, and up to 1 500 minutes, the conversion stops, and the only peaks that continues to increase are the decomposition peaks. This

indicates that an equilibrium between the two isomers is reached. From Table 3.3 it can be seen that the percentage of the *meso* form before the exposure is 6%, then it increases until it reaches 45% after 330 minutes irradiation.

Kaminsky *et al.*[10] also reported that the conversion of the two isomers from one to the other cannot be carried out up to 100%. A photostationary state is reached that is different for each metallocene. For example they found that for *rac*-$[Me_2Si(2\text{-}Me\text{-}4,6\ ^{i}Pr_2Ind)_2]ZrCl_2$ the photostationary state was reached after 4 weeks of irradiation (using sunlight) and the ration of *meso:rac* is 1:0.11. In this research using the same source of UV (sunlight) the photostationary state was reached after 330 minutes of irradiation and the *meso* to *rac* ratio was 1:1.17. The difference in the time that required reaching the equilibrium between the *rac* and *meso* isomers and the difference in the final *meso:rac* ratio is due to the difference in the substituents that are attached to the indenyl ligand (catalyst structure).

Table 3.3 *Meso*% and *rac*% vs. exposure time as obtained by NMR

Exposure time	0min	10min	30min	90min	210min	330min	10hr	25hr
race %	94	84	79	68	60	55	54.5	54.5
meso %	6	16	21	32	40	45	45.5	45.5

Kaminsky *et al.* [10], also reported isomerization of the MBI metallocene catalyst using daylight, and a final *meso:rac* ratio (reached after 4 weeks) of 1:0.35, which is different from the value we obtained (1:1.17). This is in all probability due to difference in experimental setup and solvent used.

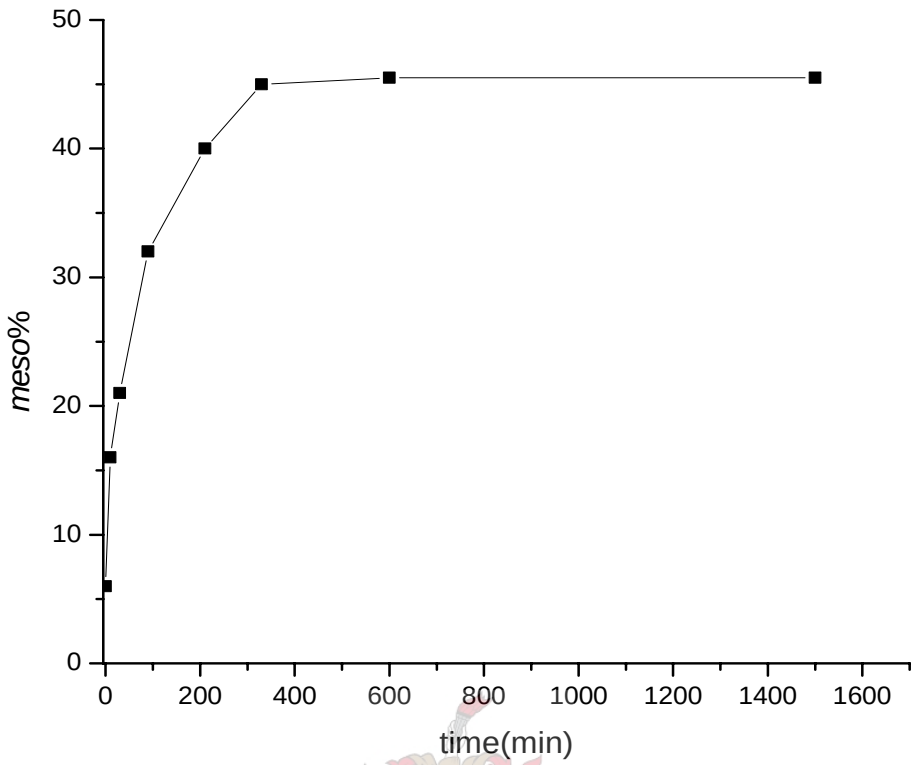

Figure 3.8 The rate of interconversion for MBI in CD_2Cl_2 using sunlight.

Figure 3.8 is a graphic representation of the data presented in Table 3.3.

Brintzinger *et al*. [6, 11] studied the isomerization of the *rac*-isomer of the complex $Me_2Si(1\text{-}Cp\text{-}2\text{-}Me\text{-}4\text{-}t\text{Bu})_2ZrCl_2$, in benzene-$d_6$, and toluene-$d_8$ using a 125 W UV lamp. The rate of the isomerization, and the *rac/meso* ratio at the photostationary state were different for each solvent. In benzene-d_6 after 105 minutes the ratio changed from 100:0 to 56:44 and stopped at this ratio, but in toluene-d_8 the final ratio was 42:58 after 1 905 minutes.

Results presented so far was obtained using CD_2Cl_2 as a solvent and attempt was made to study the effect of other solvents such as benzene-d_6 or toluene-d_8 in order to monitor the affect of different solvent in the isomerization rate. The ^{1}H-NMR spectra of these catalyst solutions that were obtained using these solvents were very poor due to low catalyst solubility, and the attempt was discontinued.

In conclusion we found that a conversion from the *rac*-isomer to the *meso*-isomer

could be observed, and the conversion rate using our experimental conditions was obtained.

3.3.1.3 UV lamp as light source

Isomerization of the MBI catalyst was investigated using a UV lamp (15 W, 257 nm) as source of the UV. Figure 3.9 shows ^{1}H NMR spectra of a MBI metallocene catalyst at different exposure times (0 min, 10 min, 90 min, and 480 min). From the spectra it can be seen that peak at 1.251 ppm does not increase with the exposure time. This means no visible isomerization occurred and the *meso*% in the catalyst solution remained almost constant.

The spectra in Figure 3.9 show the 1.53 ppm, which has been assigned to the presence of water, getting broader and decreasing in the height, as irradiation time increases, but again the peak area remained constant.

The peaks from 0.1 ppm to 0.25 ppm are due to the catalyst decomposition.

These results are confirmed by polymer structures that are produced by solutions of this catalyst exposed to different UV sources, and will be discussed in Chapter 4.

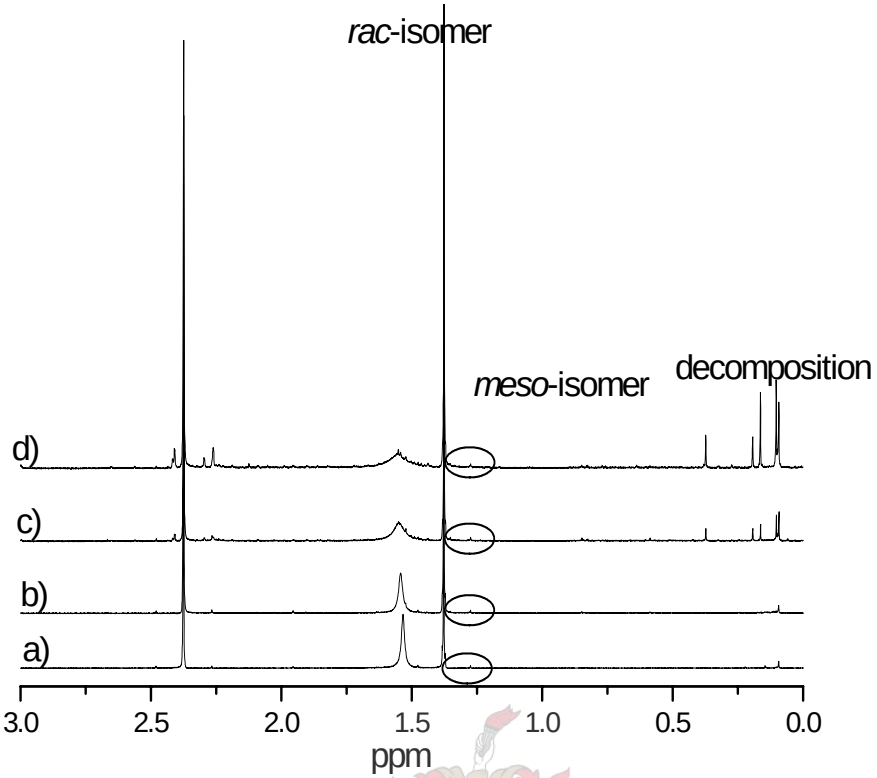

Figure 3. 9 ^{1}H-NMR spectra (0 to 3ppm) of MBI: for 0 min (a), 10 min (b), 90 min (c), and 480 min (d) exposure time respectively.

These results demonstrate that the wavelength and intensity of the UV source play an important role for the second step of the isomerization which is the rotation of the ligands around the bridge. It appears that the rate of the rotation depends on the UV wavelength. On the other hand the scission of the of the η^5-metal-cyclopentadienyl ring bond is promoted by wide range of wavelengths.

Another possible conclusion that can be drawn from our results is that the final *meso:rac* ratio (*meso:rac* at the photostationary state) depends on the wavelength. It is possible that one isomer is more stable than the other at a specific wavelength, and by changing the wavelength the relative stability of the two isomers change. From this we can conclude that for the MBI catalyst the *meso*-isomer is less stable than the *rac*-isomer at low wavelength (e.g. 257 nm), and its stability increases as the wavelength increases. So if the last explanation is true then by just changing the UV wavelength we can control the *meso:rac*

ratio in the mixture.

3.3.1.4 Effect of the catalyst solution storage time on the catalyst structure (without UV)

In order to investigate the effect of the storage time (Without UV) of the catalyst solution on the catalyst's structure in terms of the symmetry of the catalyst, and the catalyst decomposition, ^{1}H-NMR spectra of the catalyst solution was recorded after 2 days, 12 days and 35 days. The spectra are shown in Figure 3.10.

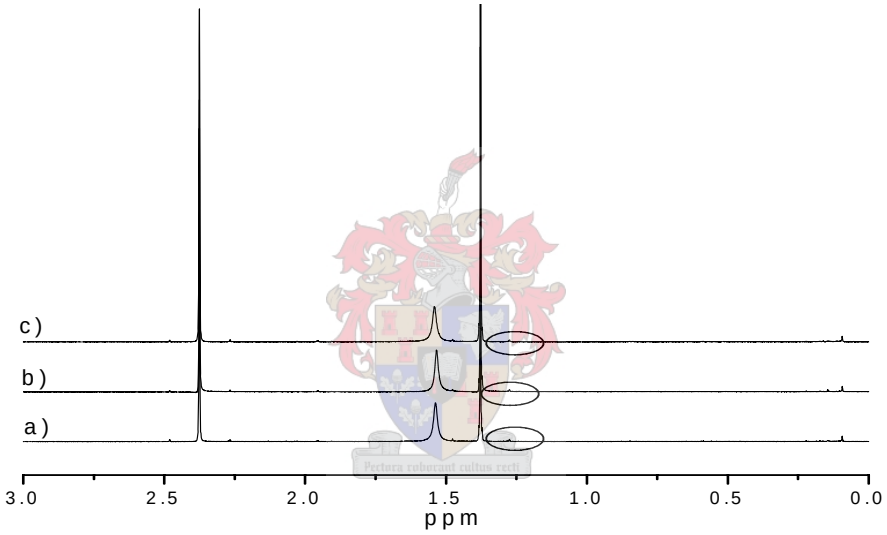

Figure 3.10 ^{1}H-NMR spectra (0ppm to 3 ppm) of MBI: for 2 days (a), 12 days (b), and 35 days (c) respectively without UV.

From the Figure 3.10 it can be seen that the structure of the catalyst remained unchanged, thus all the changes that demonstrated previously was promoted by the exposure to irradiation.

3.3.2 [*rac*-Et (Ind) $_2$] $ZrCl_2$) (EI)

The EI metallocene catalyst was selected to investigate the effect of the presence of different substituents of the ligands on the isomerization rate and on

the final photostationary state of the *meso* and *rac* isomers of the C_2-symmetric compound.

3.3.2.1 ^{1}H-NMR of the fresh catalyst

The catalyst was dissolved in CD_2Cl_2 as other deuterated solvents proved to be unsuitable.

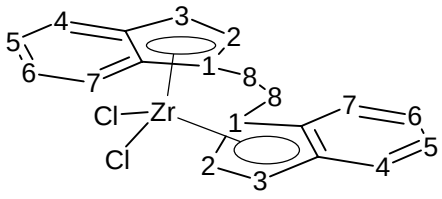

Figure 3.11 Proposed structure of the EI catalyst.

The ^{1}H-NMR spectrum of a freshly prepared solution [*rac*-Et $(Ind)_2$] $ZrCl_2$) (EI) is shown in Figure 3.12. Table 3.4 summarizes the ^{1}H NMR data of the spectrum. The signals at δ=2.9 ppm and at δ=3.37 ppm are due to the ethyl groups of the bridge in the *racemic* form of the metallocene catalyst. The signals δ=3.75 ppm is due to the protons of the carbon of the indenyl ligands which is connected with the bridge.

The peak at 6.25 ppm (designated by * in the spectrum) is a singlet peak so it is not due to the α or β-protons of the five-membered ring which has to be doublets, thus this peak has been assigned to an as yet undefined impurity.

Table 3.4 ^{1}H NMR data for EI catalyst

^{1}H NMR in CD_2Cl_2 (Figure 3.12)*	NMR shift (ppm)
H(1)	3.75
H(2)	6.25
H(3)	6.56
H(4)	7.7
H(5)	7.31
H(6)	7.2
H(7)	7.45
H(8)	2.9, 3.37

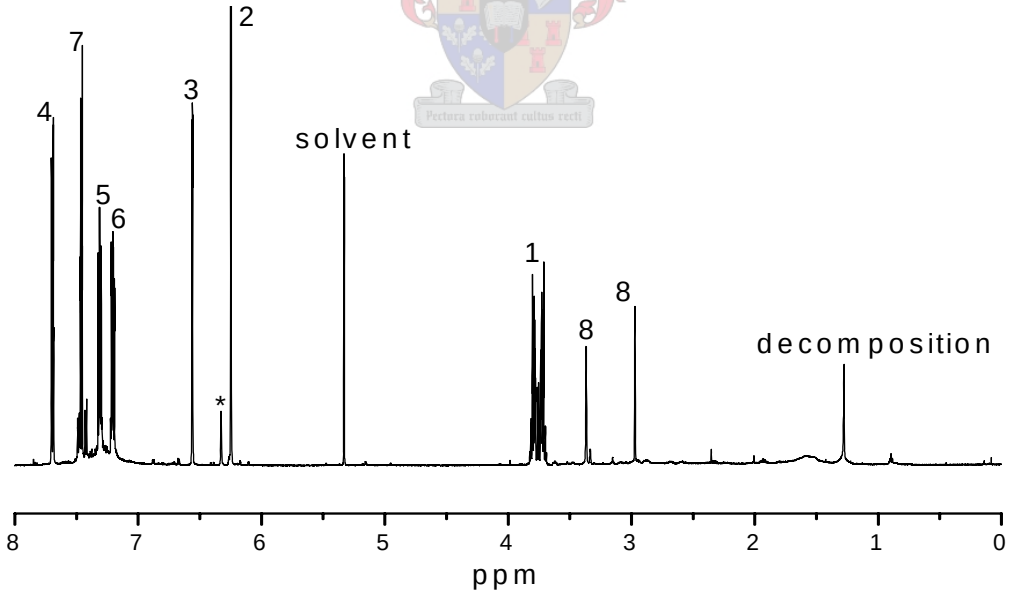

Figure 3. 12 ^{1}H-NMR spectrum of the EI metallocene catalyst in CD_2Cl_2

Figure 3.13 shows the proposed structure of the *rac*-isomer and the

meso-isomer of the catalyst, from the two structures it can be seen that the α and β-protons of the five-membered ring would experience a difference in electron density.

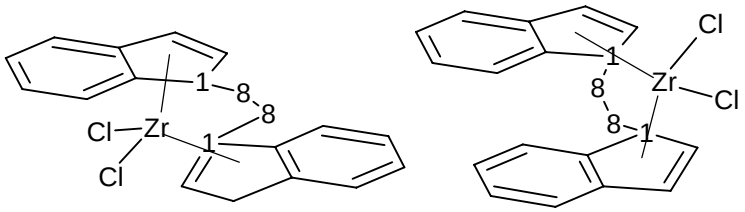

Figure 3. 13 Proposed structure of *rac* form and *meso* form of EI

The two isomers of the EI catalyst have been characterized [9, 16] by the presence of to two pairs of doublets, one with narrow and one with a widely separated pair of α, β-protons of the five-membered ring. Signals at 6.49 ppm and 6.91 ppm and at 6.07 ppm and 6.71 ppm for the *meso*-isomer and *rac*-isomer, respectively. All these four doublets peaks are present in the five-membered ring signals region and one from each isomer was used to measure the stereo-selectivity of the catalyst solution.

The signals at δ=1.23 ppm, δ=2.0 ppm, and δ=0.7 ppm are due to the protons of the bridge and other protons in the decomposed form of the catalyst. Figure 3.14 shows the increase in the decomposition rate caused by the irradiation of the catalyst.

The decomposition rate that is obtained from the ^{1}H NMR (using CD_2Cl_2 as a solvent) of the catalyst caused by the UV is very high compared with the decrease of the catalyst activity caused by UV (using toluene as a solvent). It seems that the rate of the photodecomposition promoted by conducted the isomerization process in halogenated solvents. [17]

For the EI catalyst the result obtained using UV lamp is similar with that obtained by using sunlight, thus there is no wavelength dependency on the isomerization

process for this catalyst in contrast with what happened with the MBI catalyst.

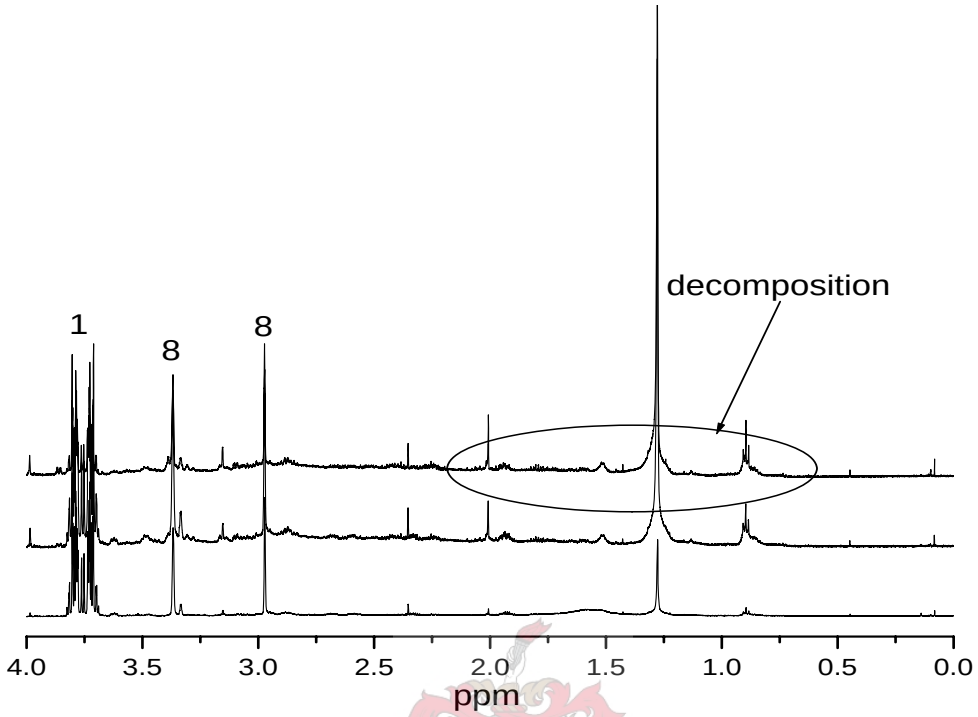

Figure 3. 14 ^{1}H-NMR spectra (0 ppm to 4.0 ppm) of EI catalyst for 0 min (bottom), 90 min (middle), and 210 min (top) exposure time, respectively.

Figure 3.15 shows the ^{1}H-NMR spectra of catalyst after 0 minutes, 90 minutes, and 210 minutes exposure time. From spectra in the Figure 3.15 it can be seen that there is no change in the intensity (and in integrals) of the *meso*-isomer and the *rac*-isomer peaks. The *meso*:*rac* ratio in the catalyst solution at 0 minutes exposure time is 1:19 (5% *meso*-isomer), and after exposing the catalyst to both sources of light this ratio remained almost constant.

These results indicate that no isomerization of the catalyst occurred in the solution (using CD_2Cl_2 as a solvent) when irradiated. The isomerization of this catalyst was also examined using a toluene as a solvent and polymerizations were preformed and the results indicated (Chapter 4) that this catalyst doesn't have the ability to inter-convert.

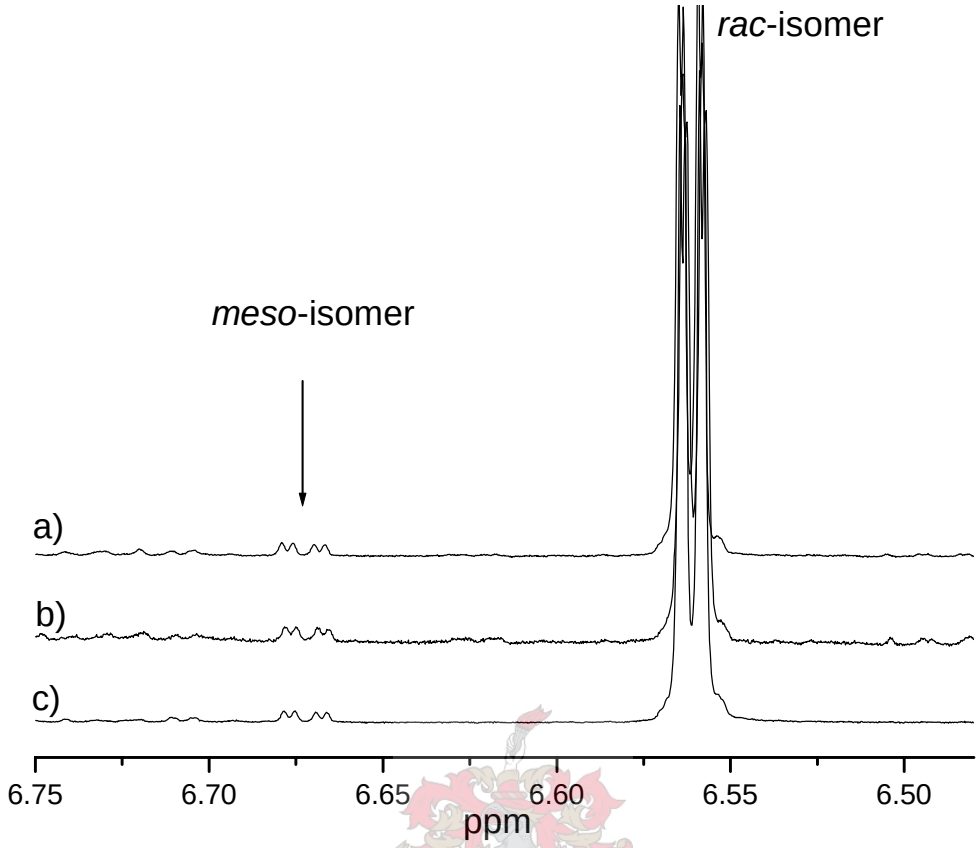

Figure 3.15 ^{1}H-NMR spectra (6.5 ppm to 6.75 ppm) of EI catalyst: a, b, c, for 0 min, 90 min, and 210 min exposure time respectively.

The substituent on the indenyl ligands seems therefore to have an effect on the ability to isomerize.

Even though the presence of the methyl and benzene substituents in the indenyl ligands of the MBI catalyst increases the steric size of the ligands and this gives the catalyst more stability in the *racemic* form than the *meso* one, the *meso:rac* ratio in the photostationary state is higher in the MBI catalyst than that in the EI catalyst. These results are in agreement with that presented by Kaminsky [10] that state that for highly substituted ligands the photostationary state is in favour of the *meso* form and with decreasing substitution the rate of the isomerization decreases, while lack of substitution on the ligands lead to isomerization of the formed catalyst upon irradiation.

3.4 References

1. Moore, E.P (Jr), Polypropylene Handbook. 1996: Munich Vienna New York. 50-53.

2. Kaminsky, W.; Kulper, K.; Brintzinger, H, Angew. Chem. Int. Ed, 1985. 24: p. 507.

3. Collins, S.; Guthier, W.; Holden, D.; Kuntz, B.; Taylar, N.; Ward, D, Organometallics, 1991. 10: p. 2061.

4. Diamond, G.; Rodewald, S.; Jordan, R .Organometallics, 1995. 14: p. 5.

5. Giardello, M.; Conticello, V.; Brand, L.; Sabat, M.; Rheingold, A.; Marks, T, J. Am. Chem. Soc, 1994. 116: p. 10212.

6. Wiesenfeldt, H.; Reinmuth, A.; Barsties, E.; Evertz, Z.; Brintzinger, H, J. Organomet. Chem, 1989. 369: p. 359.

7. Haar, C.; Stern, C.; Marks, T, Organometallics, 1996. 15: p. 1765.

8. Diamond, G.; Jordan, R.; Petersen, J, Organometallics, 1996. 15: p. 4030.

9. Wild, F.; Zsolnai, L.; Huttner, G.; Brintzinger, H, J. Organomet. Chem, 1982. 232: p. 233.

10. Kaminsky, W.; Chauwienold, A.; Freidanck, F, J. Mol. Catal. A: Chem, 1996. 112: p. 37.

11. Schmidt, K.; Reinmuth, A.; Rief, U.; Diebold, J.; Brintzinger. H, Organometallics, 1997. 16: p. 1724.

12. Rheingold, A.; Robinson, N.; Whelan,J.; Bosnich, B, Organometallics, 1992. 11: p. 1869.

13. Harrigan, R.; Hammond, G.; Gray, H, J. Organomet. Chem, 1974. 81: p. 79.

14. Spaleck, W.; Kuber, F.; Winter, A.; Rohrmann, J.; Bachmann, B.; Antberg, M.; Dolle, V.; Paulus, E, Organometallics, 1994. 13: p. 954.

15. Stehling, U.; Diebold, J.; Kirsten, R.; Roll, W.; Jungling, S.; Mulhaupt, R.; Langhauser, F, Organometallics, 1994. 13: p. 964.

16. Wild, F.; Wasiucionek, M.; Huttner, G.; Brintzinger, H, J. Organomet. Chem, 1985. 288: p. 63.

17. Collins, S.; Hong, Y.; Ramachandran, R.; Taylar, N, Organometallics, 1991. 10: p. 2349.

18. Grassman, R.; Doyle, R.; Buchwald, S, Organometallics, 1991. 10: p. 1501.

Chapter 4

Isomerised metallocenes in propylene polymerization

Abstract

Solutions of the metallocene catalysts dimethylsilyl bis(2-methyl-4,5-benzo-indenyl)zirconium dichloride [Me_2Si(2-Me-4,5-benzoind)$_2$]$ZrCl_2$ (MBI), and ethylene bis(1-indeyl)zirconium dichloride (*rac*-Et(Ind)$_2ZrCl_2$) (EI) were prepared, using toluene as solvent, and exposed to UV light (UV lamp and daylight) for different periods of time. These solutions were then used to polymerize propylene. The effect of isomerization of these catalysts in toluene on propylene polymerization is described in this chapter. The formed polymer was characterized using differential scanning calorimetry (DSC), high temperature gel permeation chromatography (HTGPC), Nuclear magnetic resonance spectroscopy (NMR), crystallization analysis fractionation (CRYSTAF), and temperature rising elution fractionation (TREF).

The effect of irradiation of the catalyst solutions on polymer properties is also compared to the results of the isomerization experiments conducted in CD_2Cl_2. In addition the effect of activating the catalysts with MAO before exposure to light is also discussed.

4.1 Introduction

Polypropylene is characterized by regio- and stereo-irregularities, distribution of defects and variable molecular masses. [1] Depending on the catalysts used and the polymerization conditions, different types of microstructural defects may be present.

The microstructure of metallocene-catalysed polypropylene strongly influences the crystal structure, the polymorphic behaviour and, as a consequence, the physical and mechanical properties of isotactic polypropylene (i-PP). So any change in the catalyst structure used could result in significant changes in the polymer properties. [2, 3]

As was shown in the previous chapter, UV irradiation of C_2-symmetric catalysts in solution in deuterated, halogenated solvents resulted in varying changes in catalyst structure, depending on the structure of the ligands in the metallocene catalyst. These results were in line with published results, [4-6] although some significant differences were observed. It has been mentioned that the activities of the polymerization of α–olefins is higher for the *meso* isomer of the C_2 symmetric catalysts than for the *rac* isomer [7].

On the other hand Ewen [4] polymerised propylene using a mixture containing 56% *rac*-Et[Ind]$_2$TiCl$_2$ and 44% *meso*- Et[Ind]$_2$TiCl$_2$. The resultant polymer was a mixture of isotactic polypropylene (63%) and atactic polypropylene (37%). He concluded that the *rac*- and *meso*-Ti isomers have similar propagation and termination rate constants and that the *rac*-isomer is slightly more active.

In order to test whether or not the irradiation of catalyst solutions to be used for polymerization would have the same type of effect as that which occurred in a controlled experiment in a halogenated solvent (Chapter 3), two isospecific *ansa*-zirconocene catalysts for propylene polymerization [Me$_2$Si(2-Me-4,5-benzoind)$_2$]ZrCl$_2$ (MBI) and [*rac*-Et(Ind)$_2$]ZrCl$_2$ (EI) were used in this investigation as catalysts for polymerization of propylene. Reactions were done both before

and after irradiation of a catalyst solution.

In the previous chapter we showed that the MBI catalyst, when using sunlight as a source of UV, converted readily from the *rac*-isomer to *meso*-isomer over time. No conversion took place when using a UV lamp as light source. The EI catalyst did not show any conversion from one isomer to the other, upon exposure the catalyst solution to the UV source.

The aim of the work reported in this chapter was to investigate the change in the polypropylene microstructure as an effect of exposing the catalyst solution light for different periods of time and relate this to the change in the catalyst structure in deuterated, halogenated solvents as studied by ^{1}H NMR.

4.2 Experimental Work

4.2.1 Materials

The catalysts, dimethylsilyl bis(2-methyl-4,5-benzo-indenyl)zirconium dichloride (*rac*-[Me_2Si(2-Me-4,5-benzoind)$_2$]$ZrCl_2$) (MBI), and ethylene bis(1-indeyl)zirconium dichloride (*rac*-Et(Ind)$_2Zr Cl_2$) (EI) were obtained from Boulder Scientific and were used as received. Toluene was dried by refluxing over sodium/benzophenone, and distilled under a nitrogen atmosphere and then stored over molecular sieves. Methylaluminoxane (MAO) was purchased from Sigma Aldrich and used as received (10% solution in toluene). Propylene was obtained from Sigma Aldrich (99.95%) and was used without any further purification.

4.2.2 Isomerization procedure

All catalyst manipulations were carried out in a glove box in a nitrogen atmosphere. Catalyst solutions were prepared in Schlenk tubes under a nitrogen atmosphere. Each Schlenk tube contained about 1 ml (2.2 µmol/ml) of catalyst solution. These solutions were exposed to UV light (UV lamp or sunlight) for times varying from 0 to 600 minutes. These solutions were then used for

propylene polymerization.

4.2.3 Polymerization procedure

MAO (8 ml of a 10% solution in toluene) was added to each of the catalyst solutions that had been prepared (see 4.2.2), and then these solutions were allowed to react for 15 minutes. The polymerization reactions were carried out in a stainless steel autoclave with two inlets and a pressure gauge. After drying the reactor, glass liner and stirrer bar overnight in an oven (120 °C), the reactor was cooled under a nitrogen stream and assembled while flushing with nitrogen. Typically, the reactor was then evacuated and flushed with nitrogen. After the reactor temperature had reached 25 ^{o}C it was charged with 30 ml toluene under nitrogen, followed by the addition of the catalyst/MAO solution. Propylene was introduced to the reactor at room temperature, and an attempt was made to maintain the amount of the propylene at around 10 g for all the polymerization reactions. The reactor was stirred at room temperature for 2 hours. In order to end the polymerization reaction the reactor was first vented and then MeOH/HCl (10% HCl) was added to the products to react with the active species. An excess of MeOH was added to precipitate the formed polymer. The resulting polymer was isolated by filtration, washed first with MeOH and then with acetone and finally dried in a vacuum oven at 65 ^{o}C for 10 hours.

4.2.4 The extraction of uncrystallizable polymer

The polymer was dissolved in xylene at 130°C, and maintained at that temperature for 2 hours (reflux). Irganox 1010 (2,6-di-tert-butyl-4-methylphenol) was added to prevent the thermal degradation of the polymer. After ensuring that all the polymer had dissolved, the solution was allowed to cool room temperature, and the precipitated polymer filtered off. The filtered (insoluble) fraction was dried in a vacuum oven at 65^{o}C for 10 hours. The soluble fraction was isolated by removal of the xylene under reduced pressure.

4.2.5 Characterization and analytical techniques

4.2.5.1 High-temperature GPC

Number average molecular weight ($\overline{Mn}$), weight average molecular weight ($\overline{Mw}$) and polydispersity (MWD) of the polymers were determined by using high-temperature gel permeation chromatography (HT-GPC). Since the two isomers (*rac*-isomer and *meso*-isomer) of the catalyst are characterized by producing polymer with high and low molecular weight, respectively, the information that obtained by HT-GPC is significant. A PL-GPC 220 high temperature chromatograph was used at flow rate of 1 ml/min at 160 ^{o}C with a differential refractive index detector. Columns packed with a polystyrene/divinylbenzene copolymer (PL gel MIXED-B [9003-53-6]) from Polymer Laboratories were used. The length and diameter of these columns were 300 mm and 7.5 mm, respectively. Particle size was 10 µm. The concentration of the samples was 1.5 mg/ml. 1,2,4-Trichlorobenzene (TCB), stabilized with 0.0125% 2,6-di-tert-butyl-4-methylphenol was used as solvent. The calibration was done with monodisperse polystyrene standards (EasiCal from Polymer Laboratories).

4.2.5.2 Differential scanning calorimetry (DSC)

Crystallization temperature (T_c), melting temperature (T_m), and degree of crystallinty (ΔHc) were determined by differential scanning calorimetry (DSC). DSC analyses on the different polymers were carried out with a TA Instruments Q100 DSC system. The DSC was calibrated by measuring the melting temperature of indium metal according to a standard procedure. All measurements were conducted under nitrogen flow, and at a purge gas flow rate of 50 ml/min. The samples (1.0 to 3.0 mg) were heated in aluminium pans from 25 to 220 ^{o}C at 10 ^{o}C/min, held isothermally at 220 ^{o}C for 5 minutes, cooled to -30 ^{o}C at a rate of 10 ^{o}C/min and the crystallization curve was recorded. At -30 ^{o}C, the temperature was kept constant for 5 minutes after which the melting curve was recorded between -30 and 190 ^{o}C at a heating rate of 10 ^{o}C/min.

4.2.5.3 High temperature ^{13}C NMR

^{13}C NMR spectroscopy was used to investigate the microstructure of the different polymers. ^{13}C NMR spectra of the samples were recorded at 120 ^{o}C on a Varian VXR 300 MHz spectrometer with a long delay time of 0.82 seconds and a pulse angle of 45^{o}. The samples were dissolved in a 9:1 mixture of 1,2,4-trichlorobenzene:C_6D_6 by using the C_6D_6 at δ=128.02 ppm as internal secondary reference. Before recording the spectra the samples were placed in an oil bath for 2 hours to allow the polymer solution to be homogenize throughout the NMR tube.

4.2.5.4 Crystallization analysis fractionation (CRYSTAF)

Crystallization analysis fractionation was carried out using a CRYSTAF Model 200 manufactured by Polymer Char S.A. (Valencia, Spain). The crystallization from solution was carried out in 5 stainless steel reactors of 60 ml capacity each where dissolution and filtration take place automatically. 20 mg of polymer was placed in each reactor. TCB was used as a solvent. The temperature was decreased from 100 ^{o}C to 30 ^{o}C at a cooling rate of 0.25 ^{o}C/min. The polymer concentration in solution was determined by an infrared detector, using a wavelength of about 3.5 μM.

4.2.6 Temperature rising elution fractionation (TREF)

Two grams of a polypropylene sample was added to 200 ml of xylene, followed by the addition of 3 mg of an anti-oxidant. The solution was heated to 135 ^{o}C to ensure dissolution. The solution was then placed in a 1L round bottom flask and placed into a preheated oil bath with attached temperature profiler. The temperature of the oil bath was stabilized at 135 ^{o}C for 3 hours and at the same time pre-heated washed sea sand was added to the solution until the solvent was completely covered. The amount of sand used depended on the initial amount of polymer and xylene used. The cooling profile for the oil bath was set at 1 ^{o}C/h.

The cooled sand/solvent mixture was transferred to a steel elution column,

then this column is transferred to an oven and eluted with xylene. Fractions were eluted at predetermined temperatures.

4.3 Results and discussion

During the polymerization experiments, it was initially found that the amount of propylene could not be kept constant. In order to make sure these results are not misleading in terms of the effect of the monomer concentration on the microstructure of the formed polypropylene and the catalyst activity (which will be used as a tool to track the isomerization process), a section of this work was dedicated to monitor the influence of monomer concentration. Table 4.1 and Figure 4.1 summarize the results obtained in this section.

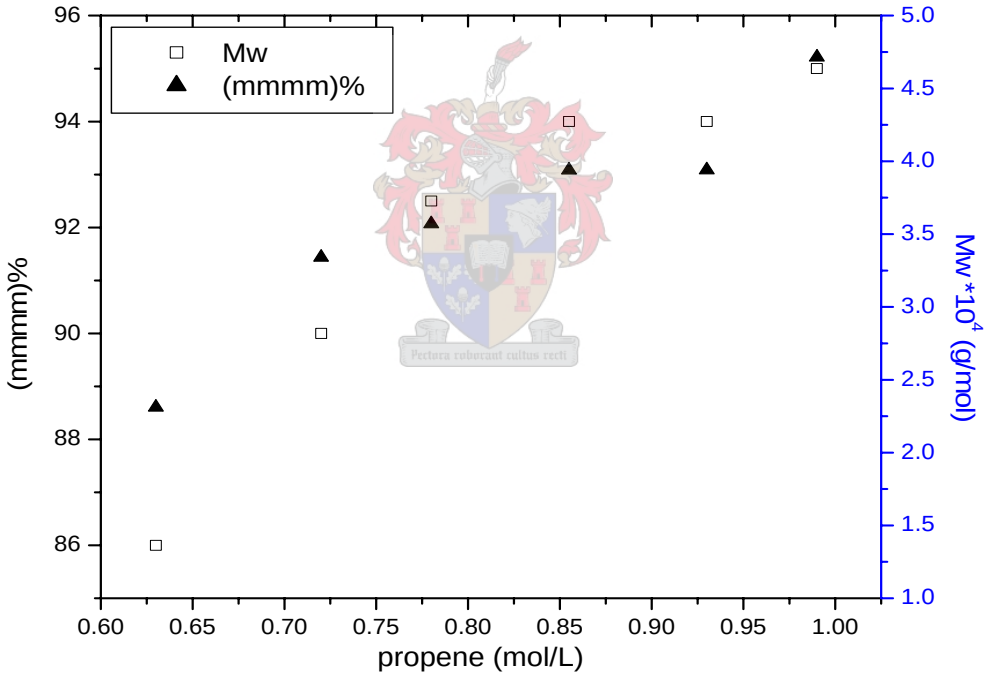

Figure 4.1 Effect of monomer concentration on of polymer molecular weight and tacticity. (EI/MAO)

Table 4.1 The effect of the monomer concentration on the polymer microstructure [A, B] (EI catalyst)

Run	Al/Zr	monomer(g)	Activity [C]	*mmmm*%	$\overline{Mw}$	MWD	Tm ^{o}C
1	6000/1	9	2350	83	23108	2.2	130
2	6000/1	10	3540	90	33400	2.187	136
3	6000/1	11	3580	92	35700	2.14	137
4	6000/1	12	3745	94	39390	2.5	138
5	6000/1	13	3750	94	39400	2.2	138
6	6000/1	14	3686	95	47150	2.3	138

[A] Polymerization time = 120 min; [metallocene] = 2.2 µmol /30 ml of toluene.

[B] All polymerizations were carried out at room temperature.

[C] kg of PP/mol of Zr:h.

From Table 4.1 and Figure 4.1 it can be seen that the monomer concentration has a significant effect on the polymer microstructure on the one hand and on the catalyst activity on the other. Increasing the monomer concentration lead to an increase in the tacticity and the $\overline{Mw}$ of the polymer produced, and, consequently the melting and crystallization temperatures will be influenced. The catalyst activity also increased as a result of increasing the monomer concentration.

Several C_2-symmetric *ansa*-zirconocenes have been studied to determine the extent of the influence of monomer concentration on catalyst activity, i-PP stereoregularity, and molecular weight. [5-8] All of these studies are in agreement with results obtained in this study.

It has been demonstrated in the previous chapter that extensive decomposition of both catalysts occurred at long exposure times of irradiation. So it must taken into account that the effective catalyst concentration is affected by with the exposure time. Polymerization runs were preformed to monitor the effect of the change in the catalyst concentration on the polymer microstructure. Runs 1 and 7 (Table

4.2) were preformed where the catalyst concentration of run 1 was double the catalyst concentration of run 7, with all the other polymerization parameters were kept constant. Results show that reducing the catalyst concentration increases the catalyst activity, stereoselectivity and polymer molecular weight.

This result is in agreement a report in the literature [9] that the activity and stereoselectivity of the catalyst is much higher at low [Zr]. Polymer molecular weight is reported to be decrease with low catalyst concentration, which is in contrast with results shown in Table 4.2.

The results for both catalysts (MBI and EI) are the same regarding the effect of monomer and catalyst concentration.

4.3.1 ^{13}C NMR spectra of the polymer

^{13}C NMR spectroscopy is a powerful tool for the determination of the microstructure of polypropylene and the polymerization mechanism. [1, 10, 11] The chemical shift of the methyl groups in polypropylene is highly sensitive to the relative stereochemistry of neighbouring monomer units, that is, each methyl C has a different chemical shift depending on the configuration of the adjacent methynes, up to five on each side (a sequence length of 11 consecutive monomer units). The degree of isotacticity can be given as the pentad, triad, or diad content (% *mmmm*, % *mm*, % *m*, respectively). The most used level of sensitivity when it comes to quoting results of stereo- sequences is the pentad level, where the methyl resonance is split in nine or ten major peaks, assigned as *mmmm, mmrr, rrrr, mmmr, mmrm, mrrr, rmmr, rmrr, mrrm, rmrm* (Chart 4.1).

^{13}C NMR spectroscopy also gives detailed information on secondary insertions (2,1 and 3,1 insertions). These are important as they cause serious disruptions of chain symmetry and consequently crystallinity and the related properties.

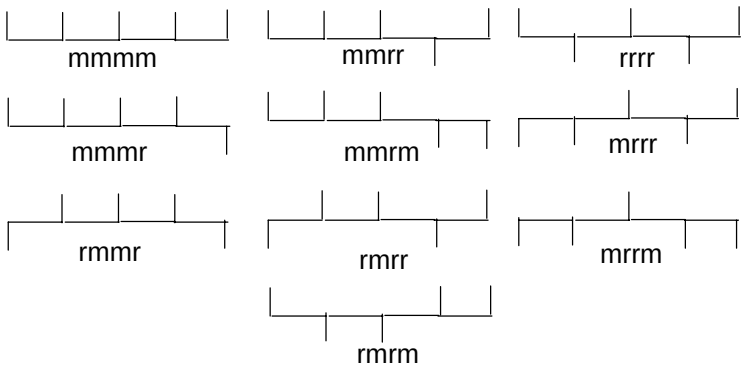

Chart 4.1 Pentad stereosequences in polypropylene.

NMR spectroscopy also gives information about the different types of end groups that can be formed in the polymer. This provides more insight into the mechanism of polymerization and termination or chain transfer.

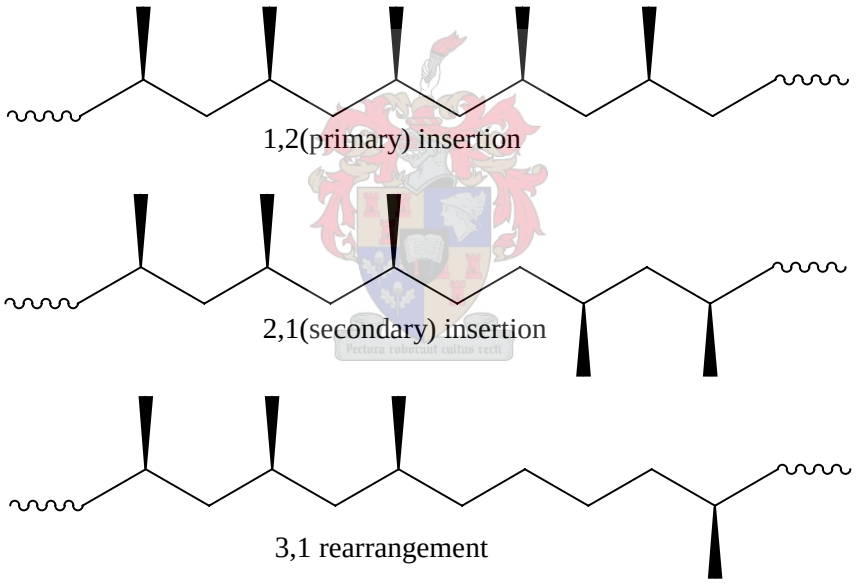

Chart 4.2 The different regioirregular sequences that can be formed in polypropylene.

4.3.2 Propylene polymerization using (*rac*-Et(Ind)$_2$ZrCl$_2$) (EI)

The results of the polymerization of the propylene with the (rac-Et(Ind)$_2$ZrCl$_2$) (EI) are summarized in Table 4.2. All polymerization runs in Table 4.2 were preformed at the same conditions in terms of: polymerization temperature (25^{o}C),

catalyst/co-catalyst ratio (1/6 000), catalyst concentration (2.2 µmol), the amount of the solvent (30 ml), and time of polymerizations (2 hours). An attempt was made in order to keep the propylene monomer per run in the range of 10-12 g.

Figure 4.2 shows a typical ^{13}C NMR spectrum i-PP prepared with EI catalyst. The three main peaks, of equal intensity, correspond to the three different C atoms in the repeating unit (methyl, methine and methylene) at 21.6 ppm, 28.36 ppm, and 46.3 ppm. [12, 13]

Table 4.2 Polymerization of propylene over EI: MAO [A, B]

Run [C]	Al/Zr	monomer (g)	Activity [D]	*mmmm*%	$\overline{Mw}$	MWD	T_m (^oC)
1	6000/1	9	2350	86	23100	2.20	130
2	6000/1	11	3540	91	39390	2.19	137
3	6000/1	11	3080	92	33400	2.14	137
4	6000/1	14	2745	94	14770	2.50	138
5	6000/1	12	1950	93	39400	2.20	138
6	6000/1	11	1410	95	41050	2.30	137
7[F]	6000/1	10	3060	94	45820	2.25	138

[A] Polymerization time = 120 min; [metallocene] = 2.2 µmol /30 ml of toluene.

[B] All polymerizations were carried out at room temperature.

[C] Difference between the runs is the exposure time of the catalyst solution: 1, 2, 3, 4, 5, 6 for 0, 30, 60, 120, 300, 600 minutes, respectively.

[D] kg of PP/mol of Zr:h.

[F] Run 7 has half the catalyst concentration of run 1.

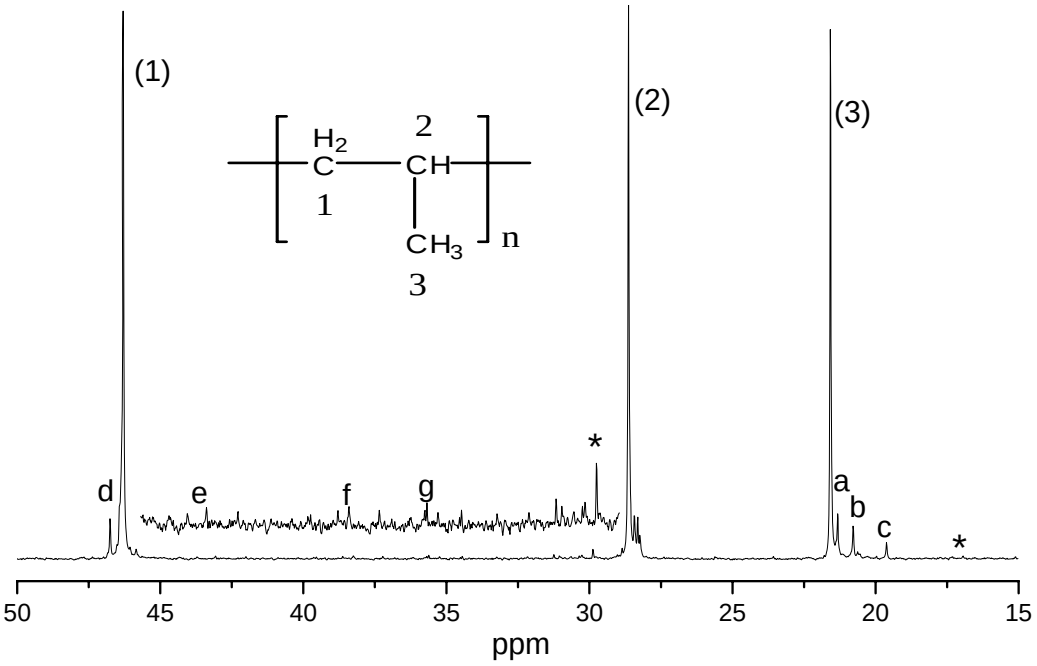

Figure 4.2 ^{13}C NMR spectrum of i-PP prepared with EI catalyst (run 1).

Usually, the methyl region is chosen for measuring the tacticity of the samples by measuring the relative intensity of the sharp peak at 21.6 ppm (methyl peak) [1, 14] to the other small peaks next to it (designated by a, b, c in the figure). These small peaks represent the stereoerrors normally associated with the site control mechanism of polymerization and represent a sensitivity of measurement at the pentad level. Peaks designated by * in Figure 4.2 are due to the regio-irregular monomeric units (2,1 and 3,1 insertions). The peaks designated by d, e, f, g in Figure 4.2 are due to the different types of end groups.

4.3.2.1 Peak assignments

Figure 4.3 shows the ^{13}C NMR spectrum of the methyl region of i-PP prepared with the EI catalyst. The spectrum (Figure 4.3) shows the different types of stereosequences that can be formed in a single chain of the polymer. Four different peaks can be seen in Figure 4.3 which are due to the stereosequences (see also Chart 4.1): *mmmm* (21.55 ppm), *mmmr* (21.3 ppm), *mrrm* (20.7 ppm), and *mrrm* (19.6 ppm).

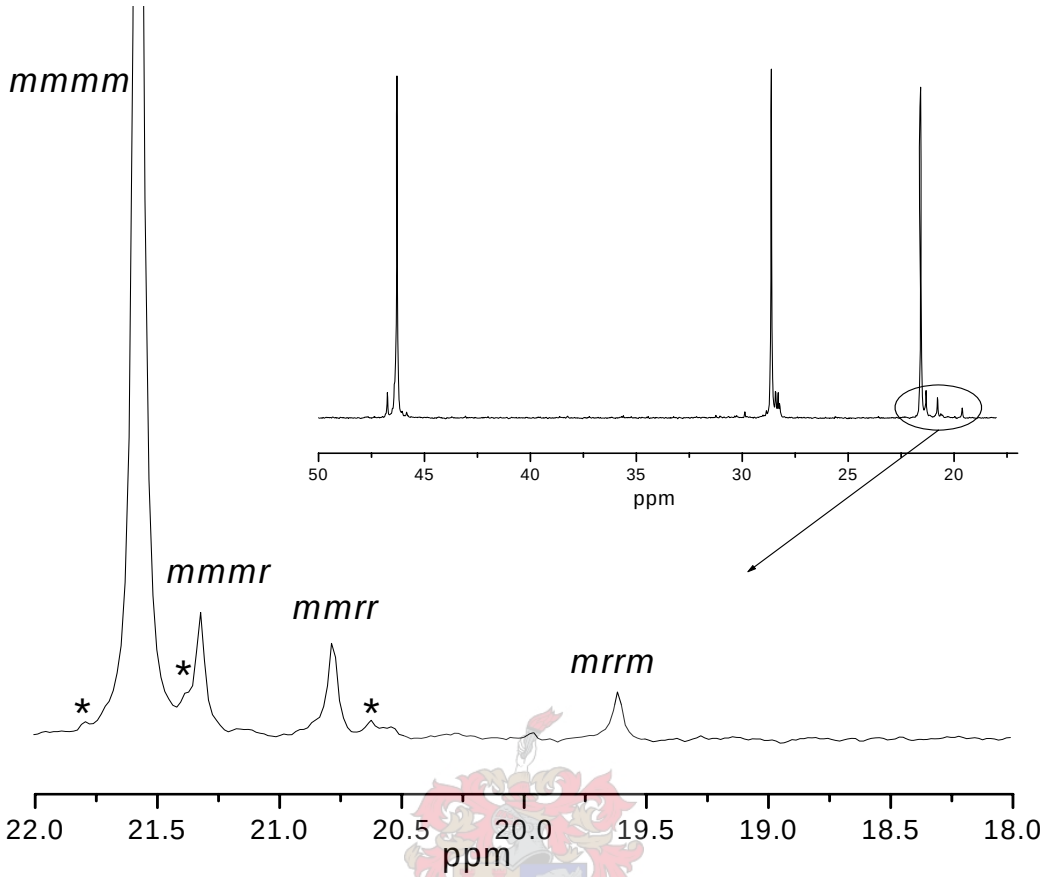

Figure 4.3 The methyl region of ^{13}C NMR spectrum of run 1.

For the peaks designated by * in Figure 4.3, it has been shown [15, 16] to be due to the ^{13}C satellites of the *mmmm* and *mmrr* resonances.

Many predictive methods have been proposed [17-19] for predicting the effect of the configuration on the chemical shifts of i-PP in ^{13}C NMR. Table 4.3 shows experimental ^{13}C NMR chemical shift values for the methyl pentads of PP produced using EI, compared with calculated ones at the same temperature that was calculated using a method proposed by Busico *et al.* [20]

Table 4.3 Experimental ^{13}C NMR chemical shift values for the methyl pentads of PP produced using EI, compared with calculated ones at the same temperature.

Pentad	δ (exp.)	$\Delta\delta$ (calc.)[25]	δ (calc.)
mmmm	21.58	0	21.58
Mmmr	21.32	-0.276	21.304
Mmrr	20.783	-0.728	20.852
Mrrm	19.615	-1.94	19.64

The percentage tacticity of all the samples was calculated by measuring the integral of *mmmm* relative to the integral of all the peaks in the methyl region, up to 19.62 ppm.

Spectra a), b), and c) in Figure 4.4 are ^{13}C NMR spectra of three different polymers that were prepared using EI catalyst solutions exposed to UV light for 0, 90, and 300 minutes, respectively. From Table 4.2 and Figure 4.4 it can be seen that run 1 has the lowest tacticity and for low exposure time (up to 15 min) no changes in the polymer microstructure were observed, and as the exposure exceeded 30 min an increase in the polymer tacticity were observed (see Figure 4.4).

This increase in the polymer tacticity confirms that no *meso*-isomer of the EI catalyst was formed (since it produces polymer with low tacticity) during the exposure of the catalyst solution to the UV source. It is been demonstrated in the previous chapter and in literature [21] that at long exposure times of irradiation, extensive decomposition of both catalysts occurred.

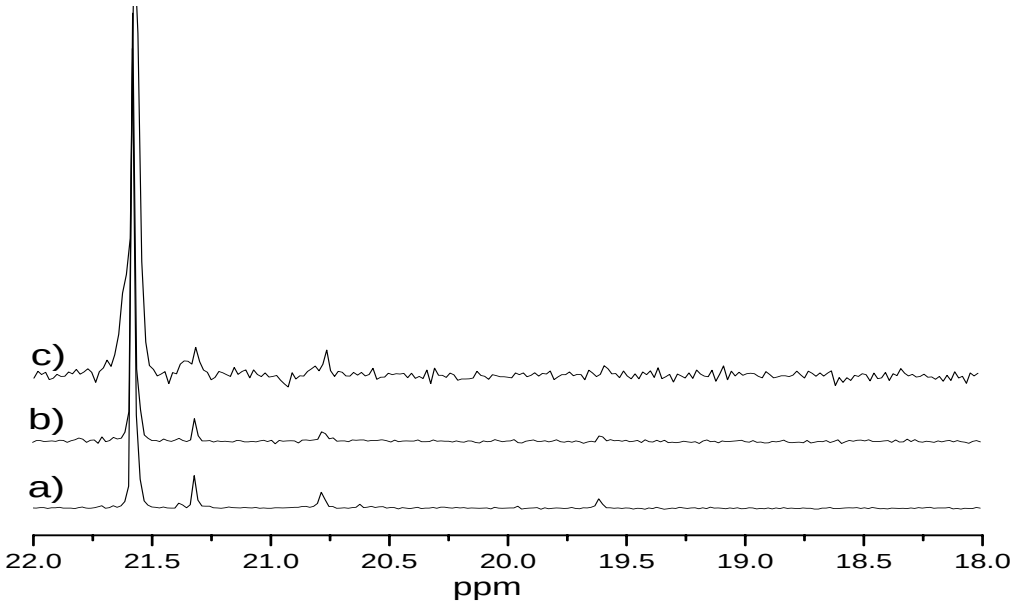

Figure 4.4 ^{13}C NMR spectra of PP prepared with EI catalyst with different exposure time to the catalyst: a, b, c, for 0 min, 90 min, and 300 min exposure time respectively.

It can be concluded that the effect of exposing solution of EI catalyst has the same effect as reducing the catalyst concentration, which leads to enhanced stereoselectivity. Catalyst activity appears to be decreasing with increased irradiation, which seems contrary to the results obtained earlier in this chapter, which seems to indicate that as decomposition takes place (effective reduction of concentration), we should see an increase in activity. The reason is of course that the activity is calculated on the original catalyst concentration.

This can be clarified by comparing the decomposition rate of the catalyst obtained from the ^{1}H NMR spectra of the catalyst and the decrease in the catalyst activity. Figure 4.5 demonstrates the decomposition rate of the EI catalyst obtained from ^{1}H NMR with the change in the catalyst activity with exposure time.

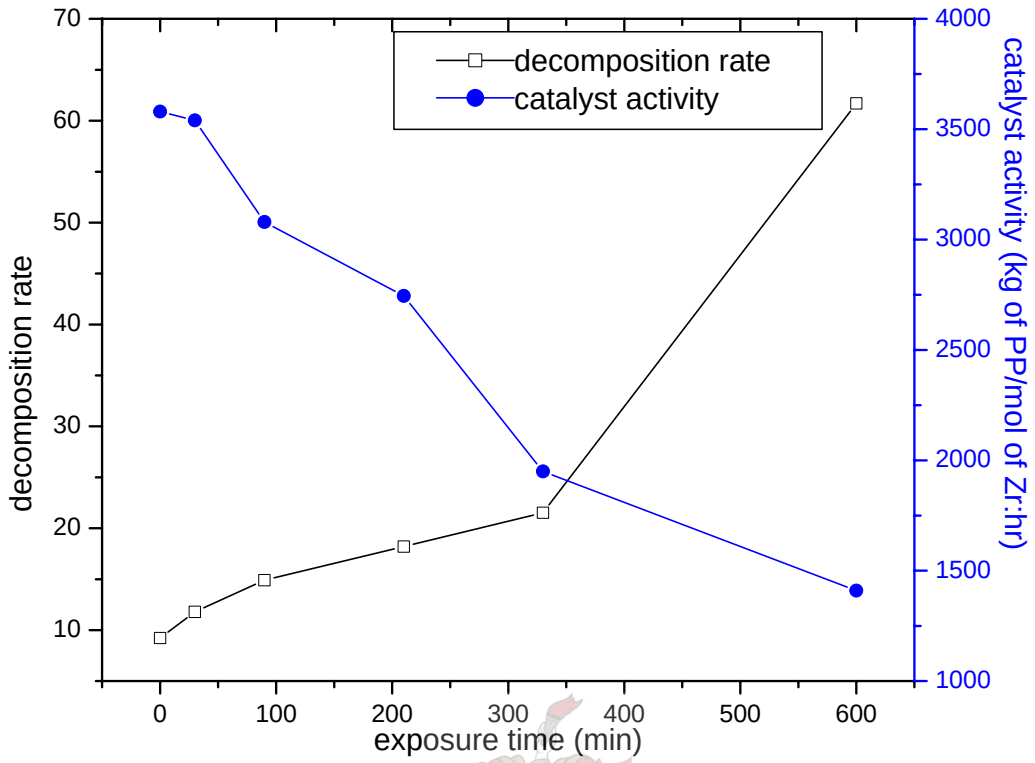

Figure 4.5 Decomposition rate of the EI catalyst obtained from ^{1}H NMR vs. the change in the catalyst activity with exposure time.

From Figure 4.5 it can be seen that as the exposure time increases the decomposition of the catalyst progresses accompanied with a reduction in the catalyst activity. After 300 minutes of exposure, the catalyst decomposition increases noticeably, but the activity does not decrease at the same rate. Since the isomerization studies were performed in halogenated solvents, it seems that the photodecomposition rate is promoted by these solvents. [22]

It must be mentioned that the results presented so far were obtained using sunlight as a UV source. When a UV lamp was used, similar results were obtained in terms of the change of the polymer microstructure. However, there were slight changes in the catalyst activity, which can be attributed to different decomposition rate caused by different UV sources.

Results also showed that the activity of the EI catalyst increases if the catalyst placed in dark after its exposure instead of using it immediately. The activity

increases by about 21% from about 1 400 to about 1 750 kg of PP/mol of Zr.h. The increase in the activity was also observed in the MBI catalyst. The increase of the activity caused by placing the catalyst in the dark is due to the recombination of the η^5-metal cyclopentadienyl ring bond, being the second step in the isomerization process.

4.3.2.2 Extraction of the atactic polymer

All the samples that were prepared with EI catalyst have stereoerrors corresponding to *mmmr, mmrr, mrrm* (see ^{13}C NMR spectra). These have always been considered to be the fingerprints of site control in stereochemical polymerization reaction typical for *ansa*-C_2-symmetric metallocene catalysts. [4, 23]

In order to ensure that these stereoerrors are not due to the presence of a small percentage of impurities of the *meso* form of the catalyst in the catalyst solution and polymers prepared with EI catalyst are free from the presence of a soluble fraction, different samples were extracted with xylene and the structure of the polymers studied before and after the extraction. Two samples were used for the extraction: run 1 which has low tacticity where the catalyst was not exposed to the UV sources and run 4 where the catalyst was exposed for 120 min in sunlight.

Figure 4.6 shows the ^{13}C NMR spectra of run 1 (a) before and (b) after extraction of the room temperature soluble fraction. The tacticity of the sample is about 86%, both before and after the extraction.

It has been stated in the previous chapter that the fresh catalyst has about 5% of *meso* form impurity and, since no soluble fraction was obtained, this amount seems to be inactive species.

Figure 4.7 shows ^{13}C NMR spectra of PP prepared by EI catalyst in run 4 (2hr exposure) before (a) and after (b) extraction. The tacticity percentage of the polymer before extraction was around 94% and this value did not change after

extraction, indicating that no soluble fraction has been produced.

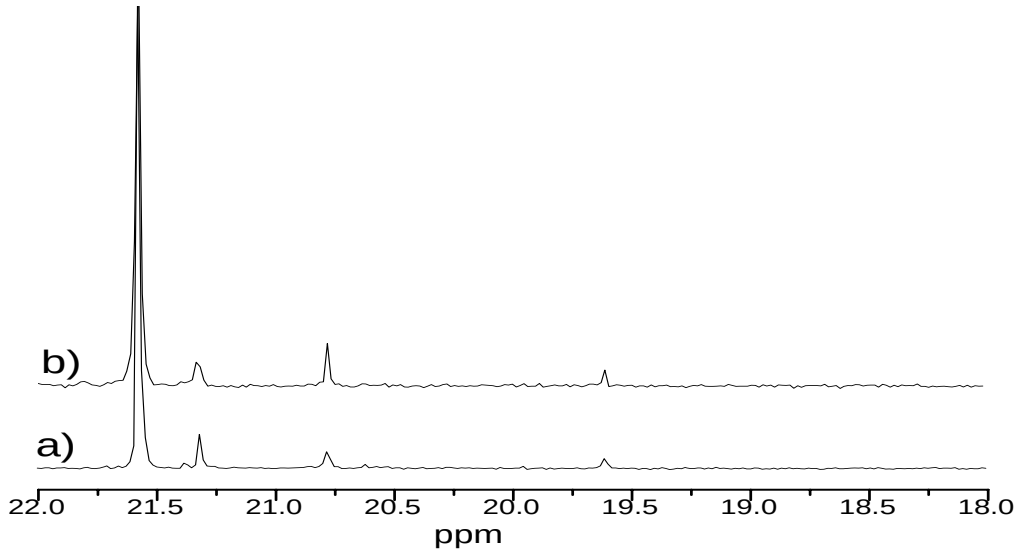

Figure4.6 ^{13}C NMR spectra of PP prepared by EI catalyst run 1: a) before extraction; b) after extraction.

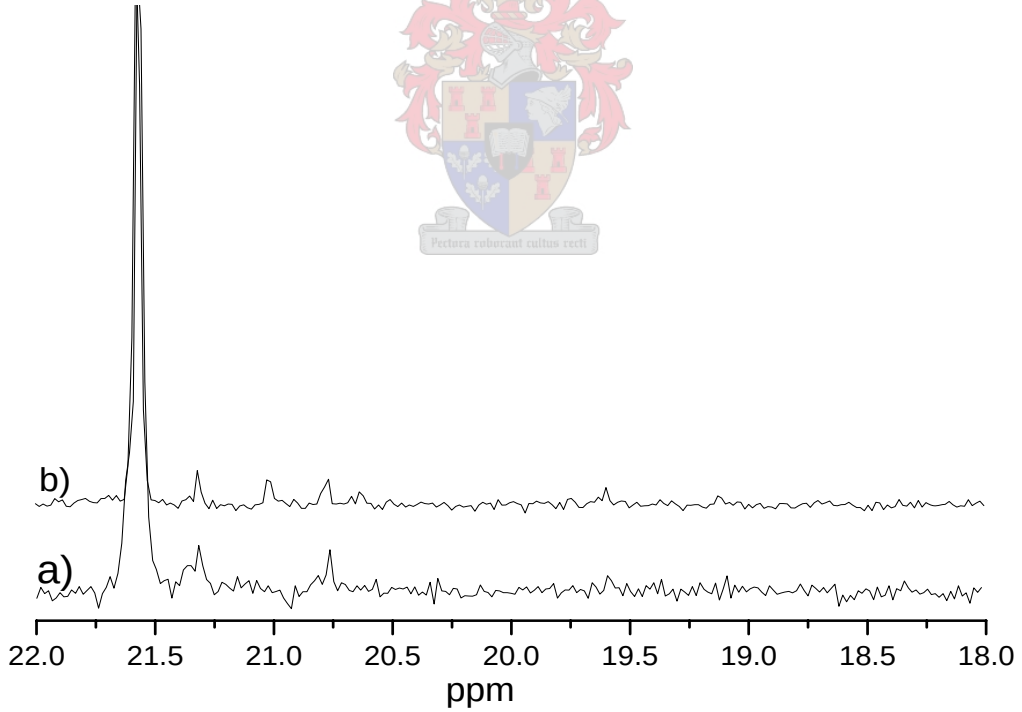

Figure 4.7 ^{13}C NMR spectra of PP prepared by EI catalyst run4: a) before extraction; b) after extraction.

4.3.2.3 Crystallization from solution (CRYSTAF)

Crystallization analysis fractionation (CRYSTAF) is based on the solution crystallization of polymer chains. This yields information about the crystallizability of the individual chains, by monitoring the changes in the concentration of polymer in a solution during a cooling process. For PP, CRYSTAF analysis gives details on the tacticity distribution and ^{13}C-NMR spectroscopy gives the overall percentage of tacticity and by combining the information that obtained from the two techniques, a complete picture of the polymer microstructure can be obtained.

Since the inter-conversion between the two isomers of the catalyst is the focus of this study, the change in the amount of the soluble fraction at room temperature will be discussed. The *meso*-isomer can be characterized as producing mainly soluble chains (atactic polymer) and the *rac*-isomer as produces mostly insoluble chains (isotactic polymer). [24-26] The change in peak broadness (and peak crystallization temperature) is a function of exposure time and activity. As tacticity increases so, the peak becomes narrower.

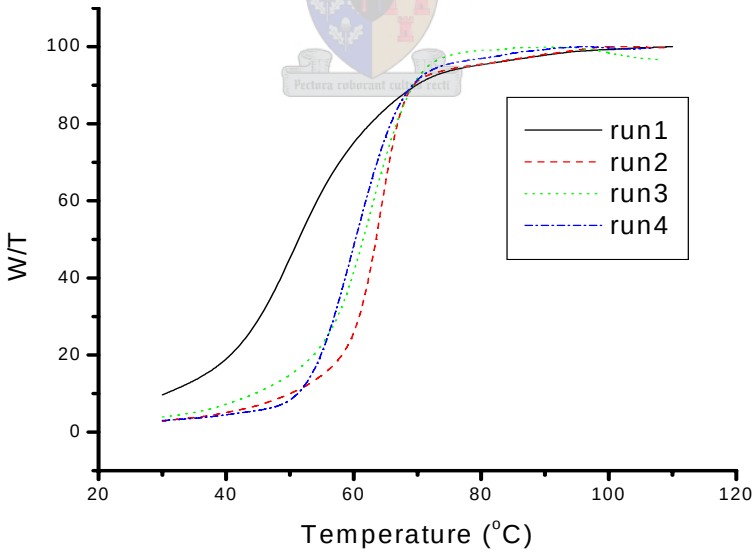

Figure 4.8 Crystallization behaviour of PP runs 1, 2, 3, and 4 as a function of temperature.

The change in the polymer concentration in solution with the temperature is shown in Figure 4.8. The first derivative of the curves in Figure 4.8 is shown in Figure 4.9.

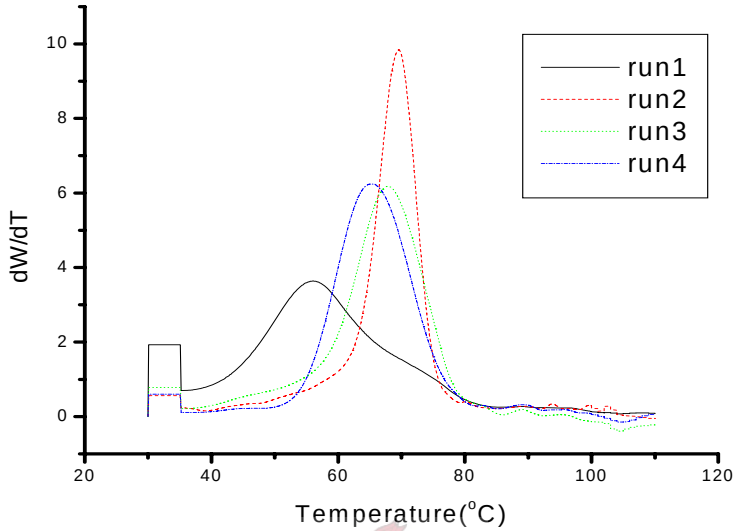

Figure 4.9 First derivative of the curves in Figure 4.8 as a function of temperature

Run 1, which has the lowest tacticity (see Table 4.2) has a broad crystallization curve with respect to the other runs, so it crystallizes over a wider range of temperatures than of the other polymers. This broadness in the crystallization temperature indicates that there is an uneven distribution of the tacticity within the polymer chains. This uneven distribution of the tacticity within the polymer chains is not a consequence of the presence of different active sites in the catalyst, but rather a result of polymerization conditions in the reactor during the polymerization, where a practical problem with the stirring rate was experienced.

Runs 2, 3, and 4 show typical first derivative crystallisation curve of i-PP, where it is characterized by sharp peak with narrow crystallization temperature. [27] The soluble fractions of these three samples are comparable and are low compared with that of run 1. The similarity in the amount of the soluble fractions in last three fractions confirms the absence of the active site that will lead the production of an atactic polymer. The slight change in the shape of the curves is due to the

changes in the catalyst concentration.

4.3.3 Propylene polymerization using (*rac*-Me_2Si(2-Me-4,5-benzoind)$_2$]$ZrCl_2$) (MBI)

The results of propylene polymerization with (*rac*-Me_2Si(2-Me-4,5-benzoind)$_2$]$ZrCl_2$) (MBI) are summarized in Table 4.5. All polymerization conditions are shown in the Table. The catalyst solutions used in runs 2, 3, 4 and 5 were exposed to the UV source (sunlight) for 0, 30, 60 and 180 minutes, respectively. The catalyst concentration in run 2 was double the catalyst concentration in run 1.

Figure 4.10 shows the change in the catalyst activity with exposure time of the catalyst solution. For the first 30 minutes of the exposure there is no change in the catalyst activity. When the exposure time exceeded 30 minutes a decrease in the activity was detected, and the activity kept on decreasing with increasing exposure time. This change in the catalyst activity was observed by using both the UV lamp or sunlight as light source.

Table 4.4 Polymerization of propylene over MBI:MAO [A,B]

Run [C]	Al/Zr	monomer (g)	activity[D]	*mmmm*%	$\overline{Mw}$	MWD	T_m °C
1	6000/1	9	5500	98	365764	2.4	152.7
2[E]	6000/1	11	7430	94	258450	2.2	152
3	6000/1	10	7400	92	232131	3.3	151
4	6000/1	10	3600	77	140231	4.2	150
5	6000/1	7	860	27.5	351493	4.7	146

[A] Polymerization time = 120 min; [metallocene] = 2.2 µmol /30 ml of toluene.

[B] All polymerizations were carried out at room temperature

[C] Runs 2, 3, 4, 5: catalyst solution irradiated for 0, 30, 60, 180 minutes

[D] kg of PP/mol of Zr:h.

[E] Run 2 had double catalyst concentration of run 1

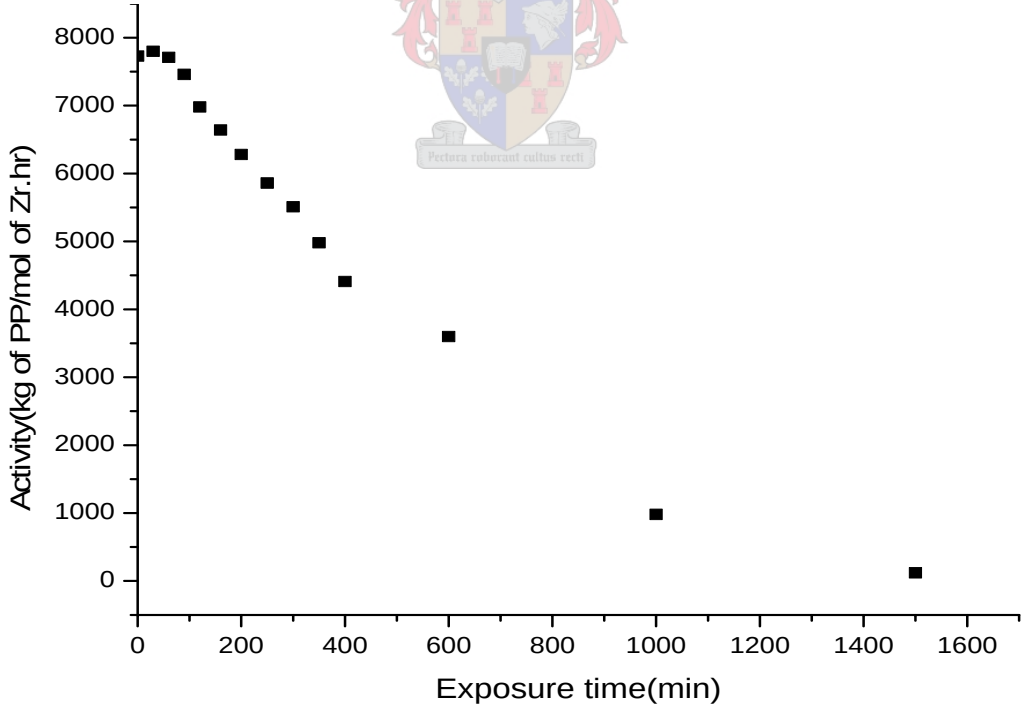

Figure 4.10 Change in the MBI catalyst activity with exposure time.

4.3.3.1 ^{13}C NMR spectra of PP prepared with MBI catalyst with different exposure times of the catalyst solutions.

Figure 4.11 shows a typical ^{13}C NMR spectrum of i-PP prepared with the MBI catalyst, where the catalyst solution has been exposed for 60 min to sunlight. The three main peaks, of equal intensity, correspond to the three different C atoms in the repeating unit (methyl, methine and methylene) at 21.6 ppm, 28.36 ppm, and 46.3 ppm. [12, 13]

The polymer, as it can be seen from its ^{13}C NMR spectrum, has a tacticity around 77%. Also it has relatively high amount of 3,1 insertions (29.9 ppm, designated by *), while no 2,1 insertions were detected in the sample.

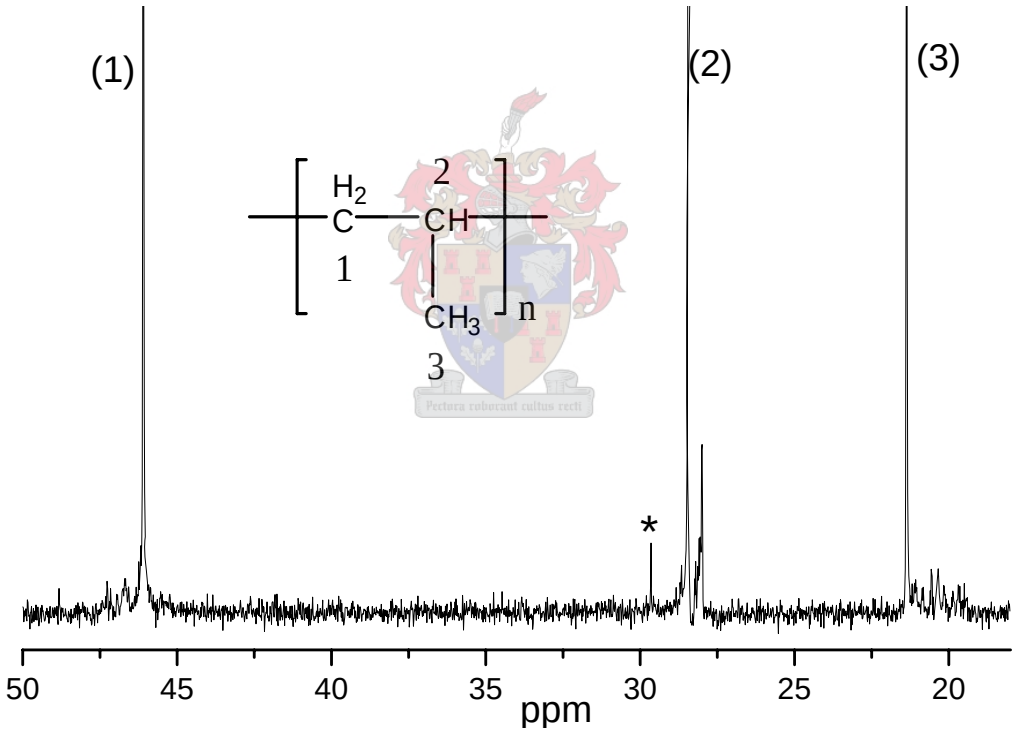

Figure 4.11 ^{13}C NMR spectrum of i-PP prepared with MBI catalyst (run 4)

No end groups can be observed, as the molecular weight of the sample is quite high.

4.3.3.2 Peak assignments.

Figure 4.12 shows the methyl region of the ^{13}C NMR spectrum of i-PP prepared with the MBI catalyst. The spectrum illustrates the different types of stereo-sequences that can be formed in a single polymer chain. Since nine different peaks can be seen in the methyl region, all the possible types of stereoerror are present. This is a clear indication that not only the *rac* C_2-symmetric form of the catalyst is present. Assignments for the stereoerror peaks can be deduced from Table 4.5.

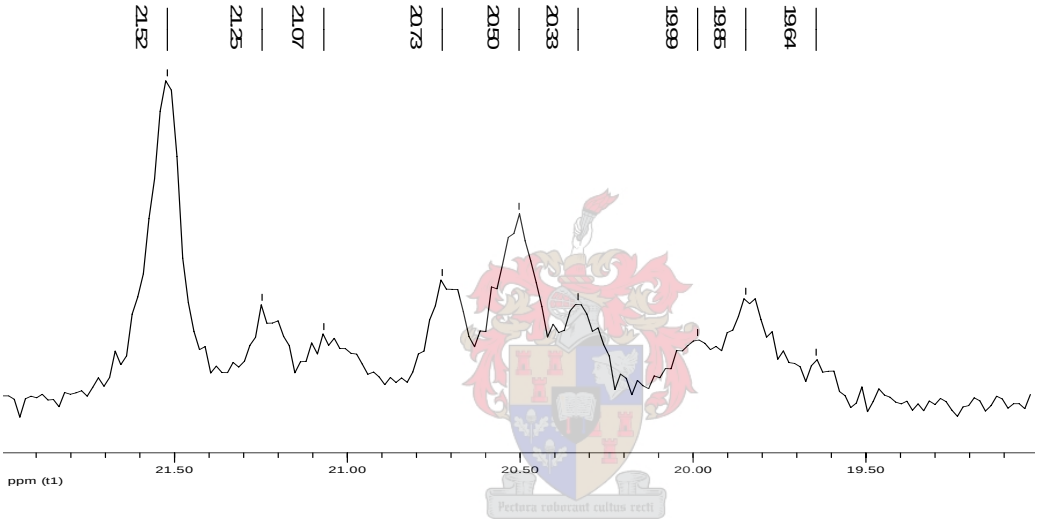

Figure 4.12 The methyl region of the ^{13}C NMR spectrum of run 5.

Table 4.5 shows the experimental ^{13}C NMR chemical shift values for the methyl pentads of PP produced using MBI, compared with calculated value was calculated using a method proposed in literature. [20]

Table 4.5 Experimental ^{13}C NMR chemical shift values for the methyl pentads of PP produced using MBI, compared with calculated values

Pentad	δ (exp.)	Δ (δ)	δ (calc.)
mmmm	21.52	0	21.52
mmmr	21.25	-0.276	21.244
rmmr	21.07	-0.55	20.97
mmrr	20.73	-0.728	20.792
rmrr	20.5	-1.009	20.511
rmrm	20.33	-1.201	20.319
rrrr	19.99	-1.499	20.021
rrrm	19.85	-1.712	19.808
mrrm	19.64	-1.94	19.58

The tacticity of the samples was calculated by measuring the integral of the of *mmmm* peak, which appears at 21.52 ppm, relative to all other peaks in the methyl region up to 19.0 ppm.

Figure 4.13 shows ^{13}C NMR spectra of PP prepared with MBI catalyst with different exposure times to the catalyst solution (using sunlight): for 0 (a), 90 (b), and 300 (c) minutes exposure time, respectively. Figure 4.13 demonstrates that there is a significant decrease in the tacticity with increasing exposure of the catalyst solution to sunlight. This is logical since exposing the catalyst solution to sunlight produces its *meso*-form as explained in the previous chapter.

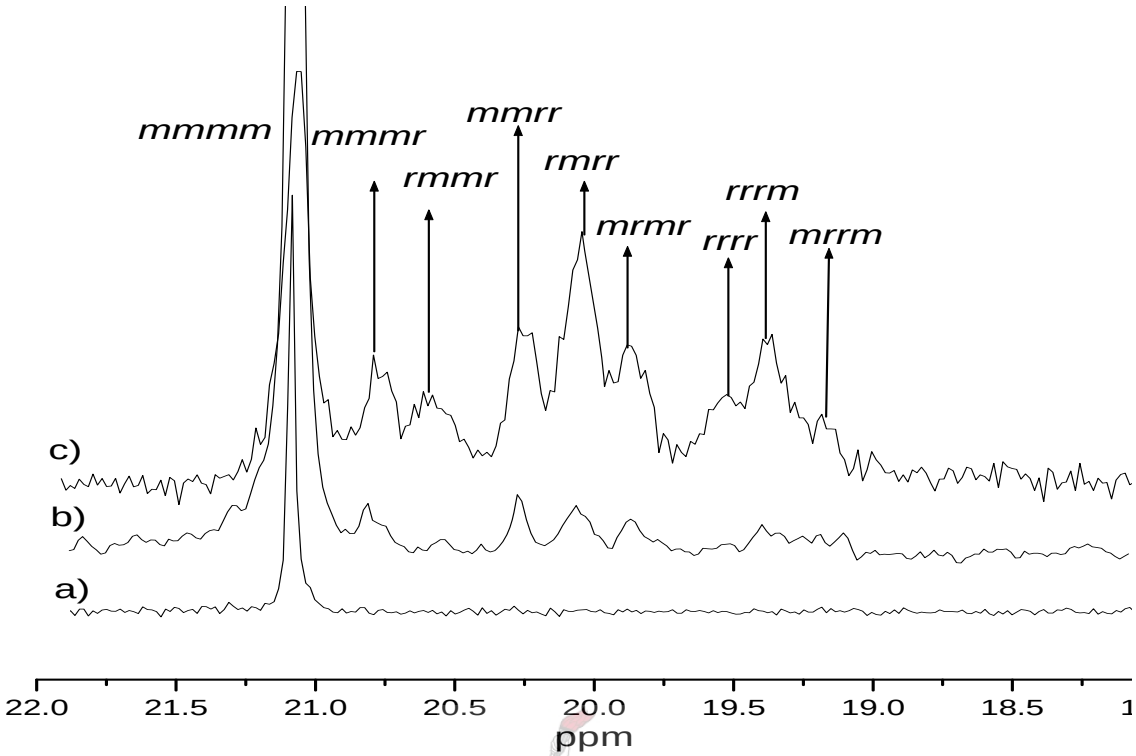

Figure 4.13 ^{13}C NMR spectra of PP prepared with MBI catalyst exposed for 0 (a), 90 (b), and 300 (c) minutes.

Figure 4.14 demonstrates the effect of the catalyst stereoselectivity on the polymer microstructure. It can be seen that rapid decrease in the isotacticity of the PP is linked to the increase in the *meso*-isomer as measured by ^{1}H NMR. When the catalyst solution reaches its photostationary state (after 330 min), the tacticity seems to be affected only by the effect of active catalyst concentration (catalyst/monomer ratio).

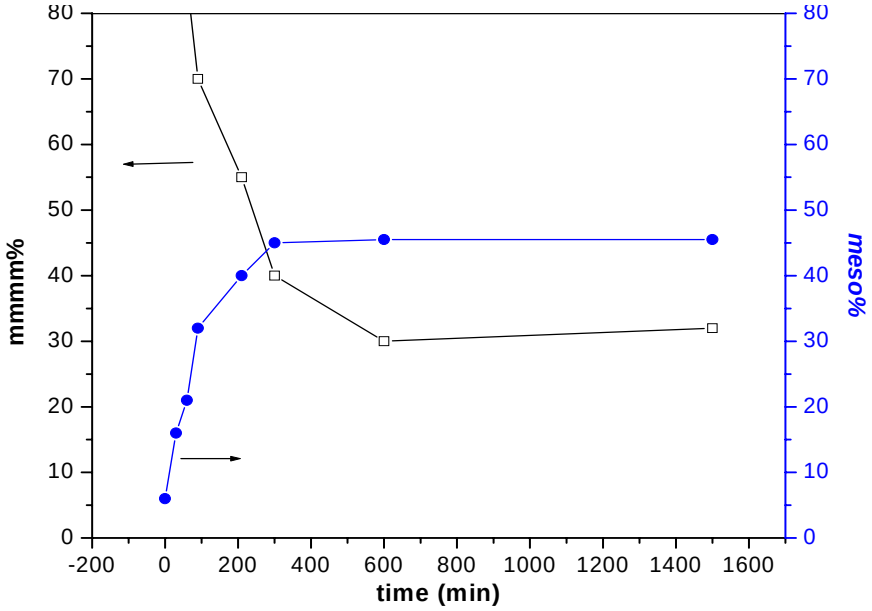

Figure 4.14 The change in the *meso*% form in the catalyst solution with exposure time and its effect on the polymer microstructure.

The ^{13}C NMR results do not conclusively prove that this decrease in the tacticity is due to two different active sites in the catalyst solution, although this is the most likely explanation. This decrease could conceivably arise from the presence of stereoirregular sequences in the polymer chains that are produced with one active site. To investigate this, an attempt was made to separate the different type of polymer chains present.

4.3.3.2 Extraction the atactic polymer

Different samples prepared with isomerised BMI catalyst were extracted with xylene and the structure of the polymers studied before and after the extraction. ^{13}C NMR spectra of PP produced by isomerised MBI catalyst: (a) after, and (b) before extraction are presented in Figure 4.15.

The tacticity of run 4 before the extraction was about 77% and after the extraction was 98.7%. This is evidence that there are two different active species in the catalyst solution, as atactic material could be completely extracted. After performing TREF analysis on the sample (see Section 4.3.3.3), the percentage of

the soluble fraction was determined to be 15.2%.

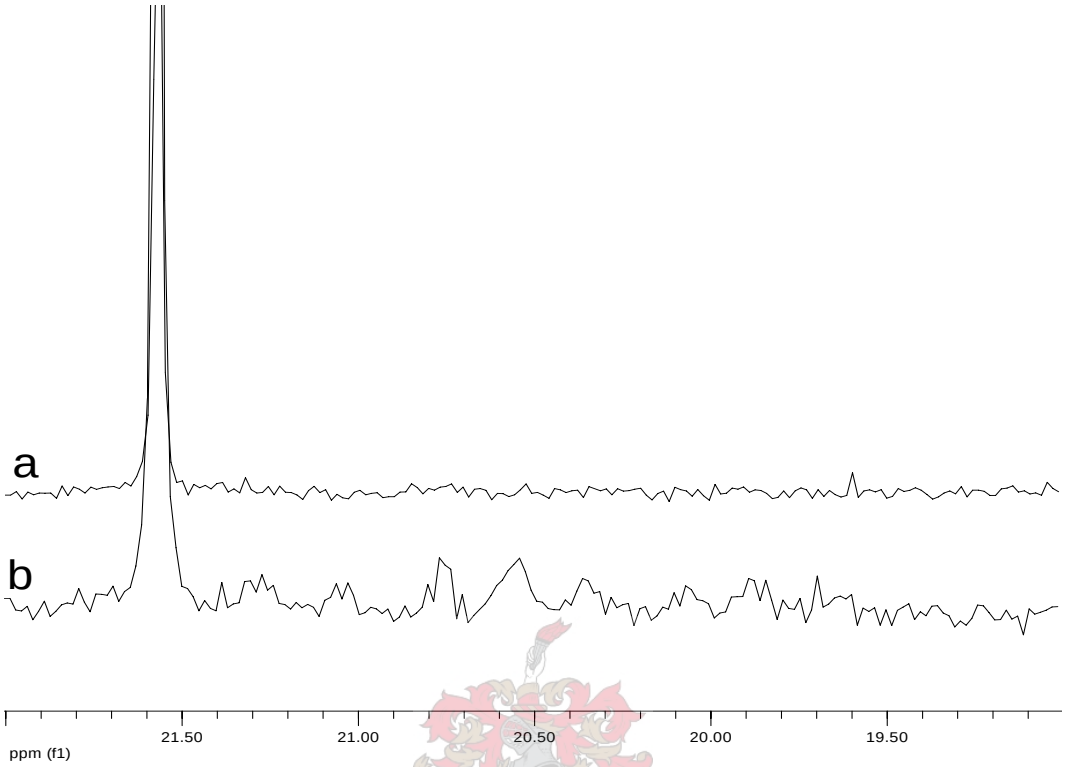

Figure 4.15 ^{13}C NMR spectra of PP prepared by MBI catalyst run4: a) after extraction; b) before extraction.

Supposing that the rate of isomerization of the MBI catalyst in deuterated dichloromethane (CD_2Cl_2) and toluene are the same, at 60 minutes exposure time the catalyst solution contains 28% *meso*-isomer and 72% *rac*-isomer. From this information it seems that the *rac*-isomer is 2.2 times more active than the *meso*-isomer.

4.3.3.3 Preparative temperature rising elution fractionation (TREF)

Table 4.6 summarizes the raw data of the TREF experiment. From Table 4.6 it can be seen that the soluble fraction which eluted at 25 ^{o}C is about 15.2% of the entire sample. The majority of the sample (60%) eluted between 90 ^{o}C and 110 ^{o}C. This is confirmed by the narrow peak in the TREF curve (weight

fraction/temperature).

Table 4.6 TREF raw data of run 4 obtained after fractionation

Temperature	Mass (mg)	Wi (%)	Σ Wi%	Δ T	Wi%/ Δ T
25	302.5	15.15	15.15	35	0.43
60	110.7	5.54	20.70	10	0.55
70	95.5	4.78	25.48	15	0.32
85	170.0	8.52	33.99	10	0.85
95	300.9	15.07	49.07	10	1.51
105	621.4	31.12	80.19	10	3.11
115	260.0	13.02	93.21	10	1.30
125	78.5	3.93	97.14	10	0.39
135	57.0	2.86	100	10	0.29

Figure 4.16 shows the weight fractions recovered for each TREF elution temperature as well as the weight fraction/temperature plot as a function of the elution temperature. The cure in Figure 4.16 illustrates that the sample has two important fractions: one characterised with narrow, sharp peak that appears between 90 ^{o}C and 110 ^{o}C and the other characterised by a broad peak that appears at lower elution temperature. These two fractions that are obtained by the TREF experiment correspond to polymer fractions that were derived from two different active species in the catalyst solution.

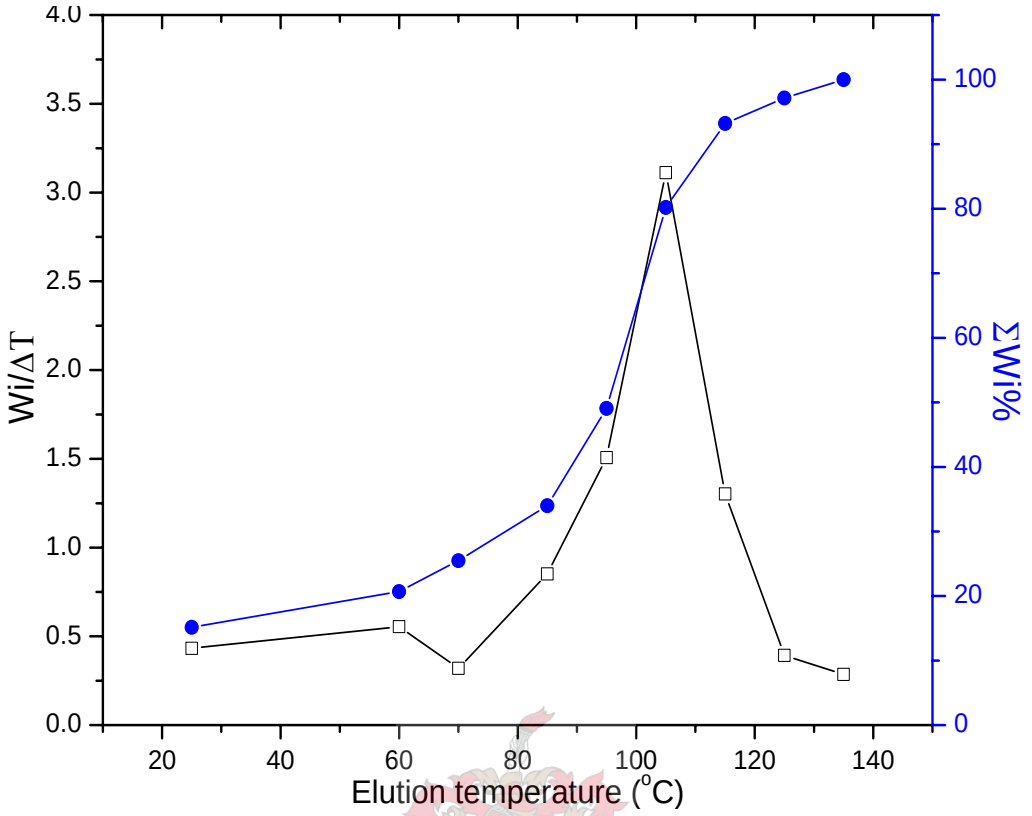

Figure 4.16 The ΣWi% and Wi%/ΔT vs the TREF elution temperature.

NMR spectroscopy was performed on one fraction from each peak (room temperature fraction and the 115 ^{o}C fraction). Figure 4.17 shows the ^{13}C NMR spectra of the room temperature fraction and 115 ^{o}C fraction. The spectra illustrates that the room temperature fraction has low tacticity (around 6%) and fraction at 115 ^{o}C has tacticity around 99%. Comparing spectra (b) in Figure 4.13 (unfractionated sample) and spectra in Figure 4.17 it can be confirmed that the unfractionated sample consists mainly of these two fractions.

Figure 4.18 shows high-temperature gel permeation chromatograms (HT-GPC) of the 25 ^{o}C fraction and the 60 ^{o}C fraction. The chromatograms indicate clearly that there is a bimodal distribution present in both fractions.

These two fractions are either atactic material or have a very low crystallinity.

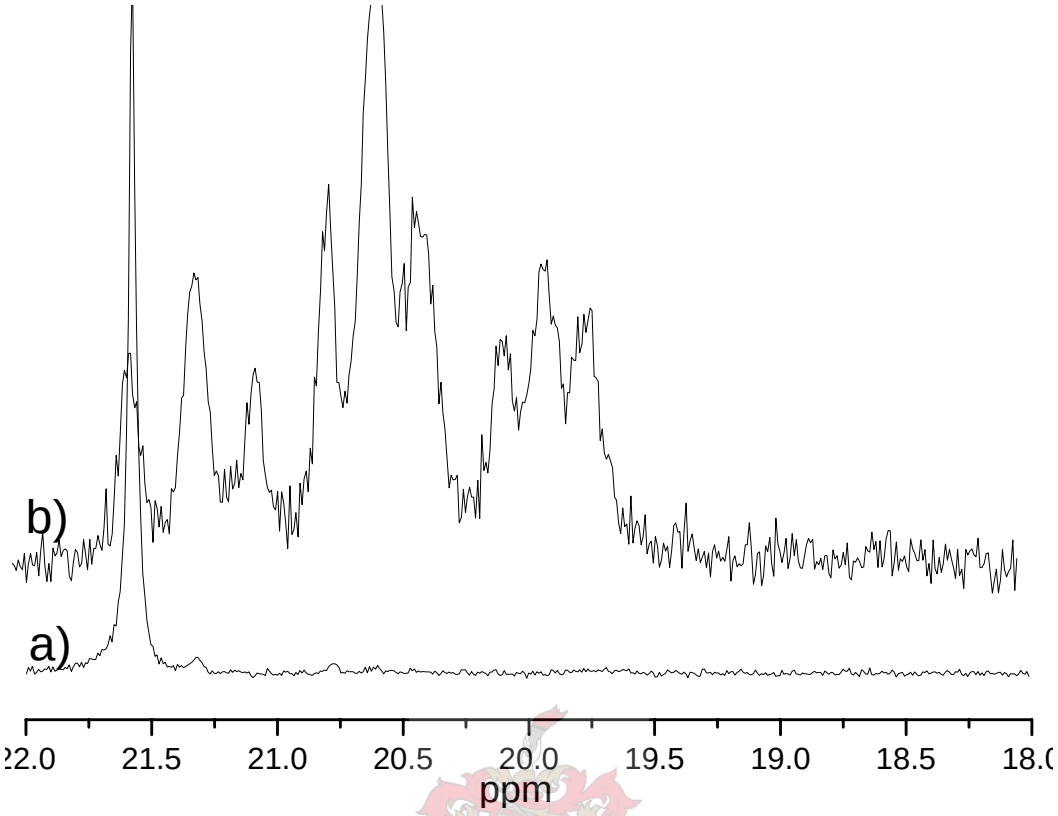

Figure 4.17 Methyl region of ^{13}C NMR spectra of; a) 115 ^{o}C fraction, and b) room temperature fraction.

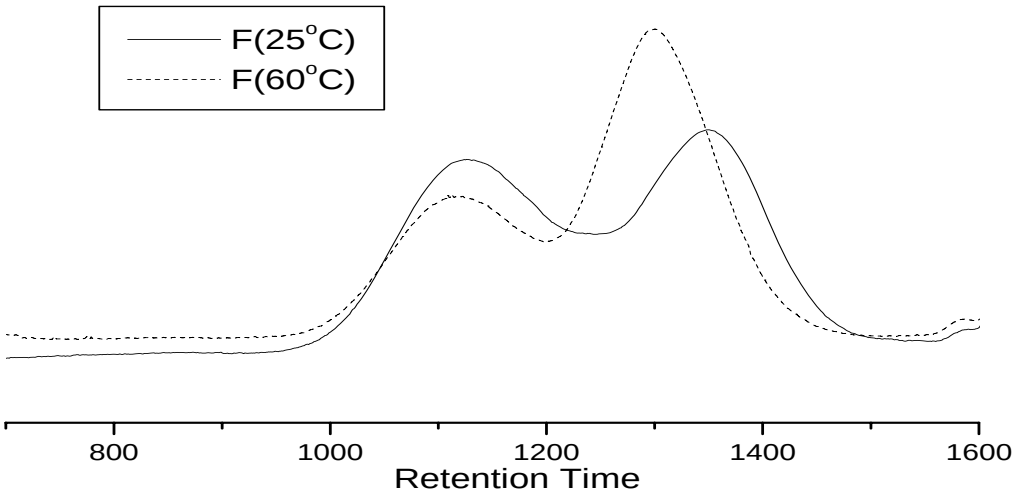

Figure 4.18 High-temperature gel permeation chromatography (HT-GPC) of low temperature fractions 25 ^{o}C, and 60 ^{o}C.

4.3.3.4 Crystallization from solution

The crystallization from solution behaviour was also studied by Crystallization Analysis Fractionation (CRYSTAF). The change in the polymer concentration in the solution with the temperature is shown in Figure 4.19. From the figure, it can be seen that the samples started to crystallize approximately at the same temperature (83 ^{o}C). This indicates that chains that crystallize at this temperature have the same configuration in terms of the percentage and distribution of the stereo- and regio-regularity.

Figure 4.20 illustrates the first derivative of the crystallization behaviour of runs 1, 2, 3, and 4. The maximum of the first derivative of the crystallization curves is taken as crystallization from solution temperature (Tc). From the derivative curves in Figure 4.20 it can be seen that Tc of the samples are roughly the same. Figure 4.19 indicates that run 1 has the lowest soluble fraction, and then the amount of the soluble fraction increases as we moved to run 2 and run 3, where run 4 has the highest soluble fraction. This was expected.

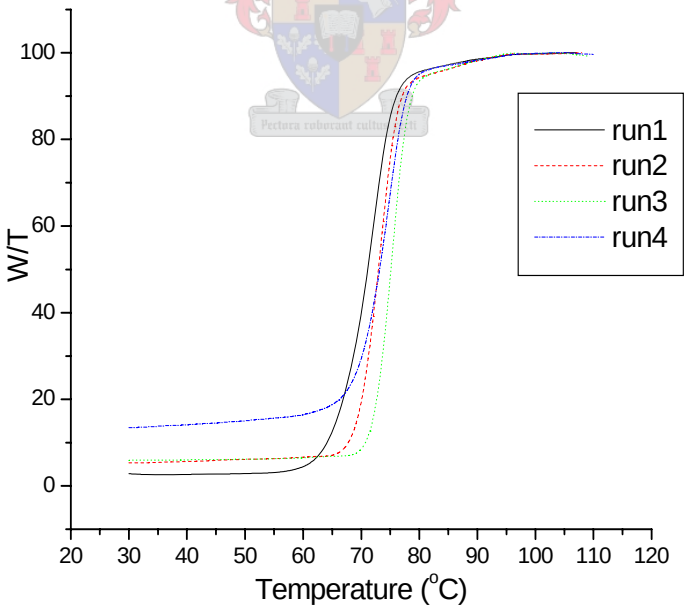

Figure 4.19 Crystallization behaviour of PP in solution; runs 1, 2, 3, and 4.

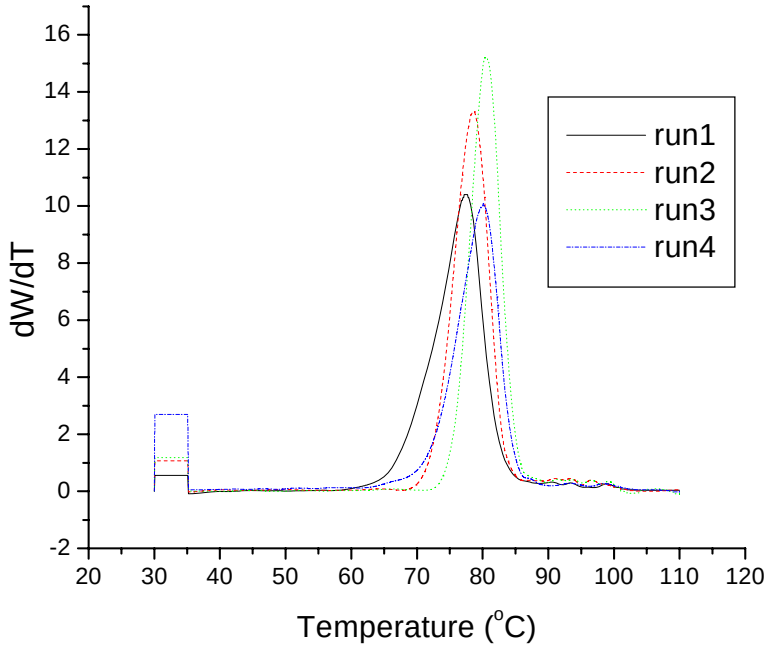

Figure 4.20 First derivative of the curves in Figure 4.18.

The soluble fractions increase as the exposure time increases. At the same time the first derivative peaks of the crystaf profiles become narrower as the exposure time of the catalyst increases. This clearly indicates the two types of catalytic sites functioning during the polymerization reactions. The narrowing of the crystaf derivative peaks indicate a narrowing of tacticity distribution of the crystallizable fraction, which is due to the effective catalyst concentration decreasing.

4.3.3.5 Molecular mass and molecular mass distribution

Figure 4.21 shows the high-temperature gel permeation chromatography (HT-GPC) of runs 1, 3, and 5.

From Figure 4.21 it is clear that as the exposure time of the catalyst solution increases so the broadness of the peak increases. This is an indication for the presence of two types of polymers due two different active sites. What is significant here is that peak shifts to a lower molecular weight than the original peak. This is evidence that the new active site produces low molecular weight

polymer compared to the original active site.

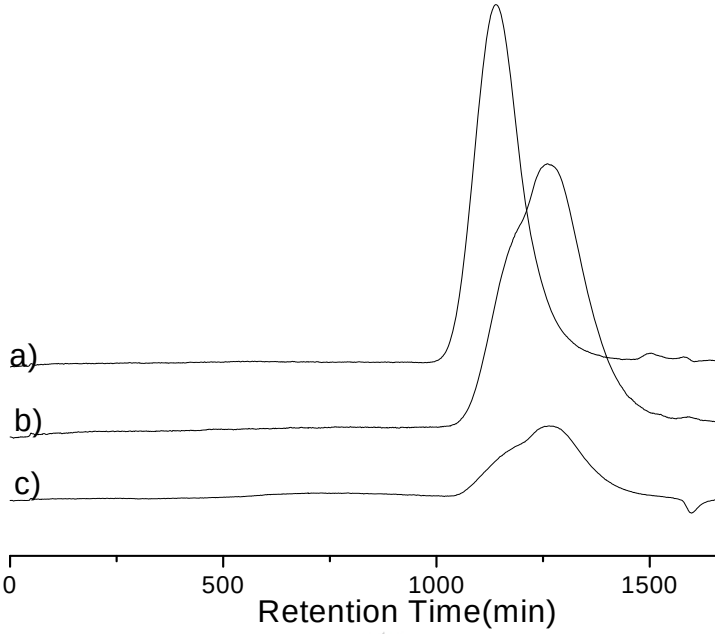

Figure 4.21 High temperature gel permeation chromatography (HT-GPC) for runs a) 1, b) 3 and c) 5.

4.3.3.6 Melting behaviour

Crystalline lamellar size and distribution within the sample will determine the shape of the melting curve and the average melting point of the sample (peak maximum temperature).

Figures 4.22 a) and b) shows the melting curves for polymers made in run 1 and run 5, respectively. From curve (a) in Figure 4.22, it can be seen that PP of run 1 has sharp melting peak at 152.7 ^{o}C.

Curve (b) is for the PP sample prepared using isomerised catalyst. From the figure it can be seen that the polymer has a broad melting peak, with a maximum at 148 ^{o}C. The broad peak is indicative of a wide distribution of lamellar thickness. This indicates that some of the chains produced by the aspecific catalyst must have some degree of crystallizability, resulting in a lower overall melting temperature (smaller crystals). Whether or not this is due to

cocrystallization is unclear.

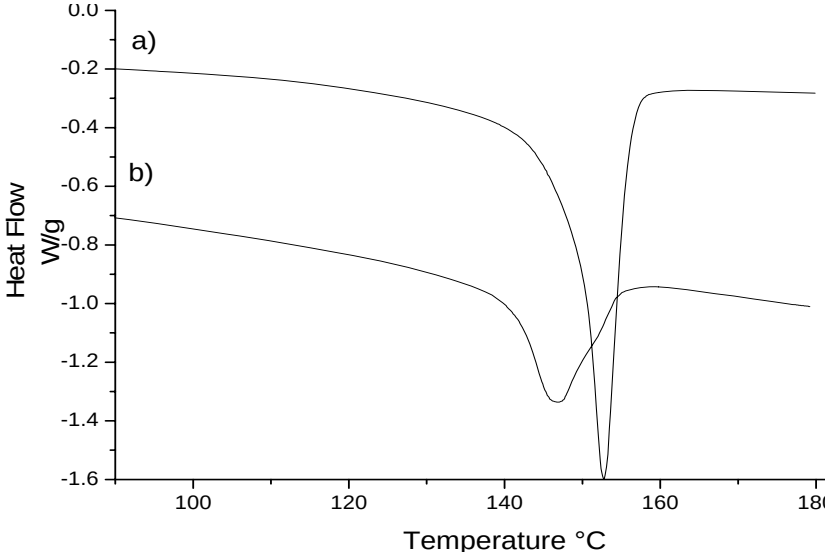

Figure 4.22 DSC melting curves of PP for runs; 1(a) and 5 (b).

All results presented so far were obtained by using sunlight for isomerization the catalyst. On the other hand, when a UV lamp (257 nm, 15W) was used as a UV source no change in the polymer microstructure was observed except slight increase in the tacticity due to decrease in the catalyst concentration, and a reduction in the catalyst activity was also observed. All these results were in line with the results that obtained during the isomerization of the catalyst (Chapter 3).

4.3.4 Activation the MBI catalyst before the isomerization process

A series of polymerization experiments were performed where the catalyst solution was first activated with MAO, and then exposed to the light. Table 4.7 shows two representative polymerization experiments. In run 1 the catalyst solution was exposed to sunlight for 3 hours and then activated with MAO and in run 2 the catalyst was activated with MAO then exposed to sunlight for 3 hours.

Table 4.7 shows that the catalyst activity in the case of activating the catalyst prior to the exposure is much higher than the catalyst activity for case where the catalyst was exposed to UV before the activation with MAO. Nevertheless the activity of the fresh catalyst (5 500 kg of PP/mol of Zr.h) is still higher than that of

the pre-activated catalyst. No change in the polymer microstructure was observed when the catalyst activated before exposure to UV compared to polymer produced using fresh (unexposed) catalyst. The pre-activated catalyst produced polymer with higher tacticity, melting temperature and molecular weight than the pre-exposed catalyst.

Table 4.7. Polymerization of propylene over MBI: MAO[A, B]

Run	Al/Zr	monomer (g)	Activity [C]	*mmmm* %	$\overline{Mw}$	MWD	T_m ^oC
1	6000/1	7	860	27.5	386396	4.7	146
2	6000/1	7	2540	99	804885	3.6	153

[A] Polymerization time = 120 min; [metallocene] = 2.2 µmol /30 ml of toluene.

[B] All polymerizations were carried out at room temperature.

[C] kg of PP/mol of Zr.hr.

During the activation of the catalyst with the cocatalyst a complex between the metallocene and the MAO is formed. The cationic Zr species associated with the anionic MAO apparently prevents isomerization of the catalyst complex in solution. The first step in the isomerization process, the homolytic cleavage of the η^5-metal cyclopentadienyl ring bond can apprently not occur. So no conversion from the *rac*-isomer to *meso*-isomer will occur.

Figure 4.23 shows ^{13}C NMR spectra of PP prepared with MBI catalyst: a) activated before exposure, and b) activated after exposure for 3hr. Spectrum b) shows the different stereoerrors that are formed due to the isomerization the catalyst solution. Spectrum (a) illustrates that the sample is highly isotactic and the presence of high percentage of regioerror as 3,1 insertion (8%) at 30ppm.

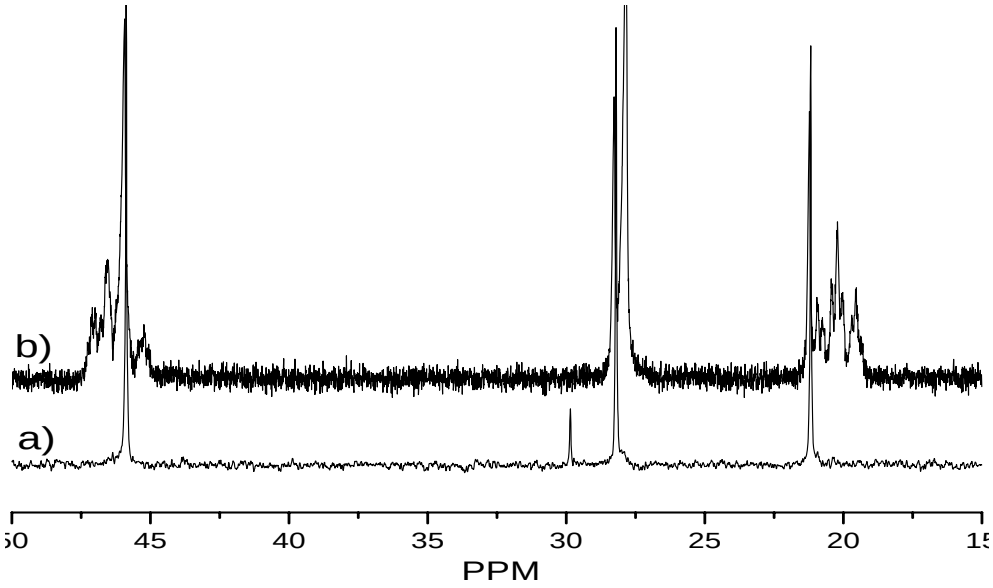

Figure 4.23 ^{13}C NMR spectra of PP prepared by MBI catalyst exposed for 3h in sunlight; a) before, b) after activation with MAO.

4.4 References

1. Resconi, L.; Cavallo, L.; Fait, A.; Piemontesi, F, Chem. Rev, 2000. 100: p. 1253.

2. Thomann, R.; Wang, C.; Kressler, J.; Mulhaupt, R, Macromolecules, 1996. 29: p. 8425.

3. Alamo, R.; Kim, M.; Galante, M.; Isasi, J.; Mandelkern, L, Macromolecules, 1999. 32: p. 4050.

4. Ewen, J.A.; J. Am. Chem. Soc, 1984. 106: p. 6355.

5. Resconi, L.; Fait, A.; Piemontesi, F.; Colonnesi, M.; Rychlicki, H.; Zeigler, R, Macromolecules, 1995. 28: p. 6667.

6. Kaminsky, W.; Ahlers, A.; Moeller, N, Angew. Chem. Int. Ed, 1989. 28: p. 1216.

7. Stehling, U.; Diebold, J.; Kirsten, R.; Roell, W.; Brintzinger, H.; Juengling, S.; Muelhaupt, R.; Langhauser, F, Organometallics 1994. 13: p. 964.

8. Jungeling, S.; Mulhaupt, R.; Stehling, U.; Brintzinger, H, J. Poly. Sci., Part A: Polym. Chem, 1995. 33: p. 1305.

9. Song, W.; Yu, Z.; Chien, J.C.W., J. Organomet. Chem, 1996. 512 p. 131.

10. Cheng, H.; Alan, D., NMR Spectroscopy of Polymers in Solution and in the Solid State. 2003, Washington, D.C American Chemical Society. 197.

11. Busico, V.; Cipullo, R, Prog. Polym. Sci, 2001. 26: p. 443.

12. Grassi, A. Zambelli, A. Resconi, L. Albizatti, E. Mazzochi, R., Macromolecules, 1988. 21: p. 617.

13. Cheng, H.; Alan, D., NMR Spectroscopy of Polymers in Solution and in the Solid State. 2003, Washington, D.C American Chemical Society. 194.

14. Resconi, L.; Abis, L.; Franciscono, G., Macromolecules, 1992. 25: p. 6814.

15. Busico, V.; Cipullo, R.; Corradini, P.; Landriani, L.; Vacatello, M.; Segre, A, Macromolecules, 1995. 28: p. 1887.

16. Busico, V.; Corradini, P.; De Biasio, R.; Landriani, L.; Segre, A, Macromolecules, 1994. 27: p. 4521.

17. Cheng, H.; Alan, D., NMR Spectroscopy of Polymers in Solution and in the Solid State. 2003, Washington, D.C American Chemical Society. 196.

18. Provasoli, A.; Ferro, D, Macromolecules, 1977. 10: p. 874.

19. Cheng, H.; Lee, G, Macromolecules, 1987. 20: p. 436.

20. Busico, V.; Cipullo, R.; Monaco, G.; Vacatello, M, Macromolecules, 1997. 30: p. 6251.

21. Rheingold, A.; Robinson, N.; Whelan,J.; Bosnich, B, Organometallics, 1992. 11: p. 1869.

22. Collins, S.; Hong, Y.; Ramachandran, R.; Taylar, N, Organometallics, 1991. 10: p. 2349.

23. Busico, V.; Cipullo, R.; Chadwick, J.; Modder, J.; Sudmeijer, O, Macromolecules, 1994. 27: p. 7538.

24. Moore, E.P (Jr), Polypropylene Handbook. 1996: Hanser Publishers, Munich Vienna New York. 124.

25. Kaminsky, W.; Kulper, K.; Brintzinger, H, Angew. Chem. Int. Ed, 1985. 24: p. 507.

26. Collins, S.; Guthier, W.; Holden, D.; Kuntz, B.; Taylar, N.; Ward, D, Organometallics, 1991. 10: p. 2061.

27. Soares, J.; Anantawaraskul, S, J. Polym. Sci. Part B: Polym. Phys, 2005. 43: p. 1557.

Chapter 5

Conclusions and Recommendations

5.1 Conclusions

C_2-symmetric metallocene catalysts are affected by UV radiation. Different catalysts are affected in different ways. Both *rac-meso* isomerization and degradation is possible, although isomerization appears to be absent on some catalysts. The substituents on the indenyl ligands have an effect in the isomerization rate and on the photostationary state. Results show that the wavelength of light has an impact on the isomerization kinetics (ligand rotation), but the scission of the of the η^5-metal-cyclopentadienyl ring bond is promoted by wide range of wavelengths.

For the MBI catalyst, when using the daylight as a source of UV, conversion of the *rac*-isomer into *meso*-isomer occurred over time, but no conversion took place when using a UV lamp as light source. The conversion of *rac*-isomer to *meso*-isomer continued until it reached a photostationary state, where the two isomers are in equilibrium in the solution mixture. On the other hand, the EI catalyst did not show any conversion from one isomer to the other upon exposure of the catalyst solution to both UV sources. At long exposure times of irradiation, extensive decomposition of both catalysts occurred.

Results show that a good correlation between isomerization studies conducted in halogenated, deuterated solvents and polymer structures arising from catalyst solutions exposed to UV light while in non-deuterated, non-halogenated solvents.

For the MBI catalyst, irradiation of the catalyst solution (used for polymerization) via sunlight reduces the polymer tacticity as a result of increasing the *meso* form of the catalyst in the catalyst solution. CRYSTAF and TREF analysis of the resultant polymer confirmed that the decrease in the stereoselectivity of the catalyst was due to the formation of the achiral C_s symmetric form of the catalyst in solution.

When using a UV lamp for the irradiation of the catalyst solution, an increase in the polymer tacticity resulted. This increase in the polymer tacticity was

due to decrease in the effective concentration of catalyst in solution. For the EI catalyst the results showed that irradiation of the catalyst solution (using both UV sources) had the same effect on the resultant polymer as the effect of reducing the catalyst concentration.

Activating the MBI catalyst before the exposure has a little effect on catalyst activity and no effect on the microstructure of the produced polymer. On the other hand, activating the EI catalyst before the exposure has no effect on catalyst activity or on the polymer microstructure.

In practice, in order to reduce the effect of the different UV sources of the resultant polymer, the results recommend the activation of the C_2-symmetric metallocene catalyst solutions immediately after preparing the catalyst solution or excluding it from the any sources of UV irradiation.

5.2 Recommendations for future investigations

Although the research objectives of this study were accomplished, a number of recommendations can be made. These recommendations can contribute to future research based on this work and lead to an increase in the commercial value of the project.

It has been shown that the isomerization depends on the UV radiation wavelength. So, depending on the UV wavelength, metallocene catalysts respond differently. The photostationary state of the individual metallocene depends on the UV wavelength. Thus by using a UV lamp where the wavelength can be adjusted it could be possible to obtain the suitable wavelength for a specific photostationary state value. This can be utilized throughout the synthesis of the catalyst, where the ratio of the two isomers of the catalyst can be manipulated.

In the case of copolymerization of propylene with other higher α-olefins, the *meso*-isomer is more active toward higher α-olefins than toward propylene

(the two monomers have different reactivity ratios with the two isomers), so isomerization of the catalyst before the polymerisation will increase the α-olefins percentage in the produced polymer, hence polymer with new inherent properties could be obtained.